

1-1-1999

Model-based integration of process design and control via process synthesis: development of highly controllable and environmentally benign processes

Yihua Yang

Follow this and additional works at: http://digitalcommons.wayne.edu/oa_dissertations

Recommended Citation

Yang, Yihua, "Model-based integration of process design and control via process synthesis: development of highly controllable and environmentally benign processes" (1999). *Wayne State University Dissertations*. Paper 1260.

This Open Access Dissertation is brought to you for free and open access by DigitalCommons@WayneState. It has been accepted for inclusion in Wayne State University Dissertations by an authorized administrator of DigitalCommons@WayneState.

**MODEL-BASED INTEGRATION OF PROCESS DESIGN AND
CONTROL VIA PROCESS SYNTHESIS:
*DEVELOPMENT OF HIGHLY CONTROLLABLE AND
ENVIRONMENTALLY BENIGN PROCESSES***

by

YIHUA YANG

DISSERTATION

Submitted to the Graduate School

of Wayne State University,

Detroit, Michigan

in partial fulfillment of the requirements

for the degree of

DOCTOR OF PHILOSOPHY

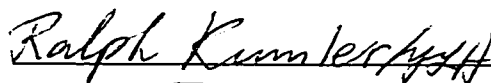
1999

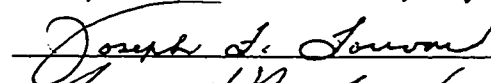
MAJOR: CHEMICAL ENGINEERING


Approved by:

 12/15/1998

Advisor Date









To Guo-Hua

TABLE OF CONTENTS

ACKNOWLEDGMENTS	iii
LIST OF TABLES	viii
LIST OF FIGURES	x
LIST OF SYMBOLS	xiv
CHAPTER 1 INTRODUCTION	1
1.1 Background	1
1.2 Objective and Significance	5
1.3 Scope of the Research	7
CHAPTER 2 DEVELOPMENT OF DISTURBANCE PROPAGATION	
MODELS FOR HEAT EXCHANGER NETWORKS	9
2.1 Introduction	9
2.2 Motivation	12
2.3 Fundamental Model	13
2.4 Unit-Based Simplified Disturbance Propagation Model	16
2.5 System Disturbance Propagation Model	20
2.6 Case Studies	23
CHAPTER 3 SYNTHESIS OF COST-EFFECTIVE AND CONTROLLABLE	
HEAT EXCHANGER NETWORKS	37
3.1 Introduction	37
3.2 Integration Strategy for Disturbance Rejection	38
3.2.1 Basic strategy	39
3.2.2 Disturbance allocation	41

3.3	Synthesis Approach	45
3.3.1	Knowledge base	45
3.3.2	Three-stage integration procedure	46
3.4	Illustrating Example	48
CHAPTER 4 SYNTHESIS OF ENVIRONMENTALLY BENIGN MASS		
	EXCHANGER NETWORKS	55
4.1	Introduction	55
4.2	Motivation	57
4.3	Unit-Based Mass Exchange Model	60
4.4	Unit-Based Simplified Disturbance Propagation Model	65
4.5	System Modeling for Waste Rejection	69
4.5.1	Generation of lumped units models	70
4.5.2	Derivation of an all-units model	72
4.5.3	Determination of a conversion matrix	73
4.5.4	Permutation of the all-units model	74
4.5.5	Evaluation formulation	75
4.6	Case Studies	76
CHAPTER 5 DESIGN OF HIGHLY OPERABLE HEAT-INTEGRATED		
	DISTILLATION PROCESSES	88
5.1	Introduction	88
5.2	Motivation	90
5.3	Basic Distillation Column Model	91
5.4	Modeling for Disturbance Propagation	92
5.4.1	Disturbance variables and their relationships	93

5.4.2	Temperature dependent enthalpy change	94
5.4.3	Fluctuation of output temperatures	95
5.4.4	Heat duty-related pressure fluctuation	97
5.4.5	Overall disturbance propagation model	101
5.5	Case Studies	104
5.5.1	Pentane-benzene binary separation process	104
5.5.2	Modification of a heat integrated distillation column process	107
CHAPTER 6 DESIGN OF CONTROLLABLE REACTION SYSTEMS		115
6.1	Introduction	115
6.2	Motivation	116
6.3	Unit-Based Disturbance Propagation Models	119
6.4	Case Studies	131
CHAPTER 7 SYNTHESIS OF OPTIMAL PLANT-WIDE WASTEWATER REUSE NETWORKS		138
7.1	Introduction	138
7.2	Elementary Wastewater Reuse	139
7.3	Modeling for a Plant-Wide Wastewater Reuse Network	141
7.4	Case Studies	146
CHAPTER 8 EXTENDED OPTIMIZATION MODELING FOR DESIGNING A WATER REUSE SYSTEM IN AN ELECTROPLATING PLANT		151
8.1	Introduction	151
8.2	Basic Strategies for Wastewater Minimization	152
8.3	Extended System Model	155
8.4	Case Study	159

LIST OF TABLES

Table 2.1	Stream Data for the HSP15R Synthesis Problem	24
Table 2.2	Comparison of the Deviations of Stream Target Temperatures in Five Solution Alternatives for H5SP1R Synthesis Problem	24
Table 3.1	Stream Data for the HSP15R Synthesis Problem	48
Table 3.2	Disturbances and Control Requirements for the HSP15R Synthesis Problem	49
Table 3.3	Comparison of the Stream Target Temperatures in Five Alternative Solutions for the H5SP1R Problem	54
Table 4.1	Stream Data for the M5SP1R Synthesis Problem	77
Table 4.2	Comparison of the Concentration Fluctuations at the Stream Outlets in Five Solution Alternatives for the M5SP1R Synthesis Problem ...	81
Table 4.3	Stream Data for the Phenol Solvent Extraction Problem	84
Table 4.4	Comparison of the Concentration Fluctuations at the Stream Outlets in Three Solution Alternatives for the Phenol Solvent Extraction Problem	87
Table 5.1	Steady-State Data of the Pentane-Benzene Separation Process	105
Table 5.2	Disturbance Specification for the Binary Separation System	105
Table 5.3	Simulation Results for the Binary Separation System	106
Table 5.4	Steady-State Data of the Heat Integrated Column Process	109
Table 5.5	Disturbance Specification for the Heat Integrated Column Process ..	110
Table 5.6	Comparison of the Simulations for the Heat Integrated Column Process Alternatives	114

Table 6.1	Types of Reactor Systems	119
Table 6.2	Design Data of a Non-Isothermal CSTR	132
Table 6.3	Prediction Precision of the Simplified Model	133
Table 6.4	Steady State Data of the Reactor Process System	136
Table 6.5	Comparison of the Results	137
Table 7.1	Maximum Water Concentrations and the Quantity of a Single Pollutant Removed from Four Major Papermaking Processes	147
Table 7.2	Comparison of Fresh Water Consumption in the Papermaking Process with and without Water Reuse	148
Table 7.3	Maximum Water Concentrations and the Quantity of Multiple Pollutants Removed from Seven Major Papermaking Processes	149
Table 7.4	Comparison of Fresh Water Consumption in the Papermaking Process with and without Water Reuse	149
Table 8.1	Process Data and Constraints in a Rinsing System	161
Table 8.2	Optimal Water Flow Rates in the Water Reuse System	166
Table 8.3	Comparison of Fresh Water Consumption between the Original and Modified Processes	167
Table C-1	Conversion Factors of Mass Flow rate Disturbances	185

Figure 3.5	Disturbance Pathways with Small Mass Flow Rate in the Hot Stream and Large One in the Cold Stream	45
Figure 3.6	Initial Grid Diagram of the H5SP1R Problem	50
Figure 3.7	Preassigned Grid Diagram of the H5SP1R Problem	51
Figure 3.8	Grid Diagram of the Optimal Solution for the H5SP1R Problem	52
Figure 3.9	Grid Diagram of an Alternative for the H5SP1R Problem	53
Figure 4.1	Flowsheet of an Integrated Plant for Product Purification	58
Figure 4.2	Grid Diagrams of the MEN in the Integrated Plant	60
Figure 4.3	Graphical Representation of Mass Transfer Mechanism	61
Figure 4.4	Concentration Driving Force between Equilibrium and Operating Lines in a Mass Transfer Process	62
Figure 4.5	Disturbance Propagation through Stream Splitting and Mixing	69
Figure 4.6	Grid Diagrams of the Five Solutions of MEN Problem M5SP1R ...	78
Figure 4.7	Flowsheet of a Phenol Solvent Extraction Process	83
Figure 4.8	Grid Diagrams of the MEN in the Phenol Solvent Extraction Process	85
Figure 5.1	A Heat Integrated Column Process	91
Figure 5.2	A Typical Continuous Distillation Column System	92
Figure 5.3	Representation of Energy Balance for the Condenser	98
Figure 5.4	Flowsheet of an Original Distillation Process	108
Figure 5.5	A Heat-Integrated Distillation Process (Solution A)	111
Figure 5.6	A Modified Distillation Process (Solution B)	113
Figure 6.1	Flowsheet of a Reactor Network	118
Figure 6.2	Modified Process Flowsheet	118

Figure 6.3	A Continuous Flow Reaction Process	120
Figure 6.4	Process Flowsheet of a Heat Integrated Reaction System	134
Figure 6.5	Modified Process Flowsheet of the Heat Integrated Reaction System	137
Figure 7.1	Removal of Multiple Contaminants in a Single Water Process	140
Figure 7.2	Superstructure Representation of a Water Reuse System	143
Figure 7.3	Potential Schemes from the Superstructure	144
Figure 7.4	Optimal Design of a Water Reuse System Containing Four Sub- Water Processes	147
Figure 7.5	Optimal Design of a Water Reuse System with Seven Sub-Water Processes	150
Figure 8.1	Sketch of a Conventional Electroplating Process	153
Figure 8.2	Mass Transfer Diagram for a Rinsing Process	154
Figure 8.3	System Representation of a Water-Reused Rinsing Process	156
Figure 8.4	Original Rinsing System in an Electroplating Plant	160
Figure 8.5	Superstructure of the Water Reuse System for Optimization	162
Figure 8.6	Modified Rinsing System	168
Figure C-1	Mass Flow Rate Disturbance at the Inlet of a Mass Exchanger	180
Figure C-2	Mass Flow Rate Disturbance at the Inlet of a Mixer	181
Figure C-3	Mass Flow Rate Disturbance at the Inlet of a Splitter	182
Figure C-4	Partial Network System for Evaluating a Conversion Factor	184
Figure D-1	Components Selected in the Fluid Package	187
Figure D-2	Data input of Feed Streams	187
Figure D-3	Column Specifications and Simulation Results	188

Figure D-4	Specifications and Simulation Results for a Heat Exchanger	190
Figure D-5	Stream Specifications and Simulation Results for a Splitter	192
Figure D-6	Stream Specifications and Simulation Results for a Mixer	193
Figure D-7	Simulation Results of the Heat-Integrated Distillation Column Process	194
Figure D-8	The PFD of the Heat-Integrated Distillation Column Process	195

LIST OF SYMBOLS

A	Heat/mass transfer area, m^2
A	Temperature/concentration-related disturbance propagation matrix
δA	Change of mass transfer area, m^2
b	Constant
B	Mass flow rate of the bottom product stream in a distillation column, kg/h
B	Heat capacity/mass flow rate related disturbance propagation matrix
δB	Maximum fluctuation of mass flow rate in the bottom product stream of a distillation column, kg/h
C	Concentration of chemical species, $\text{wt.}\%$
C	Matrix related to steady-state temperatures
C_P	Heat capacity, $\text{kJ/kg}\cdot^\circ\text{K}$
δC	Maximum concentration deviation from a nominal setting, $\text{wt.}\%$
ΔC	Concentration difference, $\text{wt.}\%$
D	Mass flow rate of the overhead product stream in a distillation column, kg/h
D	Mass flow rate disturbance propagation vector
δD	Maximum fluctuation of mass flow rate in the overhead product stream of a distillation column, kg/h
f	Conversion factor
F	Mass flow rate of the feed stream, kg/h
F	Conversion matrix
δF	Maximum disturbance of mass flow rate in the feed stream, kg/h
H	Enthalpy, kJ/kg

δH	Maximum enthalpy deviation from a nominal setting, kJ/kg
I	Unit matrix
K	Overall mass transfer coefficient/equilibrium constant
m	Constant
M	Mass flow rate, kg/h
δM	Maximum disturbance of mass flow rate from a nominal setting, kg/h
Mc_p	Heat capacity flow rate, kJ/h·°K
δMc_p	Maximum disturbance of heat capacity flow rate, kJ/h·°K
N	Number of trays in a given column
P	Pressure, kPa
P^o	Saturated vapor pressure for a pure component, kPa
δP	Maximum pressure deviation from a nominal setting, kPa
Q	Heat duty of a heat exchanger, kJ/h
Q_b	Heat load in the reboiler of a distillation column, kJ/h
Q_c	Heat load in the condenser of a distillation column, kJ/h
δQ	Maximum deviation of the heat duty of a heat exchanger, kJ/h
δQ_b	Maximum disturbance of heat load in the reboiler of a distillation column, kJ/h
δQ_c	Maximum disturbance of heat load in the condenser of a distillation column, kJ/h
R	Reflux ratio
T	Temperature, °K
δT	Maximum temperature deviation from a nominal setting, °K
ΔT	Temperature difference, °K
V	Mass flow rate of distillate in a distillation column, kg/h

r	Rich stream
s	Splitter
S	Splitters in the system

Greek

α	Relative volatility
α_p	Coefficient in the Antoine equation
β_p	Coefficient in the Antoine equation
γ	ratio of the equilibrium constants

and operating costs. Process operational issues, especially controllability, are left to the control engineers. It is conceivable that in a highly integrated plant, process units are always heavily interconnected. This gives rise to massive heat and mass interactions among process streams. These interactions create numerous paths through which severe disturbances propagate, and consequently, interfere the operations of possibly many units. This can be detrimental to process controllability (Morari, 1992; Luyben and Floudas, 1994). The worst case is unmanageable disturbance propagation (DP), which makes the process uncontrollable, no matter what control techniques are used (Papalexandri and Pistikopoulos, 1994b; Yang *et al.*, 1996). Industrial practice indicates that to have effective process integration, process controllability must be considered during a process design stage. This leads to the introduction of another type of integration: the integration of process design and control (or the integration of PD&C for short). Most recently, Downs and Sirola (1997) have provided an industrial perspective: “integrated process and control systems design can combine technical ingenuity needed to achieve superior economics with operational perspective that results in processes which are easier to run with minimum variability.”

The integration of PD&C can be initiated in different phases and at different complexity levels of overall process engineering activities. Over the past decade, studies in this field have mainly focused on process screening and control system synthesis (Calandranis and Stephanopoulos, 1988; Morari, 1992; Zhu *et al.*, 1997). The resultant processes have demonstrated improved controllability in terms of set point tracking and disturbance rejection. The available techniques can be classified into two groups, according to the types of information used. One group is based on the steady-state characteristics of a process, and the other on its dynamic characteristics and requires

approximate or complete process dynamic models. There has been a substantial development in the former. However, the latter appears to be a fertile ground for further research (McAvoy, 1987). In terms of complexity levels, the processes studied have usually been relatively simple (with only few units). For these processes, equipment design, the identification of appropriate manipulated and controlled variables, and the selection of suitable control algorithms are usually easy. Process dynamics can be realistically addressed in process modification and control synthesis. Note that very few reports have addressed improving structural controllability of complex processes, such as heat exchanger networks (HEN's), mass exchanger networks (MEN's), distillation column networks (DCN's), reactor networks (RN's), and any of their combinations. For these processes, structures are of utmost importance for effective integration of PD&C. Admittedly, this is an extremely difficult task requiring tremendous effort.

During the past two decades, a key issue addressed for the integration of PD&C at a process design stage was mainly the operational aspect of flexibility. Many approaches have been introduced to identify operable HEN's (Saboo *et al.*, 1985; Calandranis and Stephanopoulos, 1986; Linnhoff and Kotjabasakis, 1986; Papalexandri and Pistikopoulos, 1994b) and flexible MEN's (Papalexandri and Pistikopoulos, 1994a; Zhu and El-Halwagi, 1995). Their approaches have demonstrated the effective analysis of existing networks to identify the bottleneck for improving process operability.

Process structural problems should be best tackled at the process synthesis level. However, very little has been reported on process synthesis techniques by which economics and controllability can be traded off in an intelligent manner (Morari, 1992). Design-based integration approaches are basically: (i) process unit-based rather than overall flowsheet-based, (ii) detailed design-based rather than conceptual design-based,

and (iii) ad-hoc rather than systematic. Needless to say, once an integrated process is designed, enhancement of controllability through performing detailed design of specific units is functionally very limited, if not impossible. Luyben and Floudas (1994a, b) proposed a systematic procedure for analyzing the interactions of PD&C at the process synthesis stage by incorporating both steady state economic and open loop controllability measures. The procedure was successfully applied to the synthesis of a binary distillation column system and a system consisting of an isothermal reactor followed by a distillation column with a recycle. Their work demonstrates significant progress in incorporating controllability into early stages of process design.

Resorting to artificial intelligence techniques, Huang and Fan (1992, 1994) developed a unique strategy for process controllability analysis during the process synthesis phase. The approach can be used to identify and quantify process structural related DP based on knowledge-based reasoning. They classified disturbances into three degrees of severity, control requirements into three levels of precision, and propagation into four patterns. A measure of structural controllability for a developed process was then given as an index. This methodology has been successfully employed to design cost-effective and highly controllable process systems at the earliest stage of process synthesis (Huang and Fan, 1995; Huang and Edgar, 1995).

In principle, as process synthesis is to develop a flowsheet based on known design data, there must exist various opportunities for enhancing process controllability and rejecting undesirable DP to the maximum extent. It is particularly important to identify and grasp these opportunities. Apparently, a clear need for an active integration of PD&C is to conduct fundamental research on advancing process synthesis-based integration.

1.2 Objective and Significance

The objective of this research is to develop a process synthesis-based methodology for effective integration of PD&C. The methodology will be for synthesizing highly structurally controllable, cost-effective, and environmentally benign processes. Here, structural controllability is referred to structural disturbance rejection. Unlike existing approaches, the process synthesis-based integration described in this dissertation is for the development of complex networks rather than relatively simple processes. The methodology will feature the following characteristics:

Earliest integration of process design and control. As illustrated in Fig. 1.1, the integration of PD&C can be conducted in three phases of overall process engineering activities (Huang and Fan, 1992): (i) the process synthesis phase aiming at “inventing” process flowsheet, (ii) the process analysis phase focusing on the screening of process alternatives, and (iii) the control system synthesis phase centering on control system structures for a given process. Generally, the later the integration, the more the available process information and the easier the integration, since it is closer to process operation and thus operational issues can be more clearly and precisely addressed. However, later integration is much less effective in solving process structural problems. Unlike practicing integration in phase (ii) and (iii), this research project aims at the earliest integration for a complex process in phase (i). More clearly, process synthesis-based integration will be initiated at the pre-analysis stage, implemented at the structure invention stage, and enhanced at the structure evolution stage of process synthesis. This kind of integration should have the best chance to eliminate structure-related operational problems from the root; thereby greatly facilitating integration in the later phases.

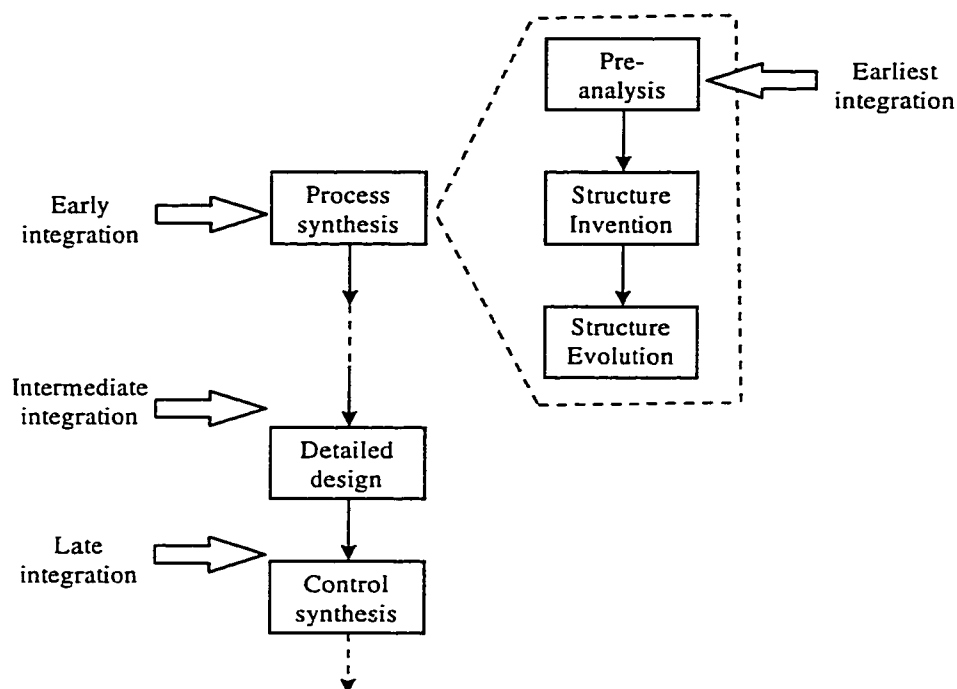


Figure 1.1. Possible ways of integrating process design and control.

Systematic rather than ad-hoc. In this methodology, a process unit operation will be generalized as a type of “processed” information flow, and structural deficiency in a process is generalized as improper DP through a heavy interaction process. To implement the integration of PD&C at a system level, each process unit will be treated as one of DP distributors in the process system. This means that the severity of DP can be detected by identifying major distributed patterns of DP through downstream paths in the plant. Thus, any uncontrollable situation can be improved by modifying improper DP pathways in a systematic manner. Moreover, the integration procedure will be modular-based, so that eventually it can be easily expanded to the design of any type of process system. This ensures that the methodology is generic rather than problem-specific.

Fundamental model-based. Effective structural disturbance rejection, especially

cleaning and rinsing information. Currently, most of research activities in this field are mainly focusing on the process development. To effectively reduce fresh water consumption and wastewater generation in manufacturing plants, a structure-based mathematical approach is derived to design an optimal WWRN. The research activities include the development of (i) a superstructure representation of a WWRN, (ii) a system model characterizing the superstructure, and (iii) an optimization strategy to determine optimal water flow patterns and water flow rates. The significance of this research will be demonstrated by effectively solving practical industrial example problems to reduce wastewater generation in electroplating plants and papermaking processes.

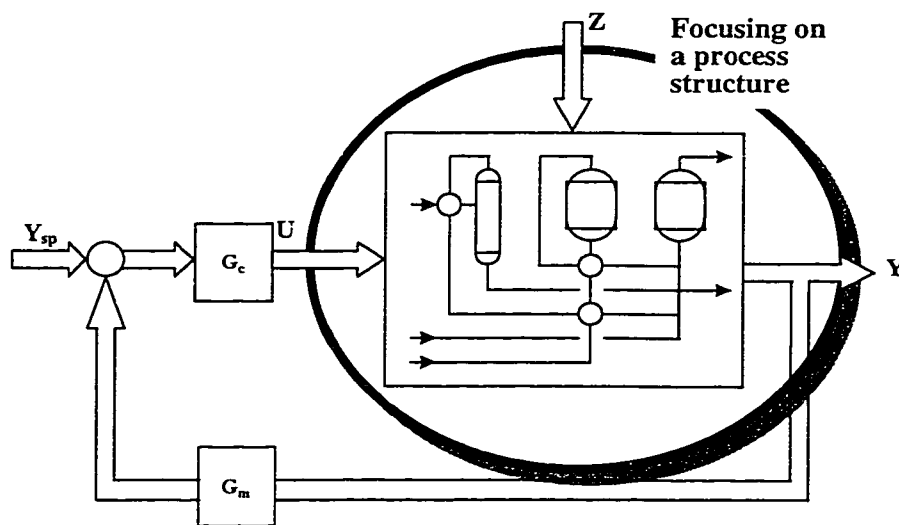


Figure 1.2. Process structure-focused integration of process design and control.

CHAPTER 2

DEVELOPMENT OF DISTURBANCE PROPAGATION MODELS FOR HEAT EXCHANGER NETWORKS

2.1 Introduction

The design of heat exchanger networks (HEN's) has been widely practiced in industries for decades to drastically reduce energy consumption. Many techniques have been proposed to synthesize HEN's featuring maximum energy recovery and minimum costs (Linnhoff and Flower, 1978a, b; Linnhoff and Hindmarsh, 1983; Cerda and Westerberg, 1983; Papoulias and Grossmann, 1983). Their methodologies have been successfully applied to the synthesis of many industrial HEN's for energy savings.

The introduction of a HEN into an integrated process plant always introduces various interconnections among process units. These interconnections create numerous downstream paths in the plant. If disturbances are present and enter the process, the disturbances propagating through the downstream paths may lead to unstable process operations (Linnhoff and Kotjabasakis, 1986). If disturbance propagation (DP) is very severe, the process will be extremely difficult to operate, or even uncontrollable regardless of advances of control techniques (Yang *et al.*, 1996). It is very important, therefore, that DP be early detected and completely evaluated.

During the last two decades, great progress has been made in identifying DP and rejecting disturbances during control system design (McLane and Davison, 1970; Commault *et al.*, 1984, 1991; Dion *et al.*, 1994). The models are applicable only to linear, but not to nonlinear, systems. A premise of using their models is that the process

structure is fixed and not to be changed. These models are not applicable to the enhancement of process controllability through process synthesis.

Probably, the earliest work on DP analysis for process synthesis was pioneered by Kotjabasakis and Linnhoff (1986). They introduced a procedure for considering flexibility right at the design stage and established a trade-off between flexibility and total cost of a heat exchanger network. Their procedure makes extensive use of what they termed sensitivity tables; thus, it is inefficient to the analysis of a complex HEN. The procedure was later improved by Ratnam and Patwardhan (1991) who adopted Kern's (1950) well known linear heat exchanger model. The basic idea of their model is that for any new operating condition considered, all temperatures in the network should be computed. That is, the system matrices in their model must be re-calculated for each new process operating condition, even if a single change of an operating variable. Thus, the model is still computationally inefficient. Moreover, the model does not provide *explicit* relationship between a set of disturbances and a set of target responses of temperature fluctuations. It is very difficult, therefore, to trace any piece of specific DP. This makes the analysis and improvement of a process very difficult. Furthermore, their model is for flexibility rather than controllability.

More recently, Li *et al.* (1994) developed linear equations for modeling DP in a HEN. Their model is also for process flexibility analysis. Li and co-workers introduced an average temperature difference to approximate logarithmic mean temperature difference, and derived approximate linear relationships between source disturbances and target temperature fluctuations. Unfortunately, their model completely ignores the cross effect of the disturbances of temperatures and those of heat capacity flowrates. This leads

to considerable computational errors when both types of disturbances exist. In addition, their model relies on the simulation of a given HEN structure when flowrate variations are considered. Through simulation, piecewise linearization for each temperature concerned can be obtained. This is very cumbersome when a number of process alternatives are to be analyzed.

Different from the aforementioned models for process flexibility analysis, the approach developed by Huang and Fan (1992) is for process controllability analysis during process synthesis phase. The approach can be used to identify and quantify DP in a process by means of artificial intelligence techniques. This methodology has been used to design highly controllable HEN's, mass exchanger networks, and work exchanger networks (Huang and Fan, 1994, 1996; Huang and Edgar, 1995). The quantification of DP in the methodology is based on approximate reasoning. They classified disturbances into three degrees of severity, control requirements into three levels of precision, and propagation into four patterns. These classifications may introduce noticeable errors for some cases and the solutions may not be preferable when more precise process evaluation is needed (Sabharwal *et al.*, 1995; Yang and Huang, 1996).

In this chapter, a simplified system model is introduced for evaluating quickly and precisely DP in a HEN. The model is developed for the analysis of controllability, rather than flexibility, during the process design stage. It is compared with rigorous models to conclude its applicability. The efficacy of using the model is demonstrated by solving practical industrial problems.

2.1 Motivation

In an integrated process plant, HEN's are always adopted to recover energy. The introduction of the HEN's to the plant usually makes the plant more interconnected. Improper interconnections, allowing various undesirable DP, may cause process structural problems.

Industrial example. An integrated process is illustrated in Fig. 2.1. This process contains many DP paths. As an example, feed stream A (stream H_1) and the bottom stream of distillation column D_2 (stream H_2) experience severe disturbances. These disturbances propagate through heat exchangers E_1 and E_2 to disturb the temperature of stream C_1 that enters reactor R_1 . The DP paths can be readily identified if the HEN is depicted in a grid diagram as shown in Fig. 2.2. The dotted lines in this figure, for example, represent a source disturbance from feed stream A propagating to affect the output temperatures of streams H_1 , C_1 , and H_2 , and the intermediate temperature of stream C_2 . In this network, the temperature fluctuations at locations A , B , C , D , E , and F should be examined in order to identify the stability of the output temperatures of all streams and, further, to reduce or even eliminate operational problems during process design.

Since disturbances can influence the stability of unit operations in the process, it is highly desirable that a simple and predictable DP model need be developed to precisely evaluate DP in a process. The reasons why we focus on the development of a simplified DP model, rather than of a rigorous one, are as follows.

(i) In the process synthesis stage, detailed disturbance information is always unavailable; this information is accessible only after a designed process is operated. It is

unnecessary for us to derive the rigorous DP model for this purpose.

(ii) Rigorous DP models are usually complicated and highly non-linear. This makes the adoption of a rigorous model into process analysis and, eventually, synthesis very difficult.

To facilitate process analysis and synthesis, a system model should (i) be as simple as possible when the model prediction is satisfactory with certain precision, and (ii) maintain explicit physical meaning in terms of model variables and parameters. To achieve this, the first-principles should be the basis in model development.

2.3 Fundamental Models

For a heat exchanger operated in a given normal operating condition, the severity of DP from one stream to another is largely dominated by the fluctuation of source temperature and that of heat capacity flow rate of each stream (δT_h^s , δT_c^s , δMc_{P_h} , and δMc_{P_c}). Note that these fluctuation data refer to the largest fluctuation ranges possibly occurring during process operation; they can be either positive or negative. A major concern of DP through the heat exchanger is the stability of the target temperature of each stream which is characterized by the largest deviations from the normal operating point; they are designated as δT_h^t and δT_c^t . A sketch of a heat exchanger and its grid diagram are shown in Fig. 2.3(a) and (b), respectively. For any heat exchanger, following energy balance and heat transfer equations at steady-state hold.

$$Q = Mc_{P_h} \Delta T_h = Mc_{P_c} \Delta T_c \quad (2.1)$$

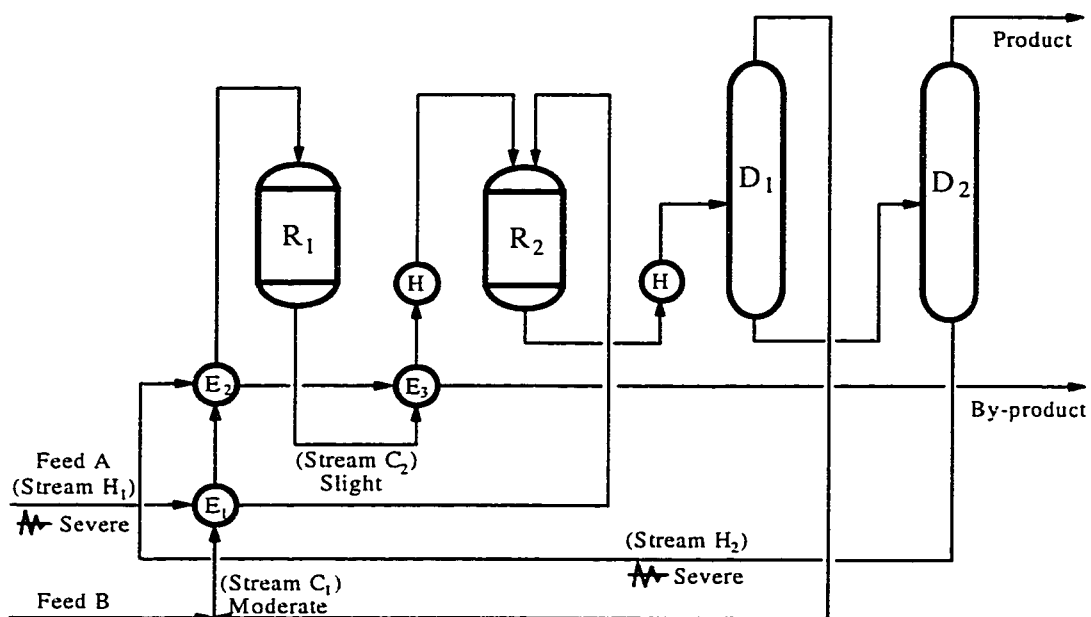


Figure 2.1. Flowsheet of an integrated plant with various DP.

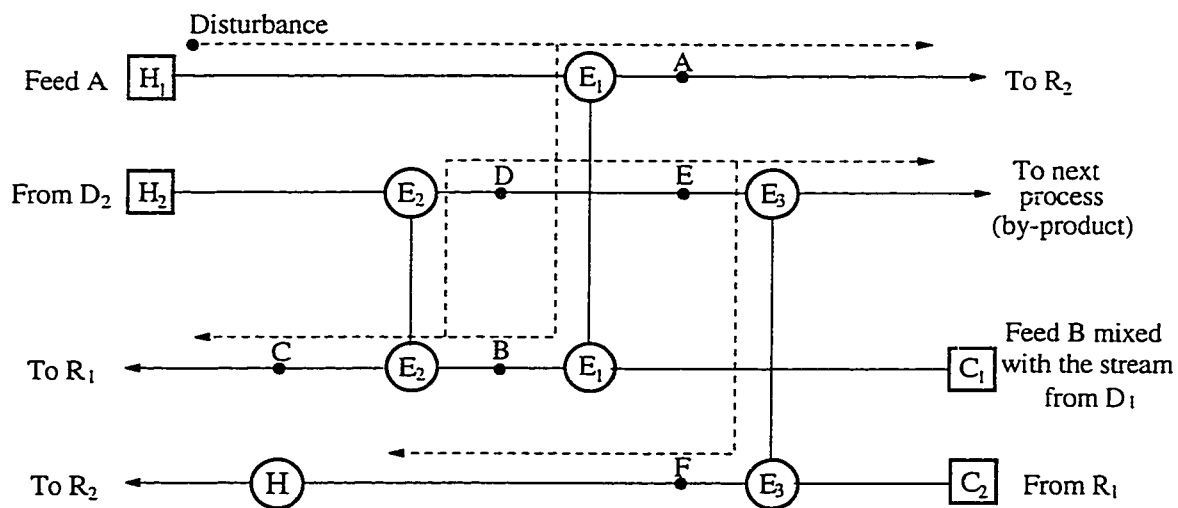


Figure 2.2. Grid diagram of the HEN in the integrated plant.

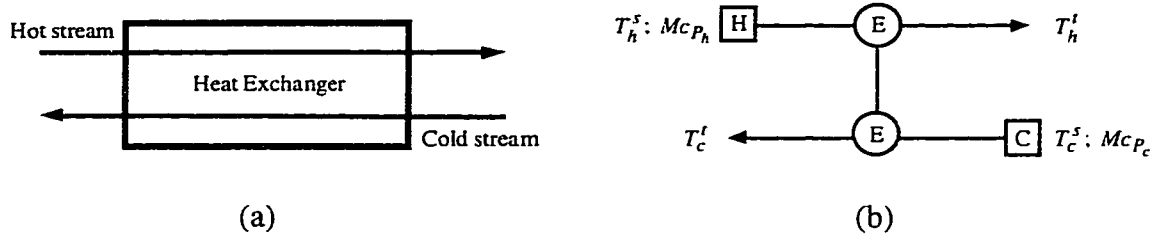


Figure 2.3. A sketch of a heat exchanger.

$$Q = UA \frac{\Delta T_{hc}^{st} - \Delta T_{hc}^{ts}}{\ln \frac{\Delta T_{hc}^{st}}{\Delta T_{hc}^{ts}}} \quad (2.2)$$

where

$$\Delta T_h = T_h^s - T_h^t \quad (2.3)$$

$$\Delta T_c = T_c^t - T_c^s \quad (2.4)$$

$$\Delta T_{hc}^{st} = T_h^s - T_c^t \quad (2.5)$$

$$\Delta T_{hc}^{ts} = T_h^t - T_c^s \quad (2.6)$$

Note that ΔT_h and ΔT_c are, respectively, the temperature change of a hot stream and that of a cold stream; ΔT_{hc}^{st} and ΔT_{hc}^{ts} are respectively the temperature difference at the hot end and that at the cold end of a heat exchanger.

Equations (2.1) and (2.2) can be extended when disturbances are taken into account. This gives their corresponding rigorous DP models below.

$$Q + \delta Q = (Mc_{p_h} + \delta Mc_{p_h})[\Delta T_h + (\delta T_h^s - \delta T_h^t)]$$

$$Q = UA \frac{\Delta T_{hc}^{st} + \Delta T_{hc}^{ts}}{2} \quad (2.9)$$

$$Q + \delta Q = UA \frac{(\Delta T_{hc}^{st} + \delta T_h^s - \delta T_c^t) + (\Delta T_{hc}^{ts} + \delta T_h^t - \delta T_c^s)}{2} \quad (2.10)$$

Simplified model. A manipulation of Eqs. (2.1), (2.7), (2.9), and (2.10) can result in a formula relating target temperature disturbances to the disturbances of source temperatures and those of heat capacity flowrates. In derivation, we adopt the following commonly used additional assumptions: (i) no phase change occurs in any heat exchanger, (ii) changes in stream pressure drops are not serious, and (iii) the second order terms, such as the product of disturbances ($\delta \cdot \delta$), are neglected.

The first two assumptions imply constant heat capacity flowrate for each process stream and heat transfer coefficient for each heat exchanger. The third assumption is mainly used for the linearization of the unit-based model; this is safe when no significant variations exist in temperature and heat capacity flowrate disturbances. A more detailed derivation can be found in Appendix A. The manipulation generates:

$$\delta T^t = A \delta T^s + B \delta Mc_P \quad (2.11)$$

where

$$\delta T^t = \begin{pmatrix} \delta T_h^t & \delta T_c^t \end{pmatrix}^T \quad (2.12)$$

$$\delta T^s = \begin{pmatrix} \delta T_h^s & \delta T_c^s \end{pmatrix}^T \quad (2.13)$$

$$\delta Mc_P = \begin{pmatrix} \delta Mc_{P_h} & \delta Mc_{P_c} \end{pmatrix}^T \quad (2.14)$$

$$\mathbf{A} = \begin{pmatrix} a_{11} & a_{12} \\ a_{21} & a_{22} \end{pmatrix} = \begin{pmatrix} 1 - \frac{\Delta T_h}{\Delta T_{hc}^{ss}} & \frac{\Delta T_h}{\Delta T_{hc}^{ss}} \\ \frac{\Delta T_c}{\Delta T_{hc}^{ss}} & 1 - \frac{\Delta T_c}{\Delta T_{hc}^{ss}} \end{pmatrix} \quad (2.15)$$

$$\mathbf{B} = \begin{pmatrix} b_{11} & b_{12} \\ b_{21} & b_{22} \end{pmatrix} = \begin{pmatrix} \frac{\Delta T_h}{2McP_h} \left(2 - \frac{\Delta T_h}{\Delta T_{hc}^{ss}} \right) & -\frac{\Delta T_c \Delta T_h}{2McP_c \Delta T_{hc}^{ss}} \\ \frac{\Delta T_h \Delta T_c}{2McP_h \Delta T_{hc}^{ss}} & -\frac{\Delta T_c}{2McP_c} \left(2 - \frac{\Delta T_c}{\Delta T_{hc}^{ss}} \right) \end{pmatrix} \quad (2.16)$$

$$\Delta T_{hc}^{ss} = T_h^s - T_c^s \quad (2.17)$$

Since both ΔT_h and ΔT_c are smaller than ΔT_{hc}^{ss} , all elements in matrix \mathbf{A} must be positive and less than 1; they are correlated in the following way:

$$a_{11} = 1 - a_{12} \quad (2.18)$$

and

$$a_{22} = 1 - a_{21} \quad (2.19)$$

Alternatively, matrix \mathbf{A} can be written as:

$$\mathbf{A} = \begin{pmatrix} 1 - a_{12} & a_{12} \\ a_{21} & 1 - a_{21} \end{pmatrix} \quad (2.20)$$

Likewise, an alternative matrix of \mathbf{B} can be derived below:

$$\mathbf{B} = \begin{pmatrix} \alpha_h (2 - a_{12}) & -\alpha_c a_{12} \\ \alpha_h a_{21} & -\alpha_c (2 - a_{21}) \end{pmatrix} \quad (2.21)$$

where

$$\alpha_h = \frac{\Delta T_h}{2McP_h} \quad (2.22)$$

2.5 System Disturbance Propagation Model

Any heat exchanger performs as a disturbance distributor, which is quantified by Eq. (2.11). In a HEN, a single disturbance may propagate through a series of heat exchangers and affect the stability of many other streams. The development of a general system model can help calculate the fluctuation of the output temperature of each stream affected by any known disturbance. The unit-based model in Eq. (2.11) can form the basis in developing such a system model.

System model. A system model for characterizing all DP through a HEN can be developed in the following form.

$$\delta \underline{T}^t = \underline{A} \delta \underline{T}^s + \underline{B} \delta \underline{M} \underline{c} \underline{P} \quad (2.28)$$

where

$$\delta \underline{T}^t = \left(\delta T_{h_1}^t \quad \delta T_{h_2}^t \quad \cdots \quad \delta T_{h_{N_h}}^t \quad \delta T_{c_1}^t \quad \delta T_{c_2}^t \quad \cdots \quad \delta T_{c_{N_c}}^t \right)^T \quad (2.29)$$

$$\delta \underline{T}^s = \left(\delta T_{h_1}^s \quad \delta T_{h_2}^s \quad \cdots \quad \delta T_{h_{N_h}}^s \quad \delta T_{c_1}^s \quad \delta T_{c_2}^s \quad \cdots \quad \delta T_{c_{N_c}}^s \right)^T \quad (2.30)$$

$$\delta \underline{M} \underline{c} \underline{P} = \left(\delta M c_{P_{h_1}} \quad \delta M c_{P_{h_2}} \quad \cdots \quad \delta M c_{P_{h_{N_h}}} \quad \delta M c_{P_{c_1}} \quad \delta M c_{P_{c_2}} \quad \cdots \quad \delta M c_{P_{c_{N_c}}} \right)^T \quad (2.31)$$

System matrices \underline{A} and \underline{B} contain temperature-related and heat capacity flowrate-related system DP information, respectively. They can be obtained through the following procedure.

Determination of system matrices \underline{A} and \underline{B} . Assume that N_h hot streams and N_c

intermediate temperatures; $\delta \underline{M} \underline{c}_P^*$ contains $(2N_e - N_h - N_c)$ redundant heat capacity flowrates. Correspondingly, \underline{A}^* and \underline{B}^* contain extra information which is not of interest. To obtain Eq. (2.28) from Eq. (2.33), vectors $\delta \underline{T}^{*in}$ and $\delta \underline{T}^{*out}$ should be permuted to $\delta \underline{T}^{in}$ and $\delta \underline{T}^{out}$, respectively, in the following manner.

$$\begin{aligned} \delta \underline{T}^{in} &= \begin{pmatrix} \delta T_{h_1}^s & \cdots & \delta T_{h_{N_h}}^s & \delta T_{c_1}^s & \cdots & \delta T_{c_{N_c}}^s & \delta T_l^m & \cdots & \delta T_{2N_e - N_h - N_c}^m \end{pmatrix}^T \\ &= \begin{pmatrix} (\delta \underline{T}^s)^T & (\delta \underline{T}^m)^T \end{pmatrix}^T \end{aligned} \quad (2.39)$$

$$\begin{aligned} \delta \underline{T}^{out} &= \begin{pmatrix} \delta T_{h_1}^t & \cdots & \delta T_{h_{N_h}}^t & \delta T_{c_1}^t & \cdots & \delta T_{c_{N_c}}^t & \delta T_l^m & \cdots & \delta T_{2N_e - N_h - N_c}^m \end{pmatrix}^T \\ &= \begin{pmatrix} (\delta \underline{T}^t)^T & (\delta \underline{T}^m)^T \end{pmatrix}^T \end{aligned} \quad (2.40)$$

In $\delta \underline{M} \underline{c}_P^*$, all redundant heat capacity flowrates should be eliminated. This reduces $\delta \underline{M} \underline{c}_P^*$ to $\delta \underline{M} \underline{c}_P$. With these definitions, we can obtain:

$$\begin{pmatrix} \delta \underline{T}^t \\ \delta \underline{T}^m \end{pmatrix} = \begin{pmatrix} \underline{A}_{11} & \underline{A}_{12} \\ \underline{A}_{21} & \underline{A}_{22} \end{pmatrix} \begin{pmatrix} \delta \underline{T}^s \\ \delta \underline{T}^m \end{pmatrix} + \begin{pmatrix} \underline{B}_1 \\ \underline{B}_2 \end{pmatrix} \delta \underline{M} \underline{c}_P \quad (2.41)$$

where $\delta \underline{T}^s$, $\delta \underline{T}^t$, and $\delta \underline{M} \underline{c}_P$ are all of the dimension of $(N_h + N_c) \times I$; $\delta \underline{T}^m$ is of the dimension of $(2N_e - N_h - N_c) \times I$. The two equations can be written separately from the above equation:

$$\delta \underline{T}^t = \underline{A}_{11} \delta \underline{T}^s + \underline{A}_{12} \delta \underline{T}^m + \underline{B}_1 \delta \underline{M} \underline{c}_P \quad (2.42)$$

$$\delta \underline{T}^m = \underline{A}_{21} \delta \underline{T}^s + \underline{A}_{22} \delta \underline{T}^m + \underline{B}_2 \delta \underline{M} \underline{c}_P \quad (2.43)$$

From Eq. (2.43), we can have

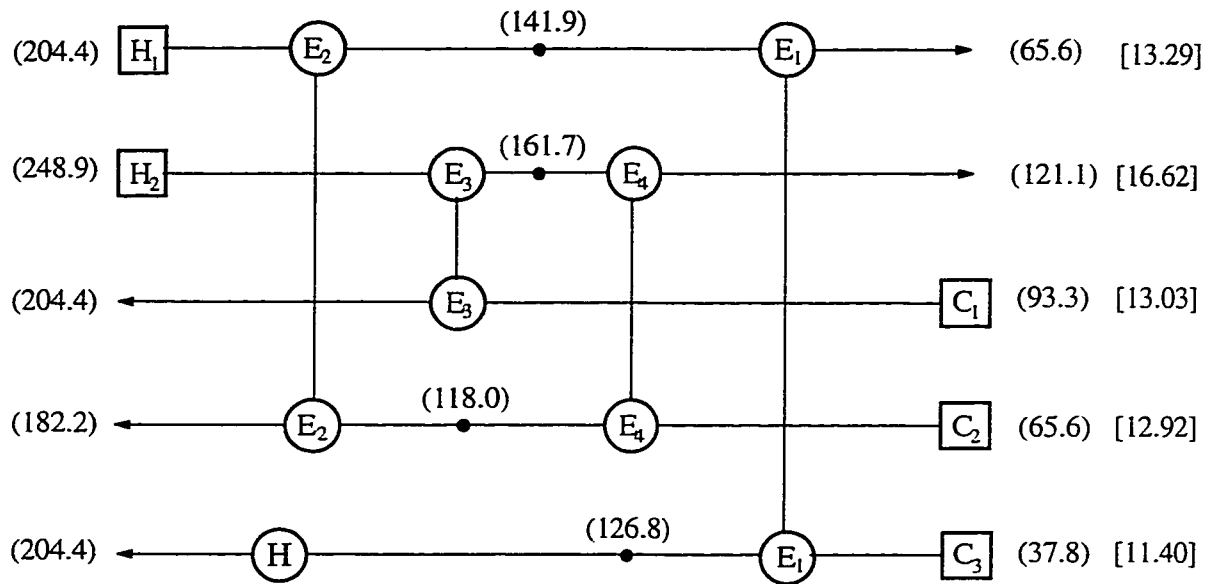
summarized in Table 2.2.

Table 2.1. Stream Data for the HSP15R Synthesis Problem

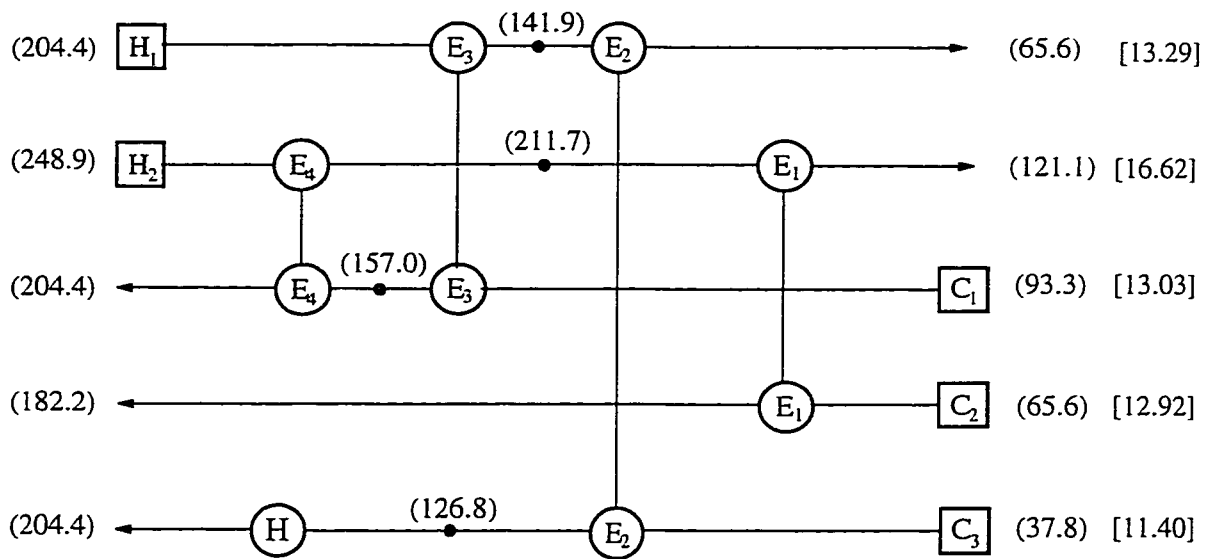
Stream No.	T^s (°C)	T^t (°C)	M_{CP} (kW/°C)	$\delta T^{s(+)}$ (°C)	$\delta T^{s(-)}$ (°C)	$\delta M_{CP}^{(+)}$ (kW/°C)	$\delta M_{CP}^{(-)}$ (kW/°C)	δT^t (°C)
H ₁	204.4	65.6	13.29	2	-2	0.4	-0.4	± 5.5
H ₂	248.9	121.1	16.62	4	-3	0.1	-0.2	± 3
C ₁	93.3	93.3	13.03	1	-0.6	0.05	-0.1	± 6
C ₂	65.6	65.6	12.92	2	-2.5	0.1	-0.05	± 7
C ₃	37.8	37.8	11.40	1	-3	0.3	-0.4	± 1

Table 2.2. Comparison of the Deviations of Stream Target Temperatures in Five Solution Alternatives for H5SP1R Synthesis Problem

Target Temp.	Control Required	Sol. A	Sol. B	Sol. C	Sol. D	Sol. E
δT_{h1}^t (C)	5.5	4.35/-5.60	4.11/-5.22	3.50/-4.71	3.50/-4.71	3.48/-3.94
δT_{h2}^t (C)	3	2.78/-3.20	3.14/-3.74	3.93/-4.22	3.28/-3.24	5.08-3.63
δT_{c1}^t (C)	6	3.88/-3.05	3.58/-2.82	3.88/-2.96	0/0	0/0
δT_{c2}^t (C)	7	3.04/-3.25	3.78/-3.91	3.70/-4.04	3.70/-4.04	8.24/-4.4
δT_{c3}^t (C)	1	0/0	0/0	0/0	7.14/-6.11	6.17/-3.99

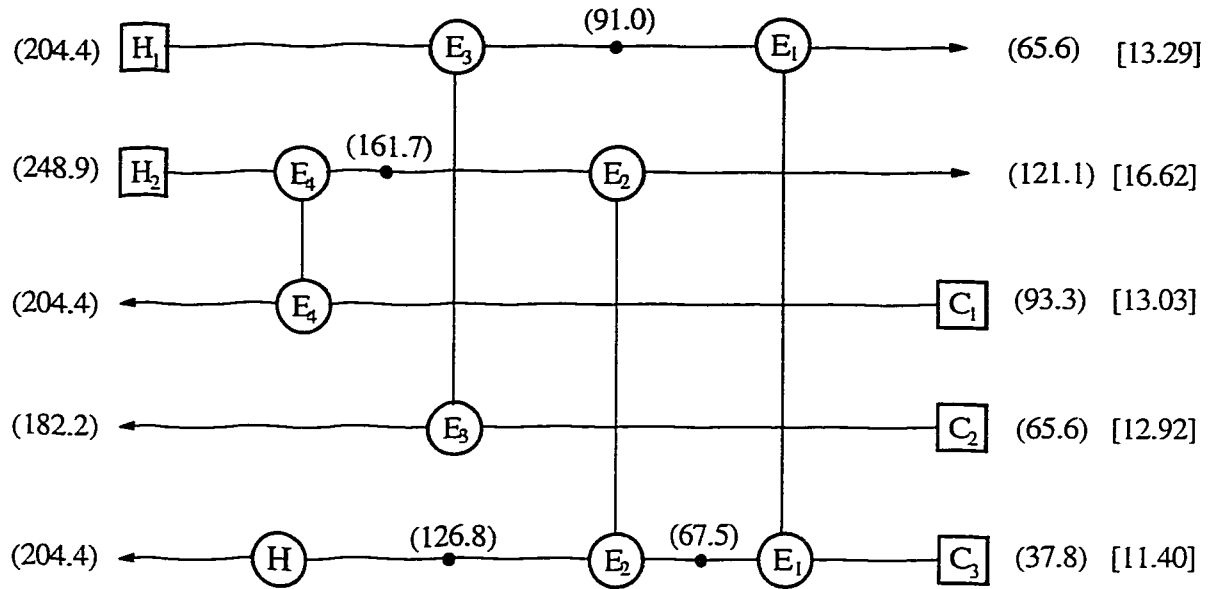


(a) Solution A

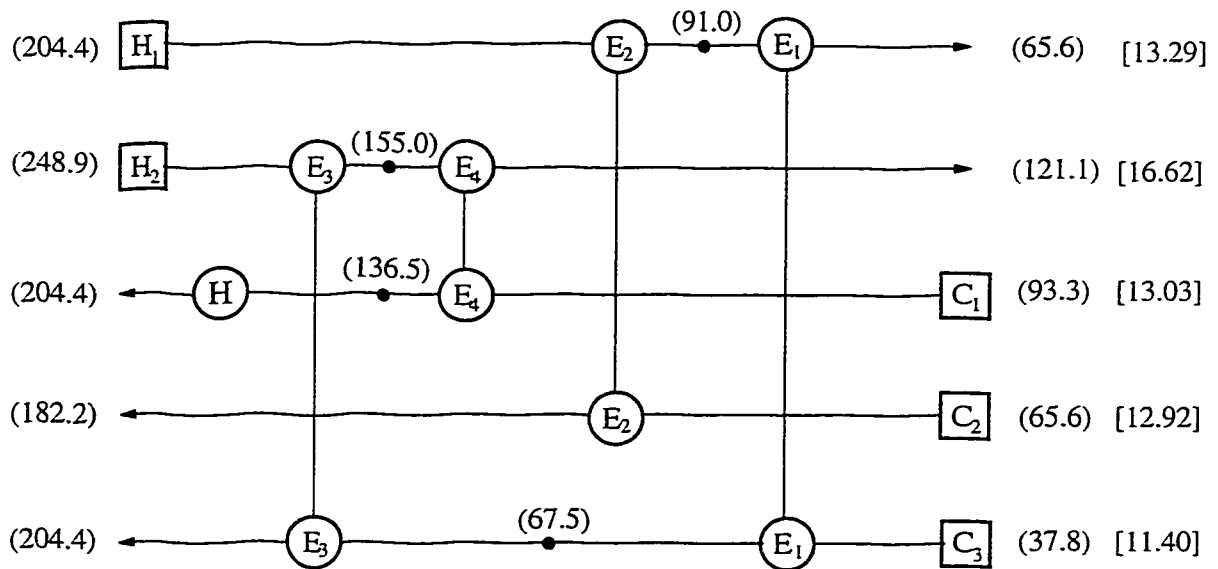


(b) Solution B

Figure 2.4. Grid diagrams of the five solutions of HEN problem H5SP1R.



(c) Solution C



(d) Solution D

Figure 2.4. Grid diagrams of the five solutions of HEN problem H5SP1R (cont'd).

$$\delta \underline{T}^s = \left(\delta T_{h_1}^s \quad \delta T_{h_2}^s \quad \delta T_{c_1}^s \quad \delta T_{c_2}^s \quad \delta T_{c_3}^s \right)^T \quad (2.47)$$

$$\delta \underline{M}_{cP} = \left(\delta M_{cP_{h_1}} \quad \delta M_{cP_{h_2}} \quad \delta M_{cP_{c_1}} \quad \delta M_{cP_{c_2}} \quad \delta M_{cP_{c_3}} \right)^T \quad (2.48)$$

$$\delta \underline{T}^t = \left(\delta T_{h_1}^t \quad \delta T_{h_2}^t \quad \delta T_{c_1}^t \quad \delta T_{c_2}^t \quad \delta T_{c_3}^t \right)^T \quad (2.49)$$

then the system matrices are:

$$\underline{A} = \begin{pmatrix} 0.0739 & 0.0463 & 0.0590 & 0.0878 & 0.7329 \\ 0 & 0.2539 & 0.3237 & 0.4225 & 0 \\ 0 & 0.7140 & 0.2860 & 0 & 0 \\ 0.7431 & 0.0616 & 0.0785 & 0.1168 & 0 \\ 0 & 0 & 0 & 0 & 0 \end{pmatrix} \quad (2.50)$$

$$\underline{B} = \begin{pmatrix} 4.4388 & 0.5260 & -0.2517 & -1.0498 & -2.8611 \\ 0 & 4.1079 & -1.3798 & -0.8567 & 0 \\ 0 & 1.8731 & -5.4825 & 0 & 0 \\ 1.7472 & 0.7002 & -0.3347 & -3.8809 & 0 \\ 0 & 0 & 0 & 0 & 0 \end{pmatrix} \quad (2.51)$$

Elements \underline{a}_{ij} in matrix \underline{A} and \underline{b}_{ij} in matrix \underline{B} represent the severity of the propagation from the inlet of stream i to the outlet of stream j . The larger the absolute value of an element, the more severe the DP. For instance, two zero elements in the second row of matrix \underline{A} mean that there exist no DP paths from streams H_1 to H_2 and from streams C_3 to H_2 . Structurally, the main contribution of DP to the outlet of stream H_2 is from stream C_2 , followed by that from streams C_1 and H_2 . It also shows that the disturbance at the inlet of stream H_1 is decayed by 92.6% when reaching its own outlet since the value of element a_{11} is very small. The last rows of matrices \underline{A} and \underline{B} contain only zero elements. This is due to a commonly adopted assumption that a heater can absorb all disturbances by adjusting steam flowrate through it. This means that the target

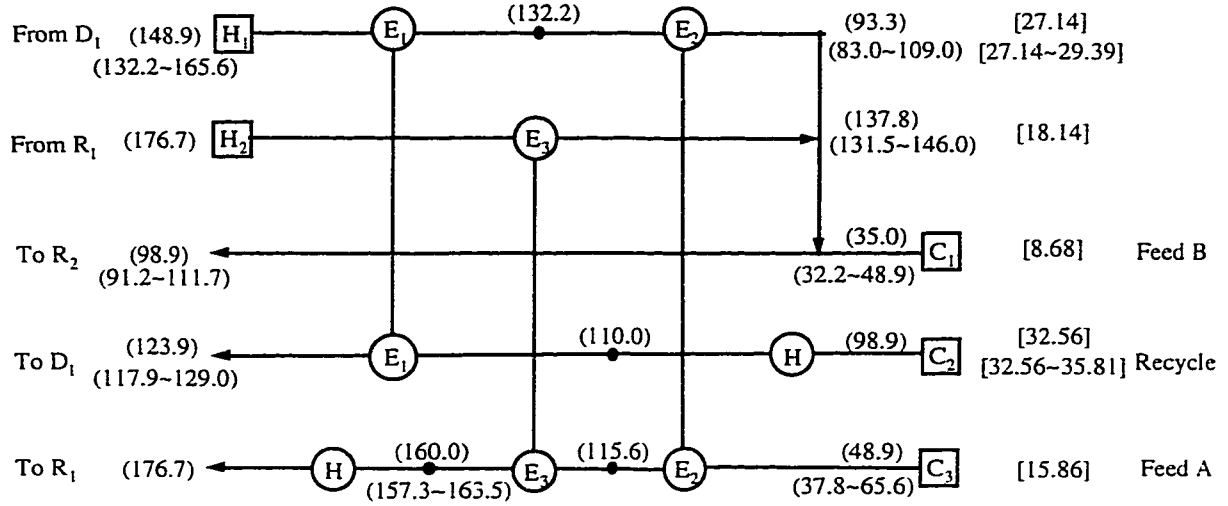
temperature of stream C_3 can be controlled very precisely.

As a comparison, Huang and Fan (1992) used the artificial intelligence-based distributed strategy to evaluate the structural controllability of all five alternatives. It turns out that solution A has the largest index value (0.958). By contrast, solutions B through E are of the index values of 0.917, 0.750, 0.083, and 0.083. This indicates that solution A is clearly the best. Solution B is much better than solution C . Solutions D and E are not acceptable.

While the evaluations by two different approaches demonstrate a good agreement in general, the simplified model can provide reliable and quantitative information of DP through a network which makes designers much more confident in process analysis. The model-based evaluation also suggests that solutions A , B , and C are all acceptable, although solution A is more preferable. Process designers should evaluate all three solutions when other design criteria are considered.

Improvement of a heat-integrated reaction-separation system supplied by the industrial partner M. W. Kellogg Company. The flowsheet of an industrial process is shown in Fig. 2.5. A recycle stream from other process is heated from 98.9°C to 123.9°C and fed to distillation column D_1 . Feed A is preheated in a series of heat exchangers and then enters reactor R_1 where a slight endothermic reaction takes place. The product stream of reactor R_1 and the column overhead stream, after cooling, are mixed with feed B . This mixture stream is fed to reactor R_2 in which catalyst is very sensitive to its operating temperature; its performance will be seriously degraded if the temperature is unstable and above 110°C. This requires that the feed stream temperature of reactor R_2 be strictly controlled between 96.1°C and 98.9°C. However, this process faces many

The grid diagram of the HEN is shown in Fig. 2.6. This process has the pinch point at 37.8°C. The minimum energy requirement is 2,022kW with minimum six heat transfer units. For this system, if we define the following disturbance vectors and control variable vector,



Key

- () : Temperature (°C)
- [] : Heat capacity flow rate (kW/°C)
- ~ : Fluctuation range

Figure 2.6. Grid diagram of the HEN for the heat-integrated reactor-separation process.

$$\delta T^s = \begin{pmatrix} \delta T_{h_1}^s & \delta T_{h_2}^s & \delta T_{c_2}^s & \delta T_{c_3}^s \end{pmatrix}^T \quad (2.52)$$

$$\delta M c_P = \begin{pmatrix} \delta M c_{P_{h_1}} & \delta M c_{P_{h_2}} & \delta M c_{P_{c_2}} & \delta M c_{P_{c_3}} \end{pmatrix}^T \quad (2.53)$$

$$\delta T^t = \begin{pmatrix} \delta T_{h_1}^t & \delta T_{h_2}^t & \delta T_{c_2}^t & \delta T_{c_3}^t \end{pmatrix}^T \quad (2.54)$$

then the system matrices are of the following values:

$$\underline{A} = \begin{pmatrix} 0.3042 & 0 & 0.2288 & 0.4670 \\ 0.2909 & 0.3633 & 0.2189 & 0.1279 \\ 0.3573 & 0 & 0.6427 & 0 \\ 0 & 0 & 0 & 0 \end{pmatrix} \quad (2.55)$$

$$\underline{B} = \begin{pmatrix} 1.3562 & 0 & -0.0488 & -0.9820 \\ 0.6117 & 1.4618 & -0.0467 & -2.4967 \\ 0.1099 & 0 & -0.3506 & 0 \\ 0 & 0 & 0 & 0 \end{pmatrix} \quad (2.56)$$

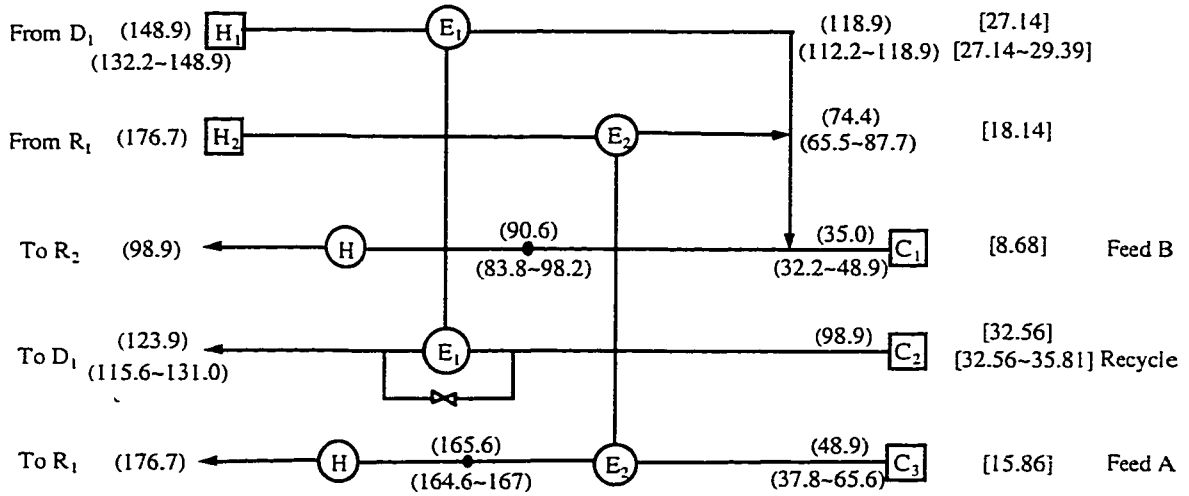
Note that in matrices \underline{A} and \underline{B} , the last row contains only zero elements, since stream C_3 is eventually heated by a heater which is capable of absorbing all disturbances. Also note that stream C_1 is not included in all vectors and matrices, since this stream is not involved in heat exchange with any stream through a heat exchanger. Instead, this stream is mixed with streams H_1 and H_2 ; the mixed stream enters reactor R_2 with the temperature fluctuation from 91.4°C to 111.7°C. This fluctuation is far beyond the tolerable range (96.1°C to 98.9°C). Thus the system cannot be operated regardless of control techniques used.

Figure 2.7 shows a modified HEN obtained by the extended distributed strategy (Yang and Huang, 1996). The derivation of this solution is out of the scope of this chapter. The modified HEN contains a by-pass and a loop design for improving system performance. In fact, when a by-pass is considered, the system model only needs to include an energy balance equation describing the relationship of the temperature disturbances before and after mixing. Since the equation gives linearity in temperature disturbances and introduces one more unknown variable, the derived form of the system model in Eq. (2.28) remains unchanged. A complete process flowsheet embedding this

HEN is depicted in Fig. 2.8, with its system matrices \underline{A} and \underline{B} listed below.

$$\underline{A} = \begin{pmatrix} 0.4 & 0 & 0.6 & 0 \\ 0 & 0.1995 & 0 & 0.8005 \\ 0.5 & 0 & 0.5 & 0 \\ 0 & 0 & 0 & 0 \end{pmatrix} \quad (2.57)$$

$$\underline{B} = \begin{pmatrix} 0.7738 & 0 & -0.2303 & 0 \\ 0 & 3.3824 & 0 & -2.9450 \\ 0.2763 & 0 & -0.5759 & 0 \\ 0 & 0 & 0 & 0 \end{pmatrix} \quad (2.58)$$



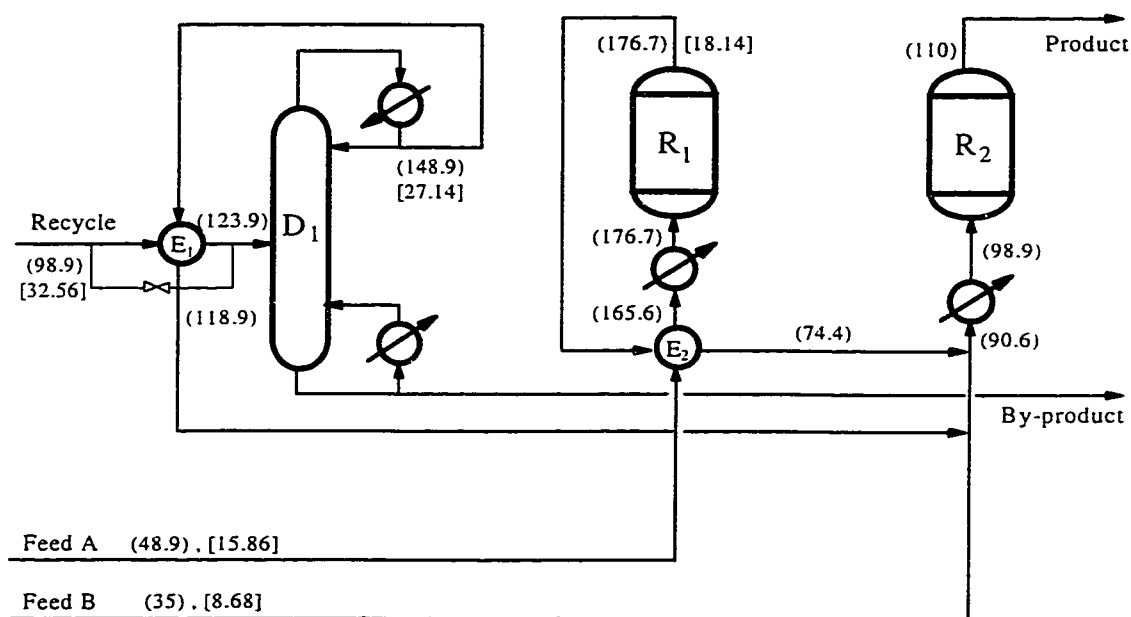
Key

- () : Temperature (°C)
- [] : Heat capacity flow rate (kW/°C)
- ~ : Fluctuation range

Figure 2.7. Grid diagram of a modified HEN for the heat-integrated reactor-separation process.

In this modified system, the temperature of the stream mixing H_1 , H_2 , and C_1 before entering a heater is between 83.8°C and 98.2°C. Through the heater, the stream

entering to reactor R_2 can be easily controlled at 98.9°C . Also note that the target temperature of stream C_2 fluctuates less severely than the original design; the temperature of stream C_3 entering a heater can be operated between 164.6°C and 167°C which shows a smaller range than that in the original design. With these changes, the original operational problems are eliminated structurally. Moreover, the modified system requires one heat exchanger less than the original system. Hence, the capital cost through process improvement can be reduced while energy cost still remains the same.



Key

() : Temperature ($^\circ\text{C}$)

[] : Heat capacity flowrate ($\text{kW}/^\circ\text{C}$)

Figure 2.8. Flowsheet of a modified heat-integrated reactor-separation process.

Discussion. While the model applications in the above cases have shown excellent agreement with the results by rigorous models based on Eqs. (2.7) and (2.8),

this may not be true for some other applications. This is due to the replacement of a logarithmic mean term by an arithmetic mean term in model development. The resultant unit-based model in Eq. (2.11) shows that the fluctuations of the target temperatures are quantified in two parts:

(a) The fluctuations due to source temperature disturbances quantified as $A\delta T^s$.

This quantification is proven to be rigorous and provides no errors regardless of the severity of any single source temperature disturbance or any combination of source temperature changes over any range.

(b) The fluctuations caused by heat capacity flowrate disturbances quantified as $B\delta Mc_P$. The prediction based on this quantification may be erroneous when δMc_{P_h} and δMc_{P_c} are significant ($\geq 20\%$ of their nominal values). To obtain a precise evaluation, we suggest the replacement of $B\delta Mc_P$ by $C_c B D_c \delta Mc_P$, where C_c and D_c are of the following forms:

$$C_c = \begin{pmatrix} f_1(a_{12}, a_{21}) & 0 \\ 0 & f_2(a_{12}, a_{21}) \end{pmatrix} \quad (2.58)$$

$$D_c = \begin{pmatrix} g_1(Mc_{P_h}, \delta Mc_{P_h}) & 0 \\ 0 & g_2(Mc_{P_c}, \delta Mc_{P_c}) \end{pmatrix} \quad (2.59)$$

The two matrices may contain non-linear forms, depending on the precision expected. With these corrections, prediction errors by the system model can be reduced to the range of 10%. Certainly, this error range is acceptable for conceptual design.

The developed model is for the analysis on DP during the first and conceptual phase of process design, i.e.; process synthesis. Thus, more practical issues, such as

design parameters of any piece of equipment and energy storage effects, are not considered here. These issues, however, must be addressed if the model is used during detailed process design and system optimization stages.

CHAPTER 3

SYNTHEIS OF COST-EFFECTIVE AND CONTROLLABLE HEAT EXCHANGER NETWORKS

3.1 Introduction

Process integration has been widely practiced in manufacturing industries for reducing cost, saving energy, and minimizing waste. As process plants become more and more integrated, process operational problems could be encountered if process structures were designed improperly. These potential problems are, in general, generated due to the lack of consideration of process operability during the process design stage (McAvoy, 1987; Sheffield, 1992; Elliott and Luyben, 1995). Traditional process design is solely focused on minimizing capital and operating costs. Process operational issues, especially controllability, are not taken into account until the design of a process control system.

Linnhoff and Kotjabasakis (1986) introduced “sensitivity tables” for analyzing different types of disturbances through process “downstream path” potentially to influence operations in a HEN. The trade-off between operability and economics are then made to identify an optimal network structure. Their approaches are particularly applicable to the analysis of an existing network process.

Different from process analysis approach, various efforts have been made to extend strict structure-based mathematical approach by incorporating flexibility and controllability requirements within the design of HENs (Floudas and Grossmann, 1986; Georgiou and Floudas, 1990; Galli and Cerda, 1991; Papalexandri and Pistikopoulos, 1994a, b). They proposed a special stream superstructure to include any configuration of

parallel, series, and bypass HENs. By taking structural controllability criteria into account, a mixed-integer nonlinear programming model is developed for minimizing annualized cost and identifying a controllable network structure simultaneously. Due to numerous process uncertainties involved in developing a process structure, it usually makes the synthesis problem very difficult to solve.

Huang and Fan (1992) introduced a knowledge-based engineering approach to synthesize cost-effective and highly structurally controllable HEN's at the earliest stage of process synthesis. They quantify disturbance propagation (DP) through a process and relate disturbances and controlled variables by means of artificial intelligence techniques. The resultant networks are ranked by the values of a structural controllability index. Due to approximate reasoning, this approach may introduce noticeable errors in quantifying DP, which may lead to excluding preferable solutions when more precise process evaluation is performed.

In this chapter, a synthesis strategy aiming at maximum disturbance rejection is introduced. By incorporating DP models derived in chapter 2, a synthesis procedure is then developed to design cost-effective and highly controllable HEN's. A synthesis problem is presented to illustrate the overall synthesis steps.

3.2 Integration Strategy for Disturbance Rejection

From the point of view of process control, perfect disturbance rejection ($Y = 0$) requires the control action $U = -G_p^+ G_d Z$ (Fig. 3.1(a)). Usually, such control does not exist (e.g., because of actuation saturation), or is not desirable due to energy concerns. A

more realistic expectation is near-perfect disturbance rejection, i.e., to keep $\|Y\|$ as close to zero as possible while $\|U\|$ is as small as possible. This is equivalent to the synthesis of a process with maximum disturbance rejection.

3.2.1 Basic strategy

Under usual constraints on capital and operating costs, a perfect disturbance rejection through process synthesis is usually unreachable (Huang and Fan, 1992; Yang *et al.*, 1996). Disturbances must propagate through “downstream paths” in a process (Kotjabasakis and Linnhoff, 1986). If a severe disturbance propagates to an output stream that should be controlled strictly, then this propagation is always intolerable. If many such situations occur, the process can be uncontrollable. On the other hand, it is also completely acceptable if a stream that need be strictly controlled is influenced by mild or negligible disturbances from somewhere else. Consequently, this analysis suggests optimally guiding DP during process synthesis.

Figure 3.1(b) illustrates the basic idea of designing optimal DP pathways. Two groups of disturbances are considered: significant disturbances (Z_1) and negligible ones (Z_2). Likewise, the output variables can also be divided into two groups: those requiring less strict control (Y_1), and those to be controlled precisely (Y_2). Thus, general disturbance rejection strategies can be:

(i) To prevent the propagation of Z_1 to Y_2 as much as possible. This means the generation of the fewest DP paths between them. If such a DP path is not preventable, the path should be as long as possible; a longer path usually provides more effective

minimum at steady state. Obviously, this kind of design will greatly simplify the design of a control system for maximum disturbance rejection.

3.2.2 Disturbance allocation

In “designing” disturbance pathways, we need to know how the placement of each unit affects DP. This can be exploited by analyzing unit-based DP using Eqs. (2.11) through (2.17) derived in chapter 2, especially Eqs. (2.15) and (2.16) for DP matrices A and B . In the following, some specific cases are investigated to reveal possible changes of temperature or heat capacity flow rate for disturbance allocation.

Case 1. Figure 3.2 (a) depicts a T - H diagram of a heat exchanger process with large driving force of heat transfer and large mass flow rates in both process streams. In this case, the temperature difference in the hot stream (ΔT_h) and that in the cold stream (ΔT_c) are, relatively, very small compared with their source temperature difference (ΔT_{hc}^{ss}). Thus, the ratios, $\Delta T_h / \Delta T_{hc}^{ss}$ and $\Delta T_c / \Delta T_{hc}^{ss}$, are nearly negligible. Thus, DP matrices A and B in Eqs. (2.15) and (2.16) can be approximated below.

$$A = \begin{pmatrix} 1 & 0 \\ 0 & 1 \end{pmatrix} \quad (3.1)$$

$$B = 0 \quad (3.2)$$

This indicates that only temperature disturbances propagate through the stream itself. As illustrated in Fig. 3.2 (b), there are no disturbance interactions between the hot and cold streams.

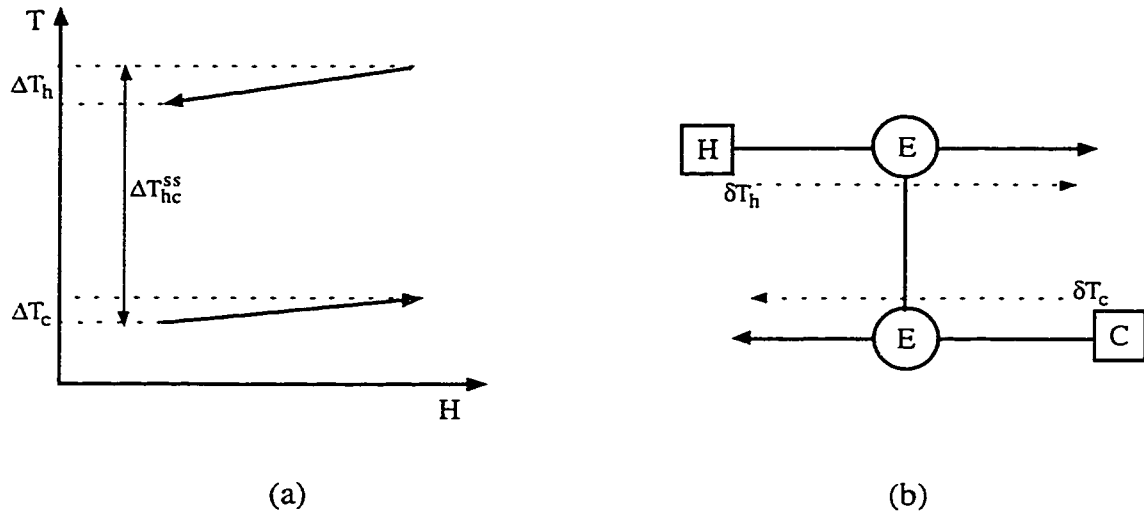


Figure 3.2. Disturbance pathways with large driving force of heat transfer and large heat capacity flow rates in both process streams.

Case 2. In this case, the driving force of heat transfer and the mass flow rates in both process streams are very small. As shown in Fig. 3.3 (a), the ratios, $\Delta T_h / \Delta T_{hc}^{ss}$ and $\Delta T_c / \Delta T_{hc}^{ss}$, nearly equal to one. After normalization, DP matrices A and B can be approximated below.

$$A = \begin{pmatrix} 0 & 1 \\ 1 & 0 \end{pmatrix} \quad (3.3)$$

$$B = \begin{pmatrix} 0.5 & 0.5 \\ 0.5 & 0.5 \end{pmatrix} \quad (3.4)$$

Matrix B in Eq. (3.4) indicates that heat capacity flow rate disturbances are quite difficult to be allocated due to severe interactions between both streams. As depicted in Fig. 3.3 (b), dotted lines and dotted dash lines show the disturbance pathways of temperatures and heat capacity flow rates, respectively.

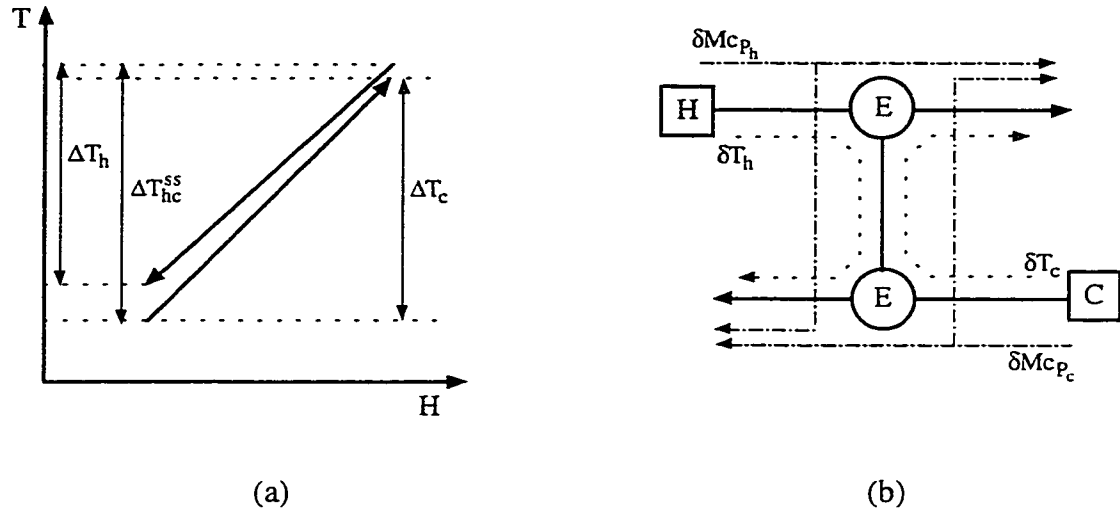


Figure 3.3. Disturbance pathways with small driving force of heat transfer and small heat capacity flow rates in both process streams.

Case 3. Different from Cases 1 and 2, the heat capacity flow rates in both hot and cold streams are significantly different. As shown in Fig. 3.4 (a), ratio $\Delta T_h / \Delta T_{hc}^{ss}$ almost approaches to zero while ratio $\Delta T_c / \Delta T_{hc}^{ss}$ closes to one. Thus, the normalized matrices **A** and **B** can be approximated as follows.

$$\mathbf{A} = \begin{pmatrix} 1 & 0 \\ 1 & 0 \end{pmatrix} \quad (3.5)$$

$$\mathbf{B} = \begin{pmatrix} 0 & 0 \\ 0 & 1 \end{pmatrix} \quad (3.6)$$

Figure 3.4 (b) shows the disturbance pathways of temperature and heat capacity flow rate. From this analysis, we conclude that cold stream splitting can reduce the effect of disturbance influence when its source temperature fluctuation is severe.

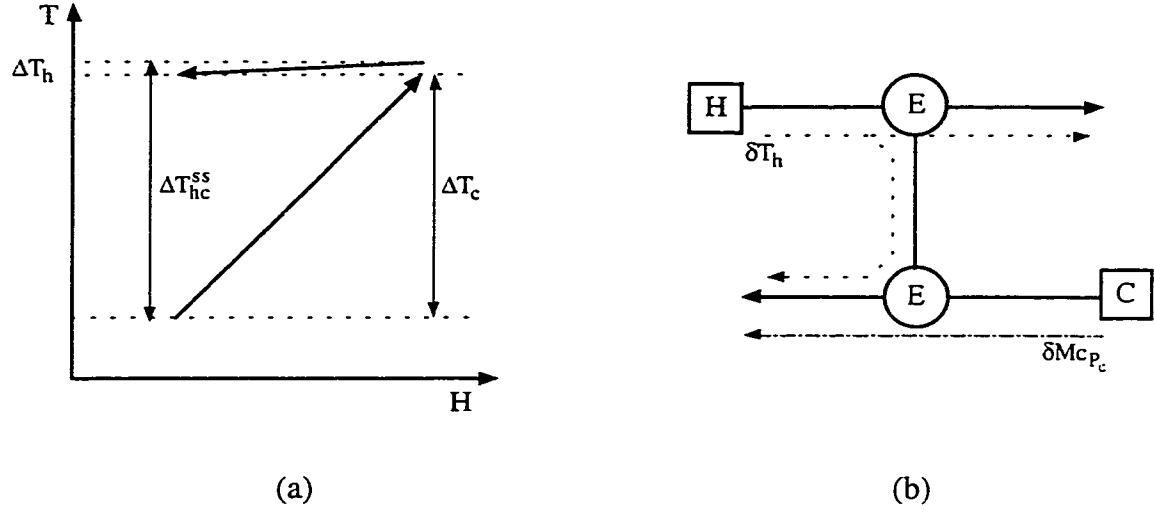


Figure 3.4. Disturbance pathways with large mass flow rate in the hot stream and small one in the cold stream.

Case 4. Figure 3.5 (a) shows a significant difference of heat capacity flow rates in both hot and cold streams. In this case, ratio $\Delta T_h / \Delta T_{hc}^{ss}$ nearly equals to one. But ratio $\Delta T_c / \Delta T_{hc}^{ss}$ almost closes to zero. DP matrices **A** and **B**, after normalization, are given below.

$$\mathbf{A} = \begin{pmatrix} 0 & I \\ 0 & I \end{pmatrix} \quad (3.7)$$

$$\mathbf{B} = \begin{pmatrix} I & 0 \\ 0 & 0 \end{pmatrix} \quad (3.8)$$

Figure 3.5 (b) depicts the disturbance pathways of temperature and heat capacity flow rate. This suggests that when the source temperature disturbance in the hot stream is severe, its splitting can diminish the severity of DP to both streams.

principles-based, simplified structural DP models are the main contents that provide deep insights on structural disturbance rejection. Fundamental knowledge is usually expressed in equations, and numerical solutions can be readily derived. Heuristic knowledge, however, can be expressed as heuristic rules for all stages of synthesis.

3.3.2 Three-stage synthesis procedure

In the synthesis procedure for integration of PD&C, the main focus is on the sequential rather than simultaneous development of a process flowsheet. This is essentially a hierarchical decision-making process. A stage-wise integration procedure involves three major stages.

Pre-analysis stage. At this stage, the total cost of the process of interest will be estimated using existing techniques, including the pinch technology (Linnhoff *et al.*, 1982). Process steady state and disturbance data should be analyzed and classified. The severity of stream disturbance information is always available to be obtained according to process characteristics. This information can provide guidance to design disturbance pathways for preventing severe disturbance propagating to those stream outputs that need be controlled strictly. The initial data analysis according to the criteria of minimum total cost and the highest degree of structural disturbance rejection will lead to the predetermination of the most favorable and least desirable placements of some units. Various rules are selected for enhancing structural controllability (Nishida *et al.*, 1981; Linnhoff *et al.*, 1982; Huang and Fan, 1992). Two of them are listed below.

Heater- and cooler-placement rule: Place a heater on the hot end of the

cold stream and/or a cooler on the cold end of the hot stream whose target temperature must be controlled precisely.

Intense-propagation-avoiding rule: *Avoid directly matching a stream, whose target temperature is to be controlled precisely, with a stream, whose source temperature and/or heat capacity flow rate is likely to experience intensive fluctuations.*

These rules enable us to restrict the possible generation of structural deficiency, and also reduce the solution space drastically. In addition, the design problem will be decomposed into several sub-problems, whenever possible. Each sub-problem will be treated independently at this level.

Structure development stage. A series of integration decisions will be made by the synthesis algorithms. The sequential placement of process units will be carried out based on the assessment of DP models and heuristic rules. In each step, the multi-targets of cost-effective and disturbance rejection will be simultaneously taken into account. Typical search approaches will be adopted to implement the overall step-wise process synthesis. One or more process alternatives will be generated for further evaluation.

Structure evolution stage. At this stage, the process structure(s) developed by preceding stages must be examined in the light of total cost and structural controllability. This can be accomplished by resorting to the DP models. Various rules will be also associated effectively to improve process system. This synthesis procedure can ensure the integration of sound process structures for maximum disturbance rejection, which eventually facilitates control system design.

3.4 Illustrating Example

A HEN synthesis problem (H5SP1R) described in chapter 2 is used to lay out the overall synthesis procedure. In this problem, there are five process streams, two hot streams and three cold streams. The original design data is given in Table 3.1 (Huang and Fan, 1992). Different disturbances are imposed on the stream source temperatures and heat capacity flow rates along with different control levels of stream target temperatures specified. All are listed in Table 3.2.

Table 3.1. Stream Data for the HSP15R Synthesis Problem

Stream	T^s (°C)	T^t (°C)	Mc_p (kW/°C)
H_1	204.4	65.6	13.29
H_2	248.9	121.1	16.62
C_1	93.3	93.3	13.03
C_2	65.6	65.6	12.92
C_3	37.8	37.8	11.40

The procedure aiming at synthesizing cost-effective and structurally controllable HEN can be carried out by the following steps:

Step 1. Data analysis and classification. According to disturbance information and control requirements listed in Table 3.2, hot stream H_2 experiences severe source disturbance; cold streams C_2 and C_3 experience mild disturbances; the remaining streams are considered to have negligible disturbances. The outlet temperatures in cold streams

C_2 and C_3 must be controlled strictly ($\leq \pm 1^\circ\text{C}$); the outlet of hot stream H_2 need be controlled in a certain degree of precision; the remaining streams do not have any control requirements in their outlet temperatures.

Table 3.2. Disturbances and control requirements for the HSP15R Synthesis Problem

Stream	$\delta T^{s(+)}$ ($^\circ\text{C}$)	$\delta T^{s(-)}$ ($^\circ\text{C}$)	$\delta M_{Cp}^{(+)}$ ($\text{kW}/^\circ\text{C}$)	$\delta M_{Cp}^{(-)}$ ($\text{kW}/^\circ\text{C}$)	δT^t ($^\circ\text{C}$)
H_1	0	0	0	0	--
H_2	6	-5	0.1	-0.15	± 3
C_1	1	-1	0	0	--
C_2	2	-1.5	0.15	-0.15	± 1
C_3	3	-3	0.1	-0.1	± 1

Step 2. Pinch analysis. In this synthesis problem, the pinch point is identified at 43.4°C ; only is hot utility needed with the minimum energy requirement of 884.6kW. The minimum number of heat transfer units is five including a heater.

Step 3. Initial grid problem. Figure 3.6 shows a grid diagram without any selection of unit placement. All stream information, such as steady state temperatures and heat capacity flow rates, source disturbances, and target-controlled temperatures, is illustrated in the figure for reference.

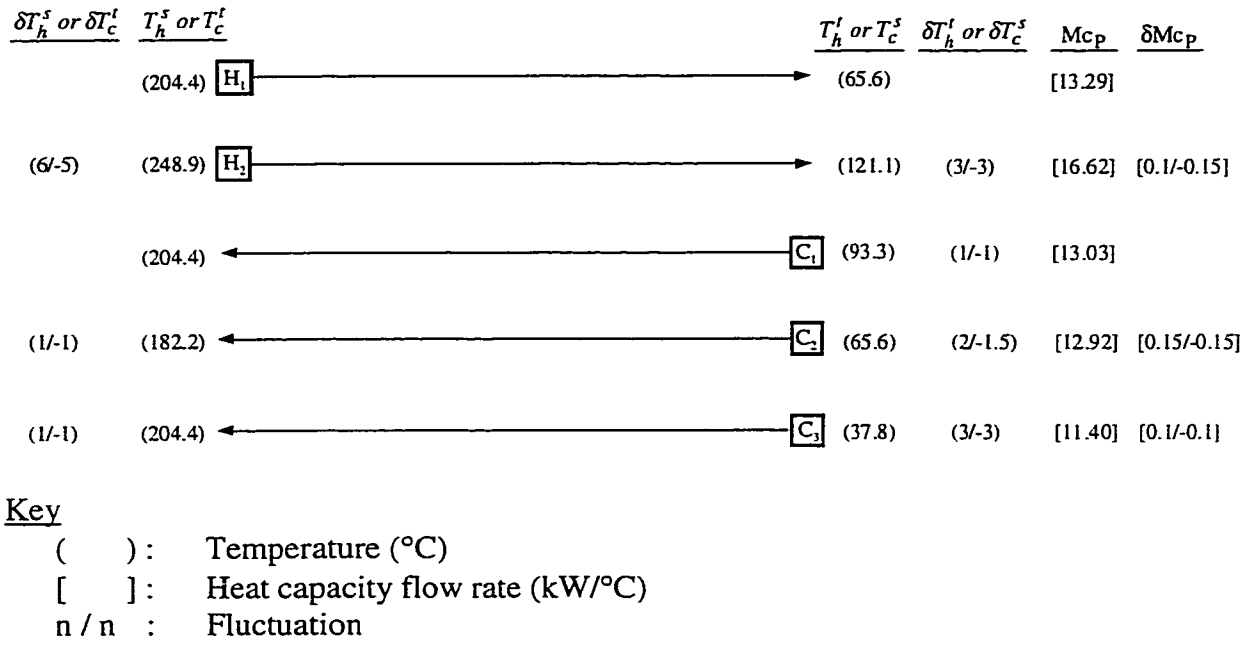


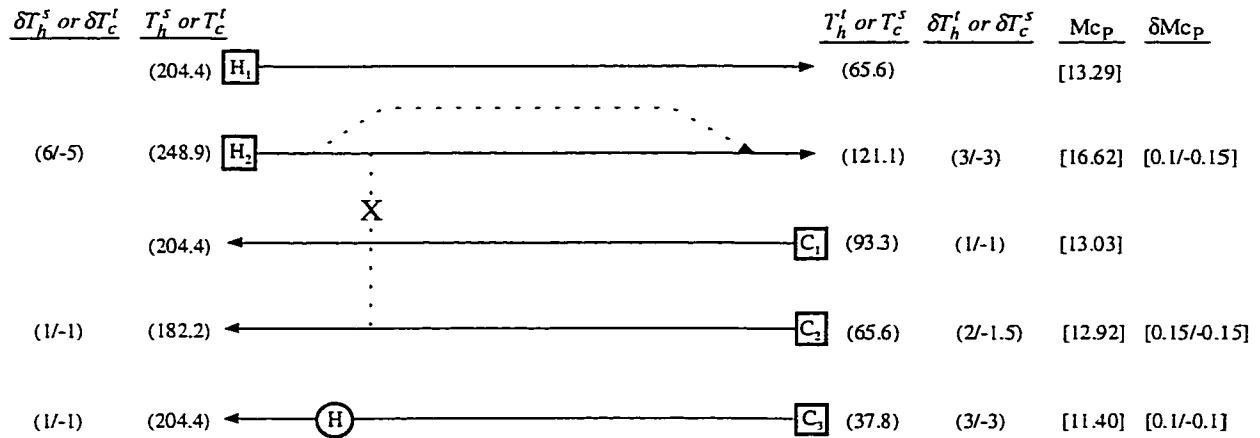
Figure 3.6. Initial grid diagram of the H5SP1R problem.

Step 4. Predetermination of unit placement. As depicted in Fig. 3.7, a heater is pre-assigned on the hot end of cold stream C_3 where the target temperature need be controlled precisely ($\leq \pm 1^\circ\text{C}$). In addition, a direct stream match between hot stream H_2 and cold stream C_2 is restricted to avoid severe disturbance propagating to cold stream C_2 where the target temperature must be controlled strictly ($\leq \pm 1^\circ\text{C}$). Because the outlet temperature of hot stream H_2 need be controlled in a certain degree of precision ($\leq \pm 3^\circ\text{C}$), the model-based analysis in Case 4 of the preceding section suggests to split hot stream H_2 in order to diminish the severe DP to its outlet.

Step 5. Process structure development. The optimal solution is obtained through step-wise unit placement, which is shown in Fig. 3.8 (Solution A). Four other alternatives are also derived without taking any restriction of stream matching into account. Figure 3.9 (Solution B) and Figures 2.3 (a) through (c) (Solutions C, D, and E) show grid

diagrams of their network structures.

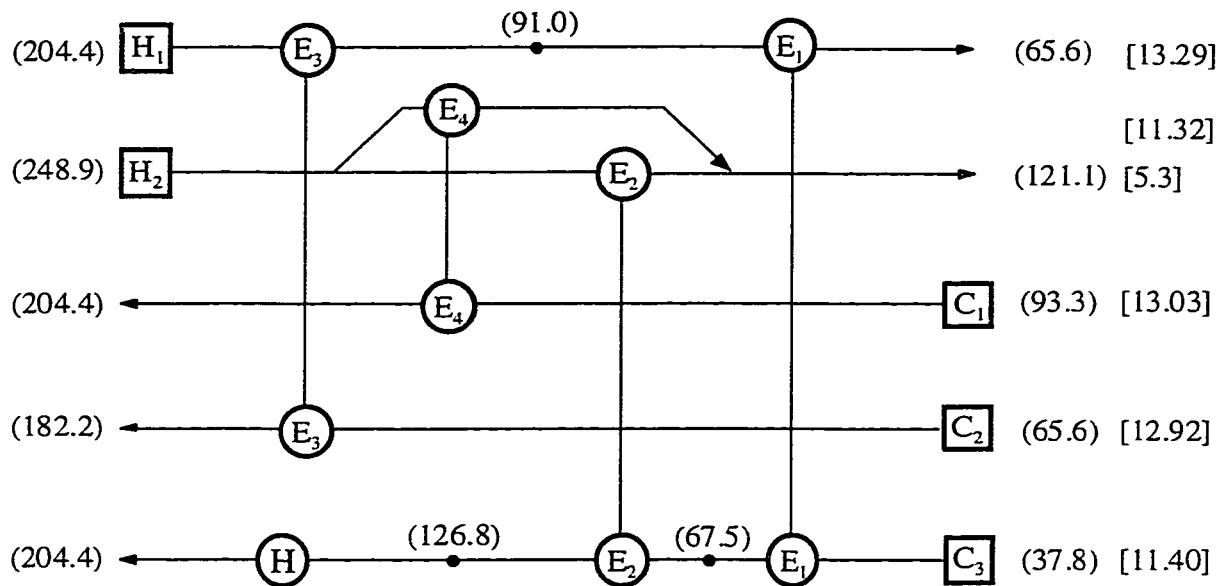
Step 6. Process evaluation. All solution alternatives are evaluated by the system DP model in Eq. (2.28). Computational results of the temperature fluctuations in the stream outlets of each solution are summarized in Table 3.3. For the target temperatures of both hot stream H_2 and cold stream C_2 , solution A is the best since it satisfies both temperature control requirements; solutions B and E can not reach the control requirement of the target temperatures in cold stream C_2 and in hot stream H_2 , respectively. Solutions C and D are undesirable due to severe fluctuations of the target temperatures in streams H_2 and C_2 . Overall, solution A is most controllable compared with the other networks.



Key

- () : Temperature ($^{\circ}\text{C}$)
- [] : Heat capacity flow rate ($\text{kW}/^{\circ}\text{C}$)
- n / n : Fluctuation

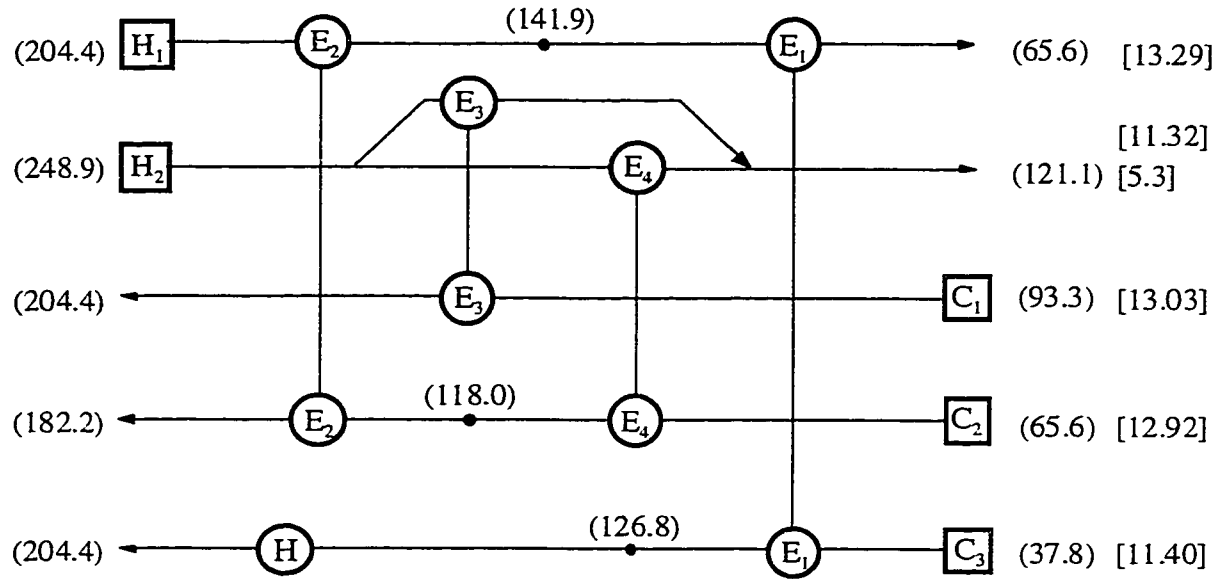
Figure 3.7. Preassigned grid diagram of the H5SP1R problem.



Key

- () : Temperature (°C)
 [] : Heat capacity flow rate (kW/°C)

Figure 3.8. Grid diagram of the optimal solution for the H5SP1R problem.
 (Solution A)



Key

- () : Temperature ($^{\circ}\text{C}$)
 [] : Heat capacity flow rate ($\text{kW}/^{\circ}\text{C}$)

Figure 3.9. Grid diagram of an alternative for the H5SP1R problem.
 (Solution B)

Table 3.3. Comparison of the Stream Target Temperatures in Five Alternative Solutions for the H5SP1R Problem

Target Temp.	Control Required	Sol. A	Sol. B	Sol. C	Sol. D	Sol. E
δT_{h1}^t (C)	--	2.64/-2.42	3.29/-3.17	3.21/-3.14	2.64/-2.64	2.64/-2.42
δT_{h2}^t (C)	± 3	3.00/-2.96	2.85/-2.75	3.23/-2.97	3.53/-3.21	3.52/-3.37
δT_{c1}^t (C)	--	4.84/-4.27	4.84/-4.27	4.76/-4.14	3.36/-2.87	4.76/-4.14
δT_{c2}^t (C)	± 1	1.10/-1.02	1.44/-1.29	1.33/-1.25	4.57/-4.17	1.10/-1.02
δT_{c3}^t (C)	± 1	0/0	0/0	0/0	0/0	0/0

CHAPTER 4

SYNTHESIS OF ENVIROMENTALLY BENIGN MASS EXCHANGER NETWORKS

4.1 Introduction

Mass separating agent (MSA) based separation processes have been widely devised for raw material preparation, product purification and separation (King, 1981). It has been naturally extended to process waste minimization (WM). As an example, the design of a mass exchanger network (MEN) contributes significantly to the removal of hazardous or toxic chemicals from process systems (El-Halwagi and Manousiouthakis, 1989; 1990a, b). The new development of MEN design includes reactive MEN, waste intercept network (WIN), and heat inducted network (HIN) (El-Halwagi and Srinivas, 1992; El-Halwagi *et al.*, 1996).

The synthesis of an MEN was previously only to minimize a total annualized cost. It has been recently recognized that operational aspects must be taken into account during process design. Papalexandri and Pistikopoulos (1994a) and Zhu and El-Halwagi (1995) discussed in detail the technical and economical attractiveness of enhancing the flexibility of MEN's, and developed systematic approaches for deriving cost-effective and flexible process systems.

Like flexibility, controllability is also an important operational aspect which should be considered in process synthesis (Fisher *et al.*, 1988; Huang and Fan, 1992; Papalexandri and Pistikopoulos, 1994b). This is especially true for the design of an MEN, since toxic chemical concentrations must be strictly controlled. Note that when a

synthesized MEN is incorporated into an existing process plant, the plant must contain various newly created interactions among process units. Process streams through these units become heavily interconnected. The interconnections may create numerous paths through which various disturbances propagate. The propagation related to the chemicals being regulated can be detrimental to waste removal and stable process operation. The undesirable severe propagation problems caused by improper process design are usually not solvable through control system design; they must be prevented during process synthesis. A conservative synthesis practice is to design a process such that the target concentrations of the regulated chemicals are well below EPA limits under a normal operating condition. Thus, when severe disturbances appear, the chemical concentrations in effluent streams are still permissible. Obviously, this is not an economical way. A much more attractive way is to design an MEN such that under the normal operating condition, the target concentrations of chemicals are just below the limits when severe disturbances exist. Certainly, this resultant network must be highly controllable structurally.

Note that sensitivity analysis has been performed to examine the flexibility and operability of heat exchanger networks (HEN's) (Kotjabasakis and Linnhoff, 1986; Ratnam and Patwardhan, 1991). A basic approach for sensitivity analysis is through a series of simulations under different operating conditions and then generates output fluctuations caused by input changes. The approach is tedious and cannot provide explicitly structural information of disturbance propagation (DP) in the process system. It is very difficult for process designers to quickly identify the main cause of DP and to tackle structure-related design problems.

Different from the sensitivity analysis approaches, Huang and Fan (1992, 1994) developed a methodology for identifying and quantifying DP in a process by resorting to artificial intelligence techniques. The methodology has been employed to design cost-effective and highly controllable heat exchanger networks (HEN's), MEN's, and work exchanger networks (WEN's) (Huang and Edgar, 1995; Huang and Fan, 1996). The quantification of DP in the methodology is based on approximate reasoning. It has been found that the approach may introduce noticeable errors for some cases and the derived solutions may not be preferable when more precise process evaluation is needed (Sabharwal *et al.*, 1995; Yang and Huang, 1996).

In this chapter, a modeling methodology is developed in a systematic manner to characterize the DP harmful for process controllability and to quantify the worst situations to occur in a process plant when an MEN is incorporated. The model is based on the first principles with reasonable assumptions for simplification. It can be used to identify the most desirable MEN during process synthesis.

4.2 Motivation

As stated in the preceding section, a cost-effective MEN is designed to reduce the target concentrations of waste chemicals to just below environmental limits under a normal operating condition. With this kind of marginal design, a process structure must be much more superior and robust. It is expected that the structural superiority be appropriately evaluated. This expectation can be further understood through the following industrial example.

An integrated process plant is illustrated in Fig. 4.1. Feed streams B and C , named rich streams R_1 and R_2 , respectively, contain a regulated chemical. These streams need be purified through this process. The bottom stream of column D and feed stream A , named as lean streams L_1 and L_2 , respectively, are used to absorb the chemical from the two rich streams. The bottom streams of exchangers E_1 and E_3 are mixed and then fed to column D where the regulated chemical in the stream is separated and removed from the overhead. In this plant, feed stream B (stream R_1) and the recycle stream (stream L_1) from column D experience severe disturbances of mass flowrates and concentrations. These disturbances propagate through all three exchangers to affect product quality. The plant in fact contains structural inferiority that can be identified by analyzing the embedded MEN.

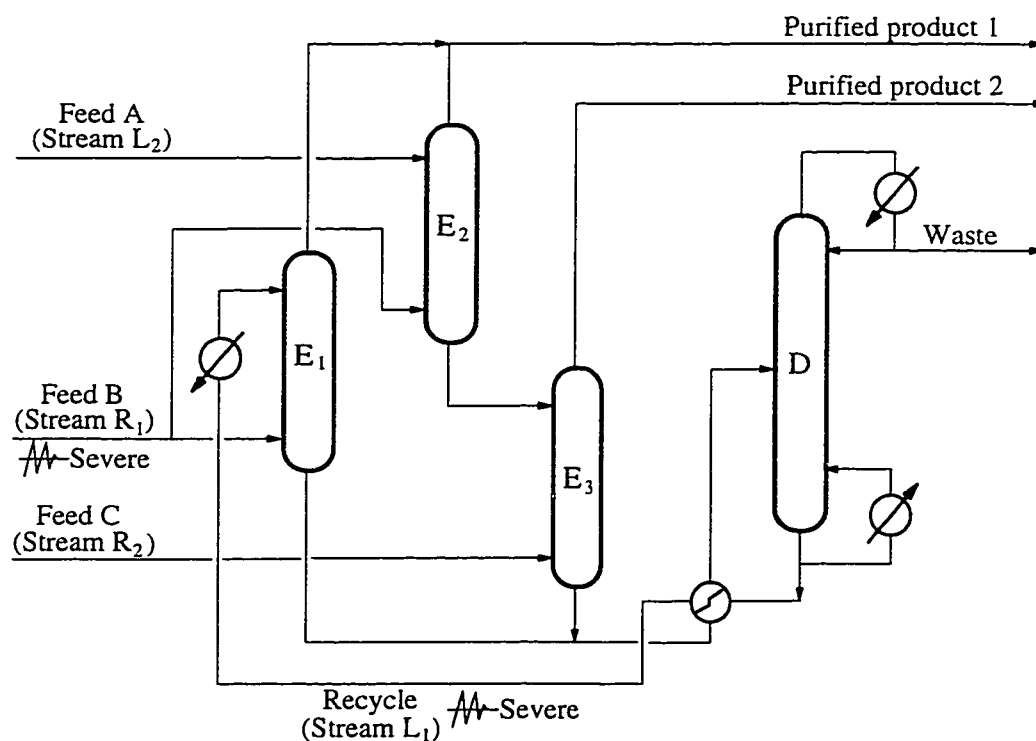
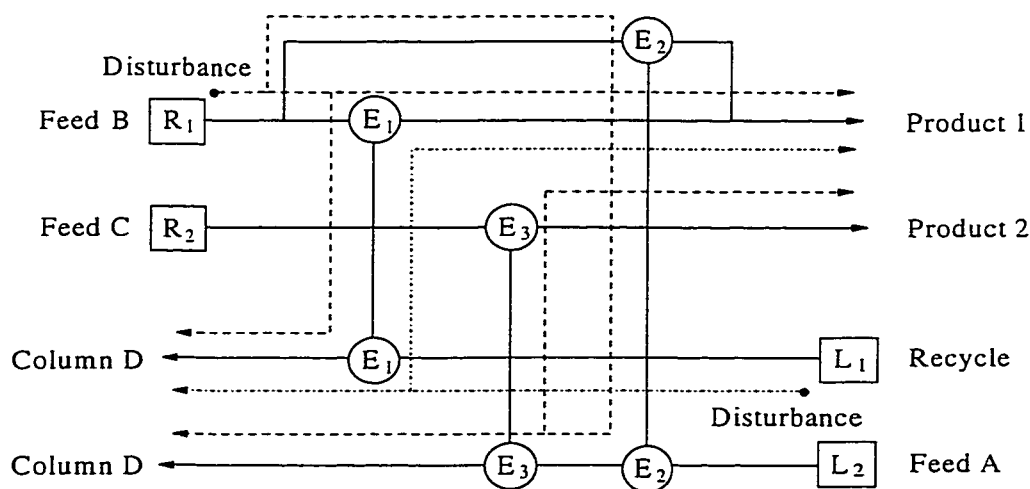


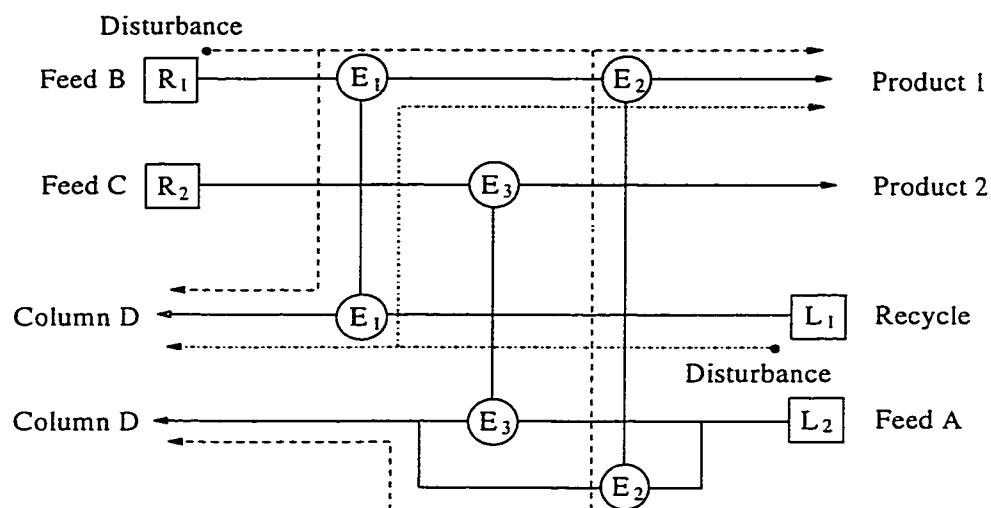
Figure 4.1. Flowsheet of an integrated plant for product purification.

The grid diagram of the MEN is illustrated in Fig. 4.2 (a). The severe DP through it is depicted by dotted lines. Clearly, the target concentration of each stream is affected by the disturbances, but with different intensities. If the MEN structure is modified as shown in Fig. 4.2 (b), the process is more acceptable in terms of disturbance rejection. Certainly, this modification should follow mass balance principles. In the modified MEN, feed stream *B* is separated twice and product 1 is purer. The disturbance from stream *B* does not propagate to product 2 since the DP path through exchanger E_3 is terminated. This modification will lead to a relatively easy design of a control system for it. The example suggests that a process structure be evaluated quantitatively from an environmental standpoint. This requires the development of a reliable model for process evaluation.



(a) Grid diagram of the original MEN.

Figure 4.2. Grid diagrams of the MEN in the integrated plant (cont'd).



(b) Grid diagram of a modified MEN.

Figure 4.2. Grid diagrams of the MEN in the integrated plant.

4.3 Unit-Based Mass Exchange Model

The type of mass separation processes discussed in this chapter refers to mass-separating-agent (MSA) based mass exchange operations, such as extraction, absorption, desorption, and ion-exchange.

Basic equations. An MSA-based separator is usually designed based on a given normal operating condition. In this type of separation unit, the key chemical species is transferred from a rich stream to a lean stream (El-Halwagi and Manousiouthakis, 1990a). As depicted in Fig. 4.3, a mass transfer between a rich stream and a lean stream is taken place through their interface, which leads to the concentration of the key component in the rich stream decreased from C_r^s to C_r^t and that in the lean stream increased from C_l^s

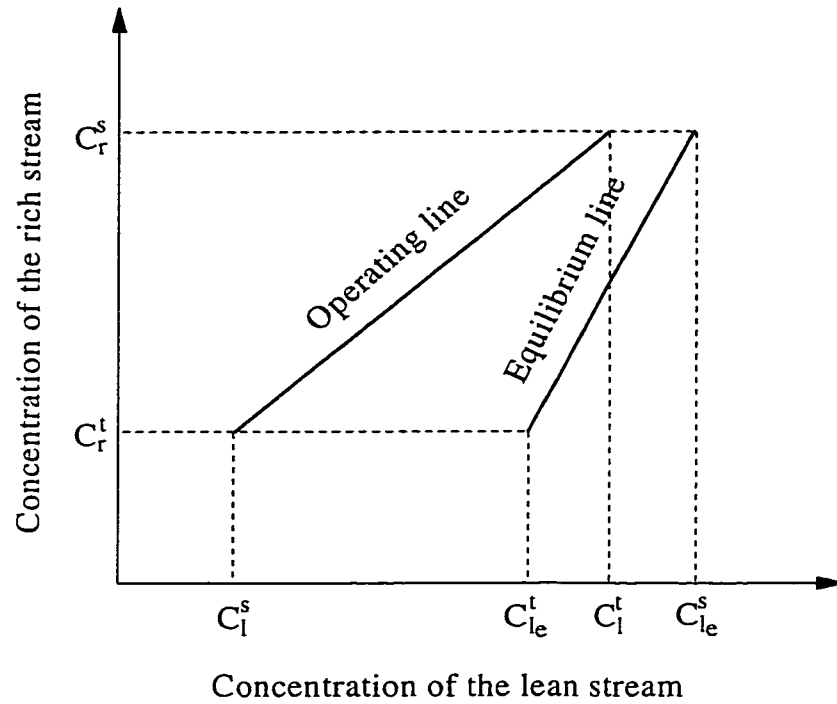


Figure 4.4. Concentration driving force between equilibrium and operating lines in a mass transfer process.

The concentration difference horizontally between the operating and equilibrium lines represents the driving force for mass transfer. The mass balance with respect to key component p is given by

$$M_p = M_r \Delta C_r = M_l \Delta C_l \quad (4.2)$$

where

$$\Delta C_r = C_r^s - C_r^t \quad (4.3)$$

$$\Delta C_l = C_l^t - C_l^s \quad (4.4)$$

The overall mass transfer equation for a mass transfer unit can be expressed below (King, 1981).

operating point (designated as δC_r^t and δC_l^t). A basic DP model for a mass exchanger can be obtained by incorporating disturbances into Eqs. (4.2) and (4.5); this gives

$$\begin{aligned} M_p + \delta M_p &= (M_r + \delta M_r) \left[\Delta C_r + (\delta C_r^s - \delta C_r^t) \right] \\ &= (M_l + \delta M_l) \left[\Delta C_l + (\delta C_l^t - \delta C_l^s) \right] \end{aligned} \quad (4.9)$$

$$M_p + \delta M_p = K(A + \delta A) \frac{\left[\Delta C_{l_e l}^{st} + (\delta C_{l_e}^s - \delta C_l^t) \right] - \left[\Delta C_{l_e l}^{ts} + (\delta C_{l_e}^t - \delta C_l^s) \right]}{\ln \left(\frac{\Delta C_{l_e l}^{st} + (\delta C_{l_e}^s - \delta C_l^t)}{\Delta C_{l_e l}^{ts} + (\delta C_{l_e}^t - \delta C_l^s)} \right)} \quad (4.10)$$

where

$$A + \delta A = A_m (M_r + \delta M_r)^n (M_l + \delta M_l)^n \quad (4.11)$$

$$\delta C_{l_e}^s = \frac{\delta C_r^s}{m} \quad (4.12)$$

$$\delta C_{l_e}^t = \frac{\delta C_r^t}{m} \quad (4.13)$$

The target concentration fluctuations, δC_r^t and δC_l^t , can be evaluated by solving Eqs. (4.9) through (4.13). Due to the existence of logarithmic and exponential terms, the model exhibits high non-linearity, and it is impossible to obtain analytical solutions for δC_r^t and δC_l^t in terms of δC_r^s , δC_l^s , δM_r , and δM_l . When the model is used to evaluate DP through a system, it becomes very cumbersome. This is especially true for the system with splitting, mixing, and loops, when a number of process alternatives need to be evaluated. The model should be simplified.

Matrices A_e and B_e are of the following forms.

$$A_e = \begin{pmatrix} 1 - a_{l2} & ma_{l2} \\ \frac{a_{2l}}{m} & 1 - a_{2l} \end{pmatrix} \quad (4.21)$$

$$B_e = \begin{pmatrix} \alpha_r(2 - a_{l2} - n(2 - a_{l2} - a_{2l})) & -\alpha_l \left(ma_{l2} + nm \frac{a_{l2}}{a_{2l}} (2 - a_{l2} - a_{2l}) \right) \\ \alpha_r \left(\frac{a_{2l}}{m} + \frac{n}{m} \frac{a_{2l}}{a_{l2}} (2 - a_{l2} - a_{2l}) \right) & -\alpha_l (2 - a_{2l} - n(2 - a_{l2} - a_{2l})) \end{pmatrix} \quad (4.22)$$

where

$$a_{l2} = \frac{\frac{1}{m} \Delta C_r}{\Delta C_{l_e l}^{ss}} \quad (4.23)$$

$$a_{2l} = \frac{\Delta C_l}{\Delta C_{l_e l}^{ss}} \quad (4.24)$$

$$\Delta C_{l_e} = C_{l_e}^s - C_{l_e}^t \quad (4.25)$$

$$\Delta C_{l_e l}^{ss} = C_{l_e}^s - C_l^s \quad (4.26)$$

$$\Delta C_{l_e l}^{tt} = C_{l_e}^t - C_l^t \quad (4.27)$$

$$\alpha_r = \frac{\Delta C_r}{2M_r} \quad (4.28)$$

$$\alpha_l = \frac{\Delta C_l}{2M_l} \quad (4.29)$$

The elements in matrices A_e and B_e are determined by only four parameters, a_{l2} , a_{2l} , α_r , and α_l , which depend on the normal operating conditions. Constants m and

n are selected based on chemical properties and the type of separators. Eq. (4.17) relates the concentration changes of the outputs to the source disturbances. Thus, the DP in a mass exchanger can be conveniently detected by this model.

Since streams splitting and mixing are always necessary for designing an MEN, splitters and mixers should also be modeled. Figure 4.5(a) depicts a stream split to S_n branches. The fluctuation of the outlet concentration of each branch is the same as that of the stream before splitting. The ratio of the fluctuation of mass flow rate to the nominal mass flow rate of each branch is the same as that of the stream before splitting. These relationships can be expressed as

$$\delta C_{s_i}^{out} = \delta C_s^{in}, \quad i = 1, 2, \dots, n \quad (4.30)$$

$$\delta M_{s_i}^{out} = \frac{M_{s_i}^{out}}{M_s^{in}} \delta M_s^{in}, \quad i = 1, 2, \dots, n \quad (4.31)$$

The correlation of the concentration fluctuations for splitting can be written in the form similar to that for a mass exchanger.

$$\delta C_s^{out} = A_s \delta C_s^{in} + B_s \delta M_s^{in} \quad (4.32)$$

$$\delta M_s^{out} = D_s \delta M_s^{in} \quad (4.33)$$

where

$$\delta C_s^{out} = \left(\delta C_{s_1}^{out} \quad \delta C_{s_2}^{out} \quad \dots \quad \delta C_{s_n}^{out} \right)^T \quad (4.34)$$

$$\delta M_s^{out} = \left(\delta M_{s_1}^{out} \quad \delta M_{s_2}^{out} \quad \dots \quad \delta M_{s_n}^{out} \right)^T \quad (4.35)$$

$$A_s = (I \quad I \quad \dots \quad I)^T \quad (4.36)$$

$$B_s = (0 \quad 0 \quad \dots \quad 0)^T \quad (4.37)$$

$$D_s = \begin{pmatrix} \frac{M_{s1}^{out}}{M_s^{in}} & \frac{M_{s2}^{out}}{M_s^{in}} & \dots & \frac{M_{sn}^{out}}{M_s^{in}} \end{pmatrix}^T \quad (4.38)$$

For a mixer, as shown in Fig. 4.5(b), the fluctuation of mass flow rate and that of concentration of the output stream after mixing can be calculated as follows.

$$\delta C_m^{out} = \frac{\sum_{i=1}^n \left(M_{m_i}^{in} + \delta M_{m_i}^{in} \right) \left(C_{m_i}^{in} + \delta C_{m_i}^{in} \right)}{M_m^{out} + \delta M_m^{out}} - C_m^{out} \quad (4.39)$$

$$\delta M_m^{out} = \sum_{i=1}^n \delta M_{m_i}^{in} \quad (4.40)$$

For consistency, the model of a mixer can also be written in the form similar to that for a mass exchanger.

$$\delta C_m^{out} = A_m \delta C_m^{in} + B_m \delta M_m^{in} \quad (4.41)$$

$$\delta M_m^{out} = D_m \delta M_m^{in} \quad (4.42)$$

where

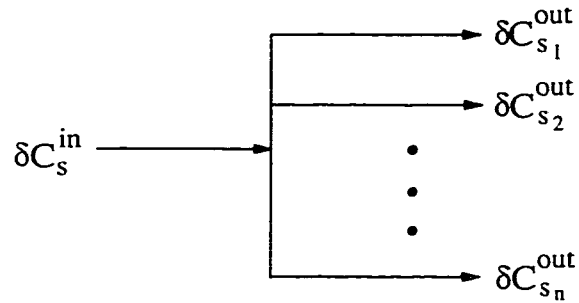
$$\delta C_m^{in} = \begin{pmatrix} \delta C_{m_1}^{in} & \delta C_{m_2}^{in} & \dots & \delta C_{m_n}^{in} \end{pmatrix}^T \quad (4.43)$$

$$\delta M_m^{in} = \begin{pmatrix} \delta M_{m_1}^{in} & \delta M_{m_2}^{in} & \dots & \delta M_{m_n}^{in} \end{pmatrix}^T \quad (4.44)$$

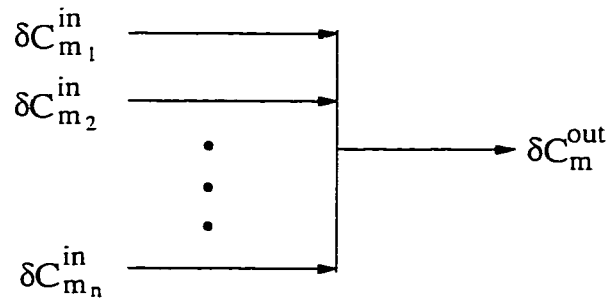
$$A_m = \begin{pmatrix} \frac{M_{m_1}}{M_m} & \frac{M_{m_2}}{M_m} & \dots & \frac{M_{m_n}}{M_m} \end{pmatrix} \quad (4.45)$$

$$B_m = \begin{pmatrix} \frac{C_{m_1}^{in} - C_m^{out}}{M_m} & \frac{C_{m_2}^{in} - C_m^{out}}{M_m} & \dots & \frac{C_{m_n}^{in} - C_m^{out}}{M_m} \end{pmatrix} \quad (4.46)$$

$$\mathbf{D}_m = (1 \quad 1 \quad \cdots \quad 1) \quad (4.47)$$



(a) Stream splitting



(b) Stream mixing

Figure 4.5. Disturbance propagation through stream splitting and mixing.

4.5 System Modeling for Waste Rejection

The main interest here is to evaluate the fluctuations of the target concentrations of all $(N_r + N_l)$ streams. These stream concentrations can be described below.

$$\delta \underline{C}_E^{out} = \left(\left(\delta C_{e_1}^{out} \right)^T \quad \left(\delta C_{e_2}^{out} \right)^T \quad \dots \quad \left(\delta C_{e_{N_e}}^{out} \right)^T \right)^T \quad (4.54)$$

$$\delta \underline{M}_E^{in} = \left(\left(\delta M_{e_1}^{in} \right)^T \quad \left(\delta M_{e_2}^{in} \right)^T \quad \dots \quad \left(\delta M_{e_{N_e}}^{in} \right)^T \right)^T \quad (4.55)$$

$$\underline{A}_E = \text{diag}(A_{e_1}, A_{e_2}, \dots, A_{e_{N_e}}) \quad (4.56)$$

$$\underline{B}_E = \text{diag}(B_{e_1}, B_{e_2}, \dots, B_{e_{N_e}}) \quad (4.57)$$

Mixers model. With N_m mixers in the MEN, we can lump all N_m mixer models, each of which is described by Eq. (4.41), to a global mixer model:

$$\delta \underline{C}_M^{out} = \underline{A}_M \delta \underline{C}_M^{in} + \underline{B}_M \delta \underline{M}_M^{in} \quad (4.58)$$

where

$$\delta \underline{C}_M^{in} = \left(\left(\delta C_{m_1}^{in} \right)^T \quad \left(\delta C_{m_2}^{in} \right)^T \quad \dots \quad \left(\delta C_{m_{N_m}}^{in} \right)^T \right)^T \quad (4.59)$$

$$\delta \underline{C}_M^{out} = \left(\delta C_{m_1}^{out} \quad \delta C_{m_2}^{out} \quad \dots \quad \delta C_{m_{N_m}}^{out} \right) \quad (4.60)$$

$$\delta \underline{M}_M^{in} = \left(\left(\delta M_{m_1}^{in} \right)^T \quad \left(\delta M_{m_2}^{in} \right)^T \quad \dots \quad \left(\delta M_{m_{N_m}}^{in} \right)^T \right)^T \quad (4.61)$$

$$\underline{A}_M = \text{diag}(A_{m_1}, A_{m_2}, \dots, A_{m_{N_m}}) \quad (4.62)$$

$$\underline{B}_M = \text{diag}(B_{m_1}, B_{m_2}, \dots, B_{m_{N_m}}) \quad (4.63)$$

Splitters model. Assume there exist N_s splitters in the MEN, the global splitter model is

$$\delta \underline{C}_S^{out} = \underline{A}_S \delta \underline{C}_S^{in} + \underline{B}_S \delta \underline{M}_S^{in} \quad (4.64)$$

where

$$\delta \underline{C}_S^{in} = \left(\delta C_{s_1}^{in} \quad \delta C_{s_2}^{in} \quad \dots \quad \delta C_{s_{N_s}}^{in} \right)^T \quad (4.65)$$

$$\delta \underline{C}_S^{out} = \left(\left(\delta C_{s_1}^{out} \right)^T \quad \left(\delta C_{s_2}^{out} \right)^T \quad \dots \quad \left(\delta C_{s_{N_e}}^{out} \right)^T \right)^T \quad (4.66)$$

$$\delta \underline{M}_S^{in} = \left(\delta M_{s_1}^{in} \quad \delta M_{s_2}^{in} \quad \dots \quad \delta M_{s_{N_s}}^{in} \right)^T \quad (4.67)$$

$$\underline{A}_S = \text{diag} \left(A_{s_1}, \quad A_{s_2}, \quad \dots, \quad A_{s_{N_s}} \right) \quad (4.68)$$

$$\underline{B}_S = 0 \quad (4.69)$$

4.5.2 Derivation of an all-units model

Note that from a system point of view, when a stream is split, each branch must have mass exchange with another stream before it mixes with other branch(es). Thus, to develop a global system model, all three types of global models described above need be lumped to obtain an all-units model, i.e.,

$$\delta \underline{C}^{out} = \underline{A} \delta \underline{C}^{in} + \underline{B} \delta \underline{M}^{in} \quad (4.70)$$

where

$$\delta \underline{C}^{in} = \left(\left(\delta C_E^{in} \right)^T \quad \left(\delta C_M^{in} \right)^T \quad \left(\delta C_S^{in} \right)^T \right)^T \quad (4.71)$$

$$\delta \underline{C}^{out} = \left(\left(\delta C_E^{out} \right)^T \quad \left(\delta C_M^{out} \right)^T \quad \left(\delta C_S^{out} \right)^T \right)^T \quad (4.72)$$

$$\delta \underline{\mathbf{M}}^{in} = \begin{pmatrix} (\delta \mathbf{M}_E^{in})^T & (\delta \mathbf{M}_M^{in})^T & (\delta \mathbf{M}_S^{in})^T \end{pmatrix}^T \quad (4.73)$$

$$\underline{\mathbf{A}} = \text{diag}\{\underline{\mathbf{A}}_E, \underline{\mathbf{A}}_M, \underline{\mathbf{A}}_S\} \quad (4.74)$$

$$\underline{\mathbf{B}} = \text{diag}\{\underline{\mathbf{B}}_E, \underline{\mathbf{B}}_M, \mathbf{0}\} \quad (4.75)$$

The total number of equations in Eq. (4.70) is N_t that can be evaluated as

$$N_t = 2N_e + N_m + \sum_{i=1}^{N_s} S_i \quad (4.76)$$

4.5.3 Determination of a conversion matrix

In the all-units model in Eq. (4.70), vector $\delta \underline{\mathbf{M}}^{in}$ may contain the variables of source and intermediate disturbances of mass flowrates (i.e., $\delta \underline{\mathbf{M}}^s$'s and $\delta \underline{\mathbf{M}}^m$'s). Since the system model in Eq. (4.48) requires only the information of $\delta \underline{\mathbf{M}}^s$'s, all $\delta \underline{\mathbf{M}}^m$'s must be converted to either $\delta \underline{\mathbf{M}}_r^s$ or $\delta \underline{\mathbf{M}}_l^s$ (see Appendix C for details). This gives rise to the introduction of the following matrix for converting vectors $\delta \underline{\mathbf{M}}^{in}$ to $\delta \underline{\mathbf{M}}^s$:

$$\delta \underline{\mathbf{M}}^{in} = \underline{\mathbf{F}} \delta \underline{\mathbf{M}}^s \quad (4.77)$$

where

$$\underline{\mathbf{F}} = \text{diag}\{f_1, f_2, \dots, f_{N_t}\} \quad (4.78)$$

Vector $\delta \underline{\mathbf{M}}^s$ contains only $\delta \underline{\mathbf{M}}_r^s$'s and $\delta \underline{\mathbf{M}}_l^s$'s. The conversion yields the all-units model in the following form.

$$\delta \underline{\mathbf{C}}^t = \underline{\mathbf{A}} \delta \underline{\mathbf{C}}^s + \underline{\mathbf{B}}' \delta \underline{\mathbf{M}}^s \quad (4.79)$$

where

$$\underline{B}' = \underline{B}^* \underline{F} \quad (4.80)$$

4.5.4 Permutation of the all-units model

A target concentration of either a rich or lean stream can be the output concentration of either a mass exchanger or a mixer, but not that of a splitter. Thus, from N_t equations in Eq. (4.70), $(N_r + N_l)$ equations describing fluctuated target concentrations should be identified and placed in the order below. The remaining $[N_t - (N_r + N_l)]$ equations only describe intermediate concentration fluctuations. The equivalent all-units model after permutation is

$$\delta \underline{C}^{*out} = \underline{A}^* \delta \underline{C}^{*in} + \underline{B}^* \delta \underline{M}^{*in} \quad (4.81)$$

where

$$\delta \underline{C}^{*out} = \left(\left(\delta \underline{C}^t \right)^T \quad \left(\delta \underline{C}^m \right)^T \right)^T \quad (4.82)$$

$$\delta \underline{C}^{*in} = \left(\left(\delta \underline{C}^s \right)^T \quad \left(\delta \underline{C}^m \right)^T \right)^T \quad (4.83)$$

$$\delta \underline{C}^t = \left(\delta C_{r_l}^t \quad \delta C_{r_l}^t \quad \cdots \quad \delta C_{r_{N_r}}^t \quad \delta C_{l_l}^t \quad \delta C_{l_l}^t \quad \cdots \quad \delta C_{l_{N_l}}^t \right)^T \quad (4.84)$$

$$\delta \underline{C}^s = \left(\delta C_{r_l}^s \quad \delta C_{r_l}^s \quad \cdots \quad \delta C_{r_{N_r}}^s \quad \delta C_{l_l}^s \quad \delta C_{l_l}^s \quad \cdots \quad \delta C_{l_{N_l}}^s \right)^T \quad (4.85)$$

$$\delta \underline{C}^m = \left(\delta C_1^m \quad \delta C_2^m \quad \cdots \quad \delta C_{N_t - N_r - N_l}^m \right)^T \quad (4.86)$$

From Eq. (4.92), we obtain

$$\delta \underline{C}^m = (\underline{I} - \underline{A}_{22})^{-1} \underline{A}_{21} \delta \underline{C}^s + (\underline{I} - \underline{A}_{22})^{-1} \underline{B}_2 \delta \underline{M}^s \quad (4.93)$$

Substituting Eq. (4.93) into Eq. (4.91) gives the system model:

$$\delta \underline{C}^t = \underline{A} \delta \underline{C}^s + \underline{B} \delta \underline{M} \quad (4.48)$$

where

$$\underline{A} = \underline{A}_{11} + \underline{A}_{12} (\underline{I} - \underline{A}_{22})^{-1} \underline{A}_{21} \quad (4.94)$$

$$\underline{B} = \underline{B}_1 + \underline{A}_{12} (\underline{I} - \underline{A}_{22})^{-1} \underline{B}_2 \quad (4.95)$$

Vectors $\delta \underline{C}^t$, $\delta \underline{C}^s$, and $\delta \underline{M}$ are defined in Eqs. (4.49) through (4.51).

4.6 Case Studies

The system model developed in the preceding section has been successfully used to evaluate process alternatives. Two case studies are illustrated below.

Evaluation of process alternatives. The MEN design problem, namely M5SP1R, specifies two rich streams and three lean streams. The original problem was solved by El-Halwagi and Manousiouthakis (1988); it was then modified by introducing various source disturbances to process streams (Huang, 1992). The design data in Table 4.1 includes the normal operating information, source disturbances, and permissible target concentration ranges of the streams. In this process, the lean streams (L_1 and L_2) and rich streams (R_1 and R_2) experience various disturbances. Lean stream L_3 is a stable external stream. In the operating range, the equilibrium relations for a key component between a rich stream (R_1 or R_2) and three lean streams (L_1 , L_2 , and L_3)

are given below:

$$C_{r_e} = 0.8C_{l_1e} + 0.002 \quad (4.96)$$

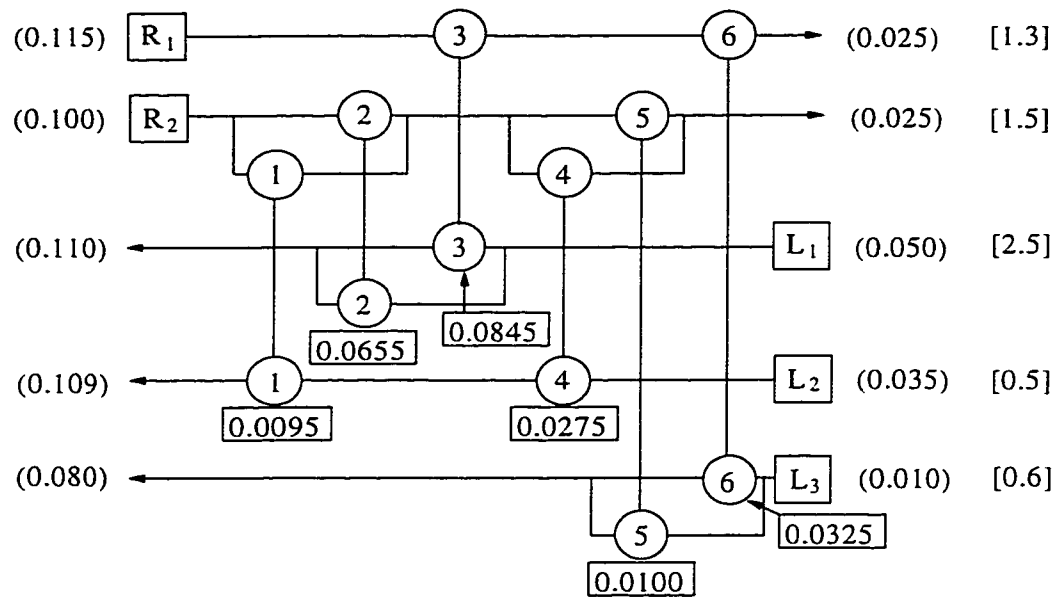
$$C_{r_e} = 0.5C_{l_2e} \quad (4.97)$$

$$C_{r_e} = 0.2C_{l_3e} \quad (4.98)$$

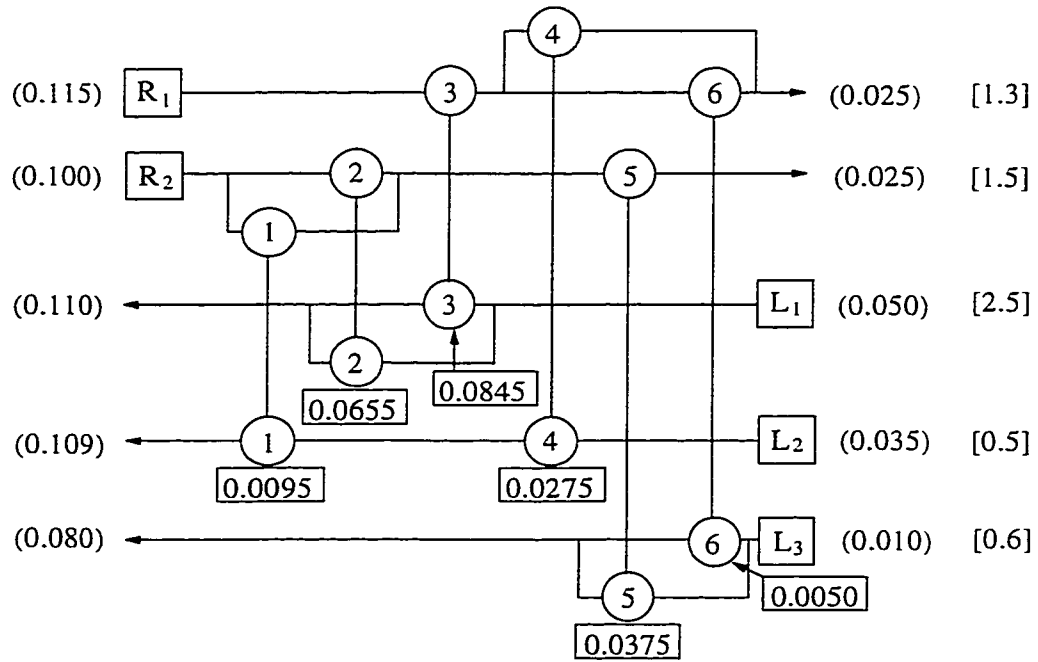
Table 4.1. Stream Data for the M5SP1R Synthesis Problem

Stream No.	C^s	C^t	M (kg/s)	δC^s	δM (kg/s)	δC^t
R_1	0.115	0.025	1.3	0.0080	0.007	0.0015
R_2	0.100	0.025	1.5	0.0060	0.010	0.0025
L_1	0.050	0.110	2.5	0.0025	0	0.0080
L_2	0.035	0.120	0.5	0.0040	0	0.0065
L_3	0.010	0.080	∞	0	0	-

The minimum allowable concentration difference between a rich stream and a lean stream is fixed at 0.01 in any mass transfer unit (MTU). Based on the normal operating condition, the pinch point is located at the concentration of 0.05 for rich streams R_1 and R_2 , and 0.05, 0.09, and 0.24 for lean streams L_1 , L_2 , and L_3 , respectively. The minimum amount of MSA required is 0.0425 kg/s, and the minimum number of MTU's is five. The permissible concentration at the outlets of streams R_1 , R_2 , L_1 , and L_2 are 0.0015, 0.0025, 0.0080, and 0.0065, respectively. With these process constraints, only exist five solution alternatives that are identified by a knowledge-based approach (Huang and Fan, 1994); their grid diagrams are depicted in Fig. 4.6.

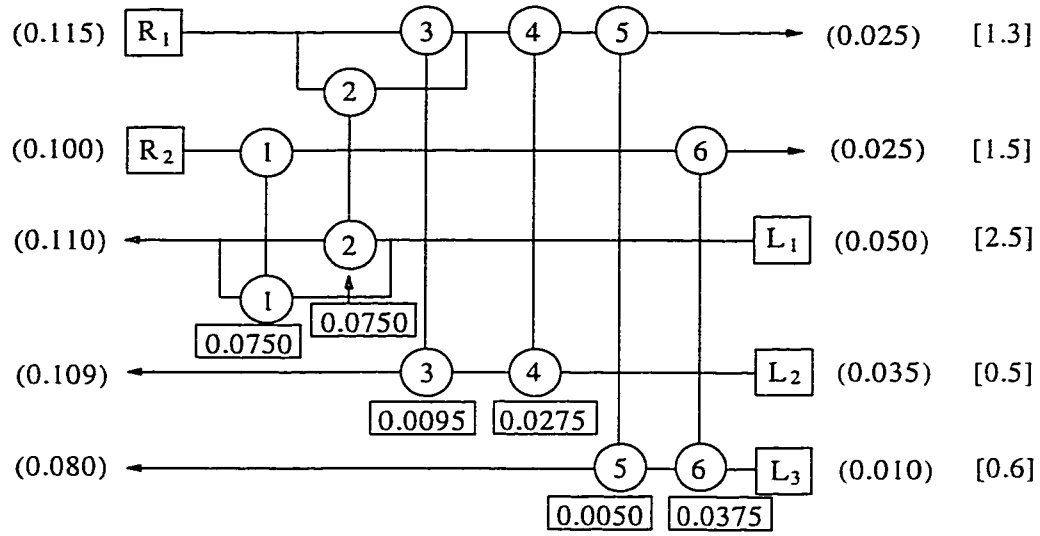


(a) Solution A



(b) Solution B

Figure 4.6. Grid diagrams of the five solutions of MEN problem M5SP1R.



(e) Solution E

Key

(): Concentration

[]: Mass flowrate (kg/s)

□: Mass transfer duty of the major component (kg/s)

Figure 4.6. Grid diagrams of the five solutions of MEN problem M5SP1R (cont'd).

The system model in Eq. (4.48) is used to evaluate these alternative solutions. For each solution, we can define two disturbance vectors and one control vector as shown below.

$$\delta \underline{C}^s = \left(\delta C_{r_1}^s \quad \delta C_{r_2}^s \quad \delta C_{l_1}^s \quad \delta C_{l_2}^s \quad \delta C_{l_3}^s \right)^T \quad (4.99)$$

$$\delta \underline{M} = \left(\delta M_{r_1} \quad \delta M_{r_2} \quad \delta M_{l_1} \quad \delta M_{l_2} \quad \delta M_{l_3} \right)^T \quad (4.100)$$

$$\delta \underline{C}^t = \left(\delta C_{r_1}^t \quad \delta C_{r_2}^t \quad \delta C_{l_1}^t \quad \delta C_{l_2}^t \quad \delta C_{l_3}^t \right)^T \quad (4.101)$$

The corresponding system matrices for solution A, for example, are:

$$\underline{A} = \begin{pmatrix} 0.0525 & 0 & 0.3413 & 0 & 0.1042 \\ 0 & 0.0434 & 0.1982 & 0.2850 & 0.0278 \\ 0.4636 & 0.4510 & 0.2683 & 0 & 0 \\ 0 & 0.5502 & 0.9342 & 0.1410 & 0 \\ 0.1222 & 0.0502 & 1.0234 & 0.0034 & 0.7083 \end{pmatrix} \quad (4.102)$$

$$\underline{B} = \begin{pmatrix} 0.0209 & 0 & -0.0052 & 0 & -0.0156 \\ 0 & 0.0145 & -0.0027 & -0.0204 & -0.0042 \\ 0.0139 & 0.0086 & -0.0134 & 0 & 0 \\ 0 & 0.0488 & -0.0129 & -0.0837 & 0 \\ 0.0463 & 0.0120 & -0.0153 & -0.0025 & -0.0717 \end{pmatrix} \quad (4.103)$$

Elements a_{ij} in matrix \underline{A} and b_{ij} in matrix \underline{B} represent the severity of DP from the inlet of stream i to the outlet of stream j . The larger the absolute value of an element, the more severe the propagation. Each zero element in matrices indicates that there exists no downstream path for DP between two relevant streams. The computed target concentration ranges for the key component of streams for each solution is summarized in Table 4.2.

Table 4.2. Comparison of the Concentration Fluctuations at the Stream Outlets in Five Solution Alternatives for the M5SP1R Synthesis Problem

Target Conc.	Control Requirement	Sol. A	Sol. B	Sol. C	Sol. D	Sol. E
$\delta C_{r_1}^t$	≤ 0.0015	≤ 0.0014	≤ 0.0014	≤ 0.0021	≤ 0.0019	≤ 0.0021
$\delta C_{r_2}^t$	≤ 0.0025	≤ 0.0019	≤ 0.0017	≤ 0.0012	≤ 0.0012	≤ 0.0013
$\delta C_{l_1}^t$	≤ 0.0080	≤ 0.0072	≤ 0.0071	≤ 0.0071	≤ 0.0071	≤ 0.0072
$\delta C_{l_2}^t$	≤ 0.0065	≤ 0.0062	≤ 0.0065	≤ 0.0071	≤ 0.0071	≤ 0.0067
$\delta C_{l_3}^t$	-	≤ 0.0042	≤ 0.0046	≤ 0.0038	≤ 0.0043	≤ 0.0039

In this design, the target concentration of stream R_I must be strictly in a permissible range all the time. In solutions A and B , the largest possible concentration change from its normal operating condition at the outlet of stream R_I is evaluated as 0.0014 which is within the permissible range. In solutions C , D , and E , however, the target concentration fluctuations of stream R_I are always far beyond the limits. Overall, solutions A and B are superior to the others.

According to Huang and Fan (1994), solutions A through E have the structural controllability index values of 0.581, 0.484, 0.355, 0.258, and 0.226, respectively. This suggests a superiority order for the solutions. However, solution A is still not highly controllable, since the index value is much less than 1. The results obtained by the proposed model show the same order of structural superiority as that by Huang and Fan (1994). However, the model provides much more precise results in terms of concentration fluctuations of all process streams. Thus, we are confident that solutions A and B are definitely highly controllable, not less controllable as suggested by Huang and Fan (1994).

Phenol waste minimization in a phenol solvent extraction process. The flowsheet of a phenol solvent extraction process is illustrated in Fig. 4.7 (Nelson, 1969). In this process, waste streams come from three process units, i.e., the raffinate tower, the water/phenol tower, and the extract stripper. These streams are mixed first and then fed to the absorber where phenol can be absorbed by heated lubricating oil stocks. It has been found that the phenol concentration in the effluent stream is much higher than the limit (≤ 0.002).

reducing the phenol concentration in the mixed stream to the tolerable range of 0.002. It is also found that mixing all phenol-containing rich streams is thermodynamically inefficient.

Table 4.3. Stream Data for the Phenol Solvent Extraction Problem

Stream No.	C^s	C^t	M (kg/s)	δC^s	δM (kg/s)	δC^t
R_1	0.15	0.002	4.3	0.0055	0.010	0.0003
R_2	0.10	0.001	1.5	0.0070	0.015	0.0002
R_3	0.07	0.0015	3.2	0.0063	0.010	0.0001
L_1	0.002	0.08	12.0	0.0002	0	0.0060
L_2	0.0007	≤ 0.01	≤ 11.0	0	0	-

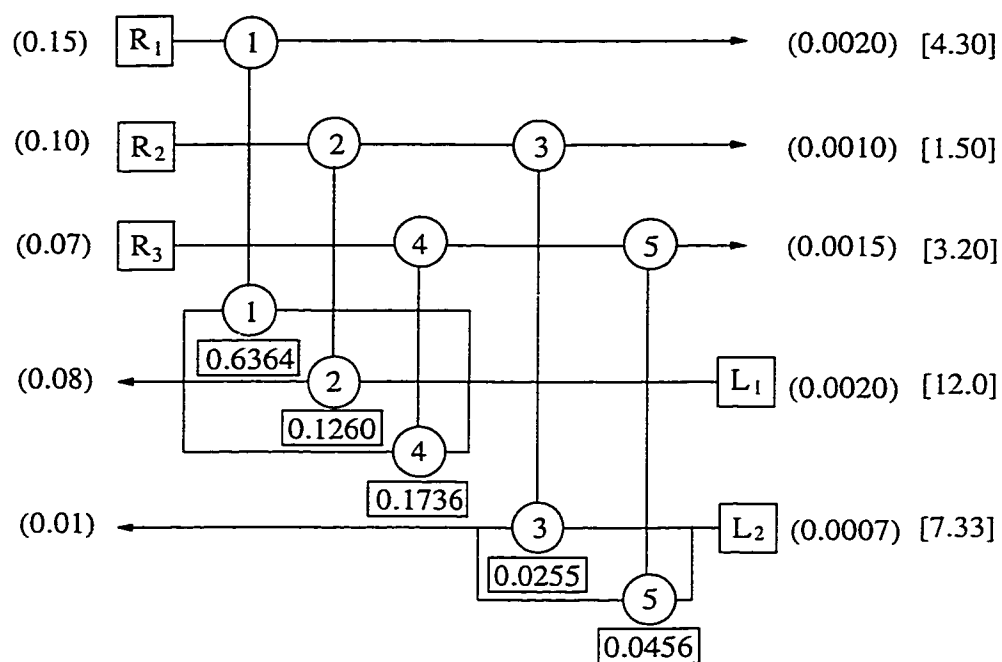
The pinch point of the system is located in the lean end of the mass composite curve, i.e., the concentrations of 0.0007 for lean stream L_2 and 0.00222 for rich streams R_1 , R_2 , and R_3 . The minimum consumption of MSA is 0.0681 kg/s with at least five units. This problem has three alternative solutions as illustrated in Fig. 4.8 (Huang and Edgar, 1995).

The system model in Eq. (4.48) is used to evaluate all three alternatives and examine the maximum phenol concentration ranges at the outlet of each rich stream. For each alternative, we define the following two disturbance source vectors and one control target vector.

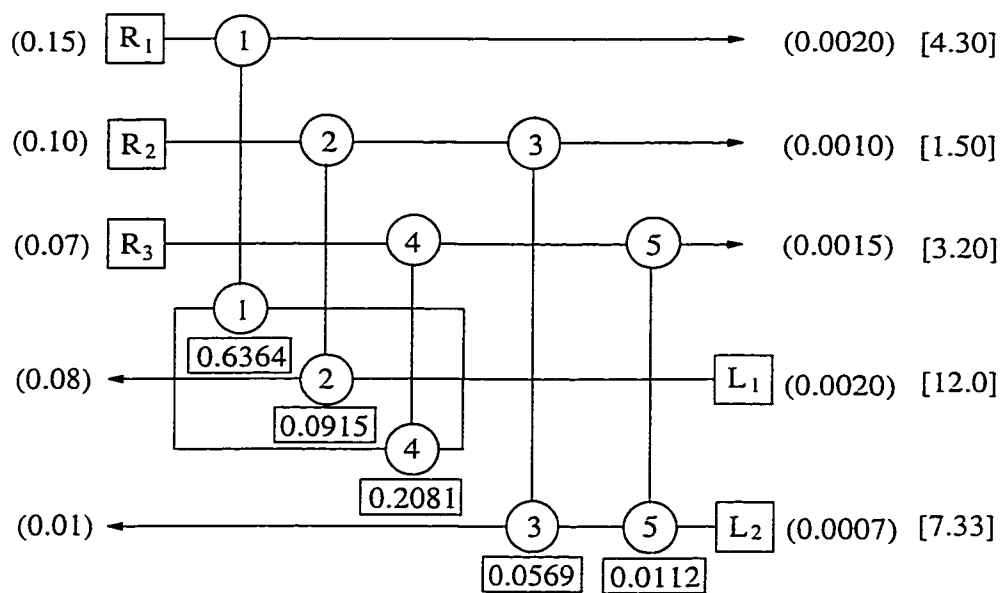
$$\delta \underline{M} = \left(\delta M_{r_1} \quad \delta M_{r_2} \quad \delta M_{r_3} \quad \delta M_{l_1} \quad \delta M_{l_2} \right)^T \quad (4.106)$$

$$\delta \underline{C}^s = \left(\delta C_{r_1}^s \quad \delta C_{r_2}^s \quad \delta C_{r_3}^s \quad \delta C_{l_1}^s \quad \delta C_{l_2}^s \right)^T \quad (4.107)$$

$$\delta \underline{C}^t = \left(\delta C_{r_1}^t \quad \delta C_{r_2}^t \quad \delta C_{r_3}^t \quad \delta C_{l_1}^t \quad \delta C_{l_2}^t \right)^T \quad (4.108)$$



(a) Solution A



(b) Solution B

Figure 4.8. Grid diagrams of the MEN in the phenol solvent extraction process.

The fluctuation ranges of the target concentrations in each solution are summarized in Table 4.4. All three solutions are acceptable from the standpoint of control of the toxic chemical.

Huang and Edgar (1995) used their structural controllability index to evaluate solutions A through C and gave the values of 0.773, 0.682, and 0.636, respectively. These results demonstrate that two different approaches give a good agreement in general. While Huang and Edgar (1995) provide an approximate measurement of process structural controllability, the system model in this work produces truly reliable information of DP through a process. Thus, those streams potentially violating regulations can be easily detected.

Table 4.4. Comparison of the Concentration Fluctuations at the Stream Outlets in Three Solution Alternatives for the Phenol Solvent Extraction Problem

Target Conc.	Control Requirement	Sol. A	Sol. B	Sol. C
$\delta C_{r_1}^t$	≤ 0.0003	≤ 0.0003	≤ 0.0003	≤ 0.0003
$\delta C_{r_2}^t$	≤ 0.0002	≤ 0.0001	≤ 0.0002	≤ 0.0001
$\delta C_{r_3}^t$	≤ 0.0001	≤ 0.0001	≤ 0.0001	≤ 0.0001
$\delta C_{l_1}^t$	≤ 0.0060	≤ 0.0043	≤ 0.0044	≤ 0.0043
$\delta C_{l_2}^t$	-	≤ 0.0010	≤ 0.0009	≤ 0.0010

CHAPTER 5

DESIGN OF HIGHLY CONTROLLABLE HEAT-INTEGRATED DISTILLATION PROCESSES

5.1 Introduction

Heat integration has been practiced in the design of distillation column systems to recover energy (Ho and Keller, 1987; Gross *et al.*, 1994). An effective approach is the heat integration between a condenser in one column and a reboiler in another to recover energy. However, such heat integration must introduce various interactions among process units. If a design is structurally inappropriate, it can cause various operational problems that may not be solvable through control system design (Barton *et al.*, 1992). In a distillation column system, various short-term and long-term disturbances enter it through feed streams, reboilers and condensers to influence on its separation quality and operational stability. Thus, how to design a system that can withstand the disturbances becomes a bottleneck for successful heat integration. Various design methods have been introduced to develop highly flexible column systems (Bagajewicz and Manousiouthakis, 1992; Hoch *et al.*, 1995). Luyben and Floudas (1994a, b) provided a systematic procedure for incorporating open-loop steady-state measures of controllability with a mathematical programming approach of process synthesis. The procedure was successfully applied to binary distillation synthesis. Elliott and Luyben (1995) proposed a capacity-based economic approach that was used to screen preliminary plant design by quantifying both steady-state economics and dynamic controllability. On the other hand, control engineers have tried to solve heat integration-related operational problems by

developing more robust control configurations; surely, the process design using the control algorithm must be controllable (Haggblom and Waller, 1990; Koggersbol *et al.*, 1996).

The notion of structural controllability involves how easily a process can reject disturbances structurally, how severely its variables interact, and how easily it can move from one operating condition to another. Thus, the characterization of structural disturbance propagation (DP) is the first step towards the integration of a highly structurally controllable process. It is conceivable that rigorous models for heat-integrated distillation column systems must be highly nonlinear due to inherent complexity. This makes their applications to enhancing structural disturbance rejection in early stages of process integration very difficult. This barrier, however, can be removed if the models are simplified to linear ones.

In this chapter, a set of steady state, first-principles-based, and simplified linear models are introduced to characterize DP through distillation column systems. The models enable us to analyze DP and identify potential operational problems in a systematic manner. Structural deficiencies in heat-integrated process can be readily detected and eliminated. Note that this development must be much more difficult than those for HEN's and mass exchanger networks (MEN's) (Yang *et al.*, 1996; Yang and Huang, 1998) since the fluctuations of temperatures, concentrations, and pressures in column systems should all be characterized simultaneously. The models developed in this chapter are particularly useful for the process analysis and evaluation in early stages of process integration. The capability of model applications is demonstrated by tackling two industrial problems.

5.2 Motivation

An introduction of heat integration between two columns can significantly reduce energy consumption. However, an improper integration may lead to various process operational problems. This can be illustrated by the following industrial example.

As shown in Fig. 5.1, feed streams A and B are, respectively, entered to columns C_1 and C_2 . The overhead stream of column C_2 , after splitting, is used to provide heat to the reboiler of column C_1 . A trim condenser is designed to condense the remaining heat of the overhead stream. In order to maintain the purity of the overhead product stream of column C_1 and the bottom product stream of column C_2 , heat duty for each reboiler should be varied. However, the changes of reboiler duty can disturb the operating pressures in the columns, which apparently leads to the temperature changes in the bottom stream of column C_1 and the overhead stream of column C_2 . The worst situation will occur when the driving force in the reboiler of column C_1 approaches to zero, which may lead to the process eventually inoperable. For effective heat integration in column systems, therefore, it is very important to carefully examine the potential integration and process operability. This requires the development of reliable models for process evaluation.

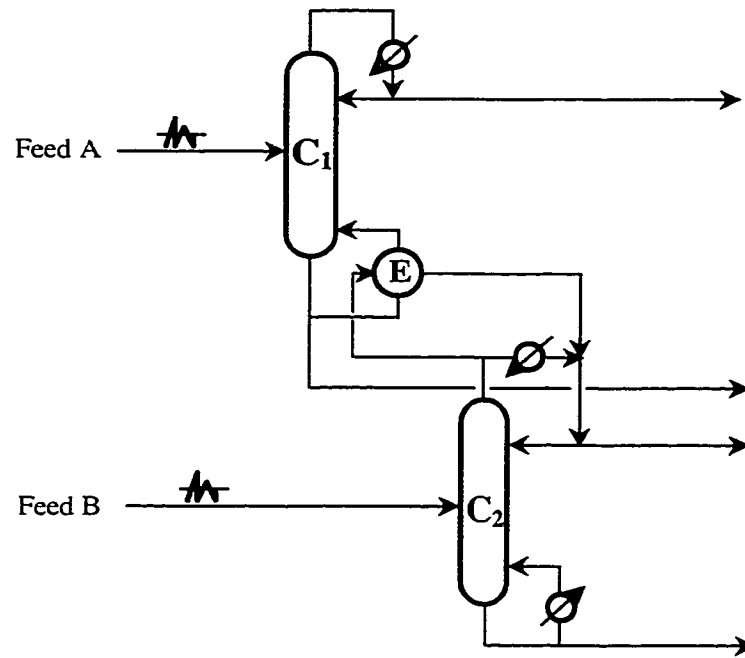


Figure 5.1. A heat integrated column process.

5.3 Basic Distillation Column Model

A typical distillation column system is sketched in Fig. 5.2. In the column, the feed stream F of mass fraction x_f enters at temperature T_f . Through separation, two product streams are generated: the overhead stream D of mass fraction x_d at temperature T_d and the bottom stream B of mass fraction x_b at temperature T_b . For the column, the overall mass balance, component mass balance, and overall energy balance are given below (McCabe *et al.*, 1993; Seader and Henley, 1998).

$$F = D + B \quad (5.1)$$

$$Fx_f = Dx_d + Bx_b \quad (5.2)$$

$$FH_f + Q_b = DH_d^l + BH_b^l + Q_c \quad (5.3)$$

The relationship between instantaneous top and bottom mass fractions can be expressed by the Fenske equation (King, 1981),

$$x_d = \frac{x_b \alpha^{N_{min}}}{1 + (\alpha^{N_{min}} - 1)x_b} \quad (5.4)$$

The basic assumption of the equation is an equimolar overflow and an ideal binary mixture where the relative volatility, α , is weakly dependent on temperature.

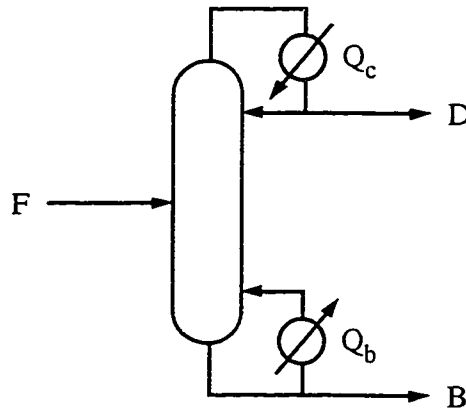


Figure 5.2. A typical continuous distillation column system.

5.4 Modeling for Disturbance Propagation

The DP models can be developed based on the above steady-state models. The new models must show how the system outputs at the top and bottom of a column are fluctuated when any disturbances appear in the feed stream, the reboiler, and/or the condenser.

5.4.2 Temperature dependent enthalpy change

In Eq. (5.7), enthalpy change need be converted to temperature change. In a steady state, the enthalpies of binary mixtures in the distillate and bottom streams can be expressed in the following general form (Smith and Van Ness, 1987),

$$H_s^l = x_s H_{s1}^l + (1 - x_s) H_{s2}^l + \Delta H_m^l \quad (5.10)$$

where subscript s can be d for the distillate stream, or b for the bottom stream. H_{s1}^l and H_{s2}^l are, respectively, the enthalpies of pure components 1 and 2 in a stream represented. ΔH_m^l is the heat of mixing; it can be treated as a constant when temperature and composition changes are insignificant in an ideal mixture. The disturbance equation can be correspondingly derived by differentiating Eq. (5.10), i.e.,

$$\delta H_s^l = x_s \delta H_{s1}^l + (1 - x_s) \delta H_{s2}^l + (H_{s1}^l - H_{s2}^l) \delta x_s \quad (5.11)$$

If we assume that the heat capacity for each component is constant for a disturbed temperature, then the following relationship holds.

$$\delta H_{si}^l = C_{P_{si}}^l \delta T_s \quad i = 1, 2 \quad (5.12)$$

Substituting Eq. (5.12) into Eq. (5.11) gives

$$\delta H_s^l = C_{P_s}^l \delta T_s + \left(\frac{H_s^l - H_{s2}^l}{x_s} \right) \delta x_s \quad (5.13)$$

where

$$C_{P_s}^l = x_s C_{P_{s1}}^l + (1 - x_s) C_{P_{s2}}^l \quad (5.14)$$

Equations (5.13) and (5.14) are general for either distillate stream or bottom stream.

Substituting them into Eq. (5.7) gives

$$F\delta H_f + H_f\delta F + \delta Q_b - \delta Q_c = H_d^l\delta D + a_2\delta x_d + a_3\delta T_d + H_b^l\delta B + a_4\delta x_b + a_5\delta T_b \quad (5.15)$$

where

$$a_2 = \frac{D(H_d^l - H_{d_2}^l)}{x_d} \quad (5.16)$$

$$a_3 = DC_{P_d}^l \quad (5.17)$$

$$a_4 = \frac{B(H_b^l - H_{b_2}^l)}{x_b} \quad (5.18)$$

$$a_5 = BC_{P_b}^l \quad (5.19)$$

To this end, four DP models have been developed; they are Eqs. (5.5), (5.6), (5.8), and (5.15). Since there are totally six output disturbance variables for a distillation column system, two more equations are needed.

5.4.3 Fluctuation of output temperatures

The fluctuations of mass fractions, temperatures, and pressures can cause a bubble point change. For the distillate stream, an equilibrium constant can be expressed as

$$K_d = \frac{P_d^o}{P_d} \quad (5.20)$$

where P_d^o is the saturated vapor pressure of a pure component under a given system

temperature. According to the Antoine's equation, we have

$$P_d^o = \alpha_p \exp\left(\frac{\beta_p}{T_d}\right) \quad (5.21)$$

where α_p and β_p are constants for a given temperature range. They can be obtained from open literature or calculated from known steady-state data.

To estimate the bubble point of a binary mixture, the following relationship for the distillate stream must hold.

$$y_{d1} + y_{d2} = K_{d1} x_d + K_{d2} (1 - x_d) = 1 \quad (5.22)$$

Substituting Eqs. (5.20) and (5.21) into Eq. (5.22) gives

$$\alpha_{p1} \exp\left(\frac{\beta_{p1}}{T_d}\right) x_d + \alpha_{p2} \exp\left(\frac{\beta_{p2}}{T_d}\right) (1 - x_d) = P_d \quad (5.23)$$

Assume that the pressure fluctuations at the top and bottom of a column are the same and designated δP . Differentiating Eq. (5.23) generates the following equation,

$$\delta T_d = a_6 \delta x_d - a_7 \delta P \quad (5.24)$$

where

$$a_6 = \frac{T_d^2 (P_{d1}^o - P_{d2}^o)}{\beta_{p1} x_d P_{d1}^o + \beta_{p2} (1 - x_d) P_{d2}^o} \quad (5.25)$$

$$a_7 = \frac{T_d^2}{\beta_{p1} x_d P_{d1}^o + \beta_{p2} (1 - x_d) P_{d2}^o} \quad (5.26)$$

Similarly, the fluctuation of the bottom stream temperature can be derived as a function of the fluctuated mass fraction and pressure as follows,

$$\delta T_b = a_8 \delta x_b - a_9 \delta P \quad (5.27)$$

be derived similar to that in liquid form, δH_d^l . Or simply, we can replace l (liquid phase) by v (vapor phase) and x by y in Eqs. (5.10), (5.11), and (5.13). The new equations are:

$$H_d^v = y_d H_{d1}^v + (1 - y_d) H_{d2}^v + \Delta H_m^v \quad (5.32)$$

$$\delta H_d^v = y_d \delta H_{d1}^v + (1 - y_d) \delta H_{d2}^v + (H_{d1}^v - H_{d2}^v) \delta y_d \quad (5.33)$$

$$\delta H_d^v = C_{P_d}^v \delta T_d^* + \left(\frac{H_{d1}^v - H_d^v}{1 - y_d} \right) \delta y_d \quad (5.34)$$

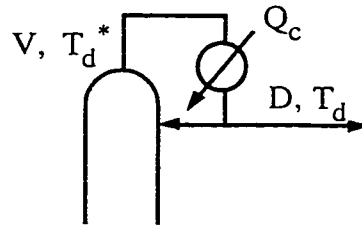


Figure 5.3. Representation of energy balance for the condenser.

For a total condenser, we have

$$y_d = x_d \quad (5.35)$$

Thus, Eq. (5.34) can be rewritten as

$$\delta H_d^v = C_{P_d}^v \delta T_d^* + \left(\frac{H_{d1}^v - H_d^v}{1 - x_d} \right) \delta x_d \quad (5.36)$$

where δT_d^* is the temperature fluctuation on the top tray of the column. It can be evaluated based on the dew point change on the tray. The basic equation for determining the dew point of a mixture is given by

$$\frac{x_d}{K_{d_1}^*} + \frac{1-x_d}{K_{d_2}^*} = 1 \quad (5.37)$$

Similar to the derivation of Eqs. (5.23) and (5.24), we can have

$$\frac{x_d}{\alpha_{p_1} \exp\left(\frac{\beta_{p_1}}{T_d^*}\right)} + \frac{1-x_d}{\alpha_{p_2} \exp\left(\frac{\beta_{p_2}}{T_d^*}\right)} = \frac{1}{P_d} \quad (5.38)$$

and

$$\delta T_d^* = \left(\frac{(T_d^*)^2 \left(\frac{1}{P_{d_2}^o} - \frac{1}{P_{d_1}^o} \right)}{\frac{x_d \beta_{p_1}}{P_{d_1}^o} + \frac{(1-x_d) \beta_{p_2}}{P_{d_2}^o}} \right) \delta x_d - \left(\frac{(T_d^*)^2 \left(\frac{1}{P_d^2} \right)}{\frac{x_d \beta_{p_1}}{P_{d_1}^o} + \frac{(1-x_d) \beta_{p_2}}{P_{d_2}^o}} \right) \delta P \quad (5.39)$$

where

$$P_{d_1}^o = \alpha_{p_1} \exp\left(\frac{\beta_{p_1}}{T_d^*}\right) \quad (5.40)$$

$$P_{d_2}^o = \alpha_{p_2} \exp\left(\frac{\beta_{p_2}}{T_d^*}\right) \quad (5.41)$$

T_d^* is the temperature on the top tray. It can be evaluated based on Eq. (5.37). Assume that

$$\gamma = \frac{K_{d_1}}{K_{d_2}} = \frac{K_{d_1}^*}{K_{d_2}^*} \quad (5.42)$$

where K_{d_i} is given by Eq. (5.20). By solving Eqs. (5.37), (5.40) through (5.42), T_d^* has the following form,

$$T_d^* = \frac{\beta_{pI}}{\ln\left(\frac{p_d(x_d + \gamma(I - x_d))}{\alpha_{pI}}\right)} \quad (5.43)$$

Substituting Eq. (5.39) into Eq. (5.36) and then Eqs. (5.36), (5.13), and (5.24) into Eq. (5.31), we can obtain the expression of δP , i.e.,

$$\delta P = \frac{a_{11}}{a_{10} - a_3 a_7} \delta D + \frac{a_{12} - a_3 a_6}{a_{10} - a_3 a_7} \delta x_d - \frac{a_{13}}{a_{10} - a_3 a_7} \delta Q_c \quad (5.44)$$

where

$$a_{10} = D \left(\frac{(T_d^*)^2 \left(\frac{C_{p_d}^v}{P_d^2} \right)}{\frac{x_d \beta_{pI}}{P_{d1}^o} + \frac{(I - x_d) \beta_{p2}}{P_{d2}^o}} \right) \quad (5.45)$$

$$a_{11} = (H_d^v - H_d^l) \quad (5.46)$$

$$a_{12} = D \left(\frac{H_{d1}^v - H_d^v}{I - x_d} + \frac{C_{p_d}^v (T_d^*)^2 \left(\frac{I}{P_{d2}^o} - \frac{I}{P_{d1}^o} \right)}{\frac{x_d \beta_{pI}}{P_{d1}^o} + \frac{(I - x_d) \beta_{p2}}{P_{d2}^o}} - \frac{H_d^l - H_{d2}^l}{x_d} \right) \quad (5.47)$$

$$a_{13} = \frac{I}{I + R} \quad (5.48)$$

With Eq. (5.44), we can eliminate intermediate variable δP in Eqs. (5.24) and (5.27). This results in the following two equations.

$$\delta T_d = \frac{a_6 a_{10} - a_7 a_{12}}{a_{10} - a_3 a_7} \delta x_d - \frac{a_7 a_{11}}{a_{10} - a_3 a_7} \delta D + \frac{a_7 a_{13}}{a_{10} - a_3 a_7} \delta Q_c \quad (5.49)$$

$$\delta T_b = a_8 \delta x_b - \frac{a_9 a_{11}}{a_{10} - a_3 a_7} \delta D - \frac{a_9 (a_{12} - a_3 a_6)}{a_{10} - a_3 a_7} \delta x_d + \frac{a_9 a_{13}}{a_{10} - a_3 a_7} \delta Q_c \quad (5.50)$$

5.4.5 Overall disturbance propagation model

Based on the derivations in preceding sections, we have all required equations for six output disturbance variables: Eqs. (5.5), (5.6), (5.8), (5.15), (5.49), and (5.50). These equations can be lumped to form an overall DP model in matrix form as follows,

$$\begin{pmatrix} A_1 & 0 \\ 0 & A_2 \end{pmatrix} \begin{pmatrix} \delta Y_1 \\ \delta Y_2 \end{pmatrix} = \begin{pmatrix} A_3 & A_4 \\ A_5 & A_6 \end{pmatrix} \begin{pmatrix} \delta X_1 \\ \delta X_2 \end{pmatrix} \quad (5.51)$$

equivalently,

$$\begin{pmatrix} \delta Y_1 \\ \delta Y_2 \end{pmatrix} = \begin{pmatrix} A_1^{-1} A_3 & A_1^{-1} A_4 \\ A_2^{-1} A_5 & A_2^{-1} A_6 \end{pmatrix} \begin{pmatrix} \delta X_1 \\ \delta X_2 \end{pmatrix} \quad (5.52)$$

or simply,

$$\delta Y = A \delta X \quad (5.53)$$

where

$$\delta Y = (\delta Y_1 \quad \delta Y_2)^T \quad (5.54)$$

$$\delta X = (\delta X_1 \quad \delta X_2)^T \quad (5.55)$$

$$\delta Y_1 = (\delta D \quad \delta x_d \quad \delta T_d)^T \quad (5.56)$$

$$\delta Y_2 = (\delta B \quad \delta x_b \quad \delta T_b)^T \quad (5.57)$$

$$\delta X_1 = (\delta F \quad \delta x_f \quad \delta H_f)^T \quad (5.58)$$

$$\delta X_2 = (\delta Q_c \quad \delta Q_b)^T \quad (5.59)$$

$$A = \begin{pmatrix} A_1^{-1} A_3 & A_1^{-1} A_4 \\ A_2^{-1} A_5 & A_2^{-1} A_6 \end{pmatrix} \quad (5.60)$$

$$A_1 = \begin{pmatrix} (x_d - x_b) & \left(D + \frac{B}{a_1}\right) & 0 \\ b_1 & b_2 & a_3 \\ b_4 & -b_5 & b_6 \end{pmatrix} \quad (5.61)$$

$$A_2 = \begin{pmatrix} (x_b - x_d) & (a_1 D + B) & 0 \\ b_7 & b_8 & a_5 \\ b_4 & b_{11} & -b_{12} \end{pmatrix} \quad (5.62)$$

$$A_3 = \begin{pmatrix} (x_f - x_b) & F & 0 \\ (H_f - H_b^I) & 0 & F \\ 0 & 0 & 0 \end{pmatrix} \quad (5.63)$$

$$A_4 = \begin{pmatrix} 0 & 0 \\ -b_3 & I \\ I & 0 \end{pmatrix} \quad (5.64)$$

$$A_5 = \begin{pmatrix} (x_f - x_d) & F & 0 \\ b_9 & 0 & F \\ b_4 & 0 & 0 \end{pmatrix} \quad (5.65)$$

$$A_6 = \begin{pmatrix} 0 & 0 \\ -b_{10} & I \\ -I & 0 \end{pmatrix} \quad (5.66)$$

Equation (5.53) shows a linear relationship between a set of five input disturbance variables and a set of six output disturbance variables. The elements in submatrices A_i

through A_6 are determined by the steady-state information. The constants b_1 through b_{12}

in relevant elements are in the following forms.

$$b_1 = H_d^l - H_b^l - \frac{a_5 a_9 a_{11}}{a_{10} - a_3 a_7} \quad (5.67)$$

$$b_2 = a_2 + \frac{a_4 + a_5 a_8}{a_1} - \frac{a_5 a_9 (a_{12} - a_3 a_6)}{a_{10} - a_3 a_7} \quad (5.68)$$

$$b_3 = 1 + \frac{a_5 a_9 a_{13}}{a_{10} - a_3 a_7} \quad (5.69)$$

$$b_4 = \frac{a_{11}}{a_{13}} \quad (5.70)$$

$$b_5 = \frac{a_6 a_{10} - a_7 a_{12}}{a_7 a_{13}} \quad (5.71)$$

$$b_6 = \frac{a_{10} - a_3 a_7}{a_7 a_{13}} \quad (5.72)$$

$$b_7 = H_b^l - H_d^l + \frac{a_7 a_{10} a_{11}}{a_{10} - a_3 a_7} \quad (5.73)$$

$$b_8 = a_1 a_2 + a_4 + \frac{a_1 a_{10} (a_6 a_{10} - a_7 a_{12})}{a_{10} - a_3 a_7} \quad (5.74)$$

$$b_9 = H_f - H_d^l + \frac{a_{10} a_7 a_{11}}{a_{10} - a_7 a_3} \quad (5.75)$$

$$b_{10} = 1 + \frac{a_7 a_{10} a_{13}}{a_{10} - a_3 a_7} \quad (5.76)$$

$$b_{11} = \frac{a_8 (a_{10} - a_3 a_7) - a_1 a_9 (a_{12} - a_3 a_6)}{a_9 a_{13}} \quad (5.77)$$

$$b_{12} = \frac{a_{10} - a_3 a_7}{a_9 a_{13}} \quad (5.78)$$

5.5 Case Studies

The DP model in Eq. (5.53) has been used to tackle a variety of distillation process design problems. Two examples are delineated in this section. The first one is to demonstrate the precision of the model prediction, as compared with the simulation results from a HYSYS simulator. The second one is to illustrate a model-based process modification.

5.5.1 Pentane-benzene binary separation process

The separation of a pentane-benzene mixture in a column is typical in the petrochemical industries. A nominal operating condition of the column is listed in Table 5.1. The column has 12 trays with reflux ratio R of 1.35. The desired purity for overhead and bottom product streams can be achieved when the process is operated under a stable condition.

The disturbances in the feed stream (δF , δX_f , and δH_f), the reboiler (δQ_b), and the condenser (δQ_d) are given in Table 5.2. Note that some of the disturbances, such as δH_f , are very severe. The model in Eq. (5.53) is used to evaluate the fluctuations of the overhead and bottom streams and the pressure perturbation in the column. The input and output vectors for the process are defined, respectively, as

$$\mathbf{A} = \begin{pmatrix} 0.0540 & 654.2 & 0.1862 & 7.815 \times 10^{-4} & 3.052 \times 10^{-4} \\ 0.0005 & 0.0067 & -0.0002 & -8.400 \times 10^{-7} & -3.200 \times 10^{-7} \\ 0.0087 & 1204.6 & 0.3822 & -6.452 \times 10^{-4} & 6.265 \times 10^{-4} \\ 0.9460 & -654.2 & -0.1862 & -7.815 \times 10^{-4} & -3.052 \times 10^{-4} \\ 0.0008 & 0.0121 & -0.0004 & -1.500 \times 10^{-6} & -6.300 \times 10^{-7} \\ -0.1114 & 1588.4 & -0.1114 & -6.303 \times 10^{-4} & 9.136 \times 10^{-4} \end{pmatrix} \quad (5.81)$$

Each element in matrix \mathbf{A} represents the severity of DP from a disturbance source to a process output. After the process output fluctuations are estimated, the pressure perturbation of the column can be then obtained by Eq. (5.44). As a comparison, the distillation process was simulated by a HYSYS simulator where various rigorous models are embedded. Table 5.3 summarizes the results from the simplified model and that from the simulator. The prediction errors in the last column of Table 5.3 show the difference between the HYSYS and the model results. Clearly, the model prediction is well acceptable for process analysis.

Table 5.3. Simulation Results for the Binary Separation System

Output variable	Unit	Simplified model	HYSYS simulator	Prediction Error
$D + \delta D$	kg/h	294.69	295.41	0.72
$x_d + \delta x_d$	wt. %	94.62	93.92	-0.70
$T_d + \delta T_d$	°K	331.53	331.77	0.24
$B + \delta B$	kg/h	325.31	324.59	-0.72
$x_b + \delta x_b$	wt. %	0.50	0.60	0.10
$T_b + \delta T_b$	°K	393.16	392.54	-0.62
$P + \delta P$	kPa	196.9	200.0	3.10

In this case study, the simplified model demonstrates its advantages as (i) model simplicity, (ii) requirement of only limited process design data, and (iii) fast computation with well acceptable precision. All those facilitate the adoption of the models for identifying a highly controllable distillation column system. As a comparison, there is some inconvenience in using a HYSYS. In the simulator, two sets of operating conditions are needed: one for a normal operation, and the other for the operation when disturbances are exerted. The HYSYS needs to run twice to obtain simulation results. The difference of the output results under two operating conditions reflects the deviation of the process outputs.

5.5.2 Modification of a heat integrated distillation column process

A heat integrated column process is shown in Fig. 5.4. In this system, feed streams S_1 and S_2 are preheated by stream S_3 through heat exchangers E_1 and E_2 , respectively. In this design, the heat required in reboilers is provided by steam, while the heat in condensers is released to cooling water. The nominal operational data of the process is listed in Table 5.4. It is desired to identify the best design for energy recovery, while the product quality can be maintained, especially for the overhead stream of column C_1 whose purity is critical.

Disturbances in this process include (i) the perturbations of mass flowrates, temperatures, and mass fraction of the key component in streams S_1 and S_2 , and (ii) the source temperature fluctuation of stream S_3 . Their magnitudes are listed in Table 5.5.

These disturbances can cause very unstable operation in columns C_1 and C_2 , if heat integration is improper.

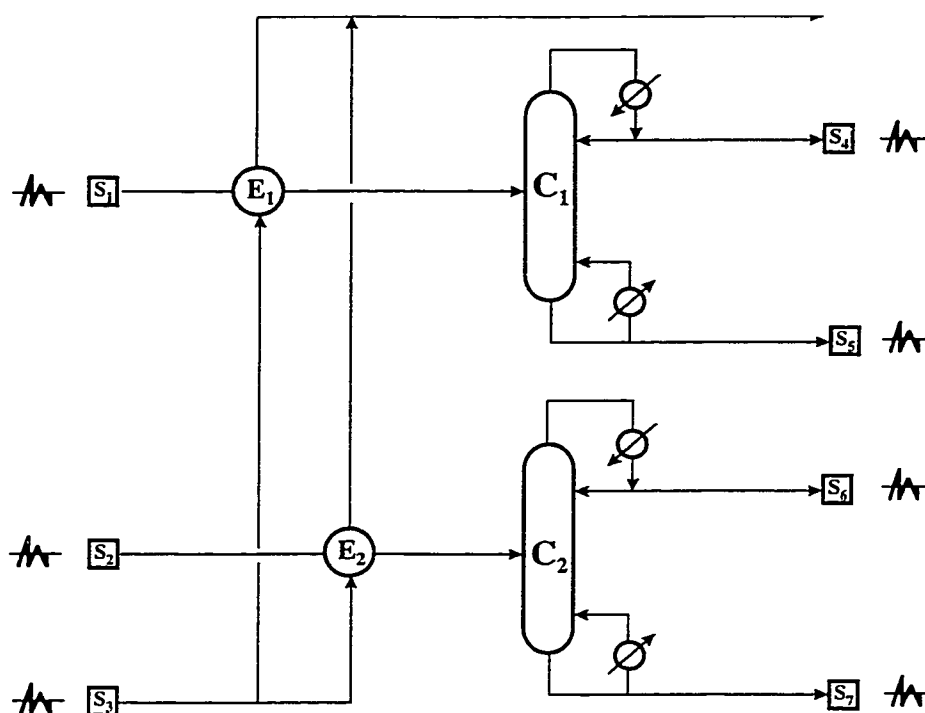


Figure 5.4. Flowsheet of an original distillation process.

Table 5.4. Steady-State Data of the Heat Integrated Column Process

Process Variable	Symbol	Unit	Value
Mass flow rate of stream S_1	F_1	kg/h	620
Heat capacity of stream S_1	C_{p1}	kJ/kg-C	2.34
Mass fraction of stream S_1	xf_1	wt. %	27.0
Input temperature of stream S_1	T_{s1}	°K	393.15
Feed stream temperature of column C_1	T_{f1}	°K	453.15
Mass flow rate of stream S_2	F_2	kg/h	560
Heat capacity of stream S_2	C_{p2}	kJ/kg-C	3.30
Mass fraction of stream S_2	xf_2	wt. %	42.0
Input temperature of stream S_2	T_{s2}	°K	423.15
Feed stream temperature of column C_2	T_{f2}	°K	503.15
Mass flow rate of stream S_3	F_3	kg/h	900
Heat capacity of stream S_3	C_{p3}	kJ/kg-C	3.0
Input temperature of stream S_3	T_{s3}	°K	533.15
Output temperature of stream S_3	T_3	°K	450.55
Mass flow rate of stream S_4	D_1	kg/h	165.35
Mass fraction of stream S_4	xd_1	wt. %	99.3
Temperature of stream S_4	T_{d1}	°K	377.58
Heat load of the condenser in column C_1	Q_{c1}	kJ/h	1.6×10^5
Mass flow rate of stream S_5	B_1	kg/h	454.65
Mass fraction of stream S_5	xb_1	wt. %	0.4
Temperature of stream S_5	T_{b1}	°K	468.49
Heat load of the reboiler in column C_1	Q_{b1}	kJ/h	1.5×10^5
Mass flow rate of stream S_6	D_2	kg/h	234.83
Mass fraction of stream S_6	xd_2	wt. %	98.8
Temperature of stream S_6	T_{d2}	°K	479.39
Heat load of the condenser in column C_2	Q_{c2}	kJ/h	2.1×10^5
Mass flow rate of stream S_7	B_2	kg/h	325.17
Mass fraction of stream S_7	xb_2	wt. %	0.44
Temperature of stream S_7	T_{b2}	°K	579.15
Heat load of the reboiler in column C_2	Q_{b2}	kJ/h	2.8×10^5

$$\delta T_e^t = A_e \delta T_e^s \quad (5.82)$$

where

$$\delta T_e^t = (\delta T_h^t \quad \delta T_c^t)^T \quad (5.83)$$

$$\delta T_e^s = (\delta T_h^s \quad \delta T_c^s \quad \delta M c p_h \quad \delta M c p_c)^T \quad (5.84)$$

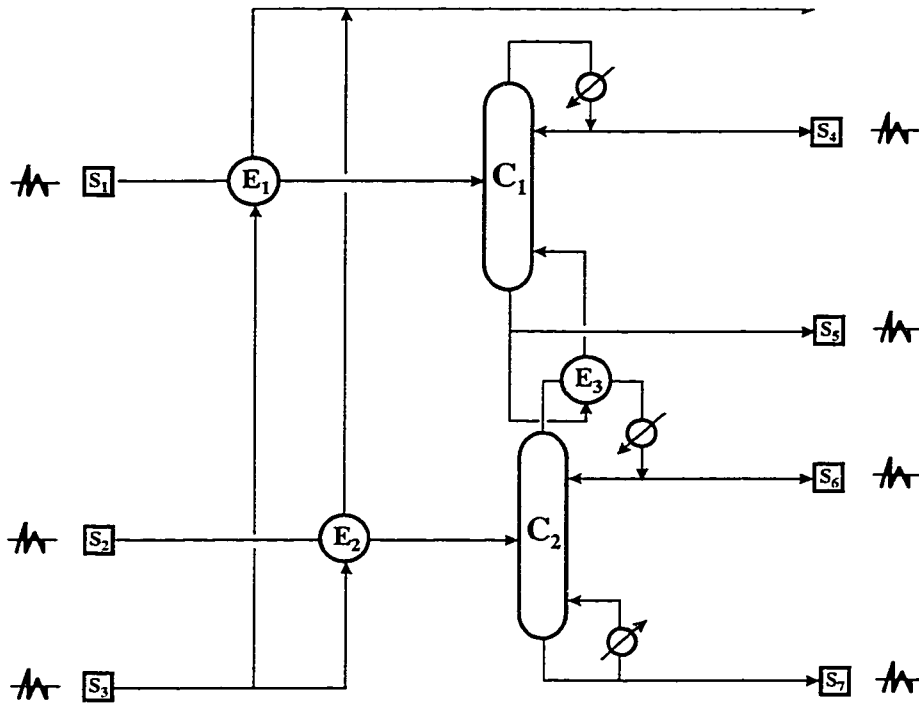


Figure 5.5. A heat-integrated distillation process (Solution A).

With this model and the column model in Eq. (5.53), we can develop the following system model for the whole process, using the procedure for a system model generation provided by Yang *et al.* (1996).

$$\delta Y = A_{sys} \delta X \quad (5.85)$$

where

$$\delta Y = \begin{pmatrix} \delta Y_1 & \delta Y_2 & \delta Y_3 & \delta Y_4 & \delta T_{s_2}^t \end{pmatrix}^T \quad (5.86)$$

$$\delta Y_1 = \begin{pmatrix} \delta D_1 & \delta x_{d_1} & \delta T_{d_1} \end{pmatrix}^T \quad (5.87)$$

$$\delta Y_2 = \begin{pmatrix} \delta B_1 & \delta x_{b_1} & \delta T_{b_1} \end{pmatrix}^T \quad (5.88)$$

$$\delta Y_3 = \begin{pmatrix} \delta D_2 & \delta x_{d_2} & \delta T_{d_2} \end{pmatrix}^T \quad (5.89)$$

$$\delta Y_4 = \begin{pmatrix} \delta B_2 & \delta x_{b_2} & \delta T_{b_2} \end{pmatrix}^T \quad (5.90)$$

$$\delta X = \begin{pmatrix} \delta X_1 & \delta T_{s_2}^s & \delta X_3 & \delta Q_{c_1} & \delta Q_{c_2} & \delta Q_{r_2} \end{pmatrix}^T \quad (5.91)$$

$$\delta X_1 = \begin{pmatrix} \delta F_1 & \delta x_{f_1} & \delta T_{s_1} \end{pmatrix}^T \quad (5.92)$$

$$\delta X_3 = \begin{pmatrix} \delta F_3 & \delta x_{f_3} & \delta T_{s_3} \end{pmatrix}^T \quad (5.93)$$

The computation using the model in Eq. (5.85) shows that, with the known entering disturbances, the purity of the overhead stream (S_4) of column C_1 of this solution can be as low as 98.78% which is 0.52% below the nominal value. It is expected to identify a better design with higher purity of the overhead under the same disturbance input condition. An alternative solution (Solution B) in Fig. 5.6 shows a change of the flow of stream S_3 . In this solution, the temperature fluctuation at the inlet of column C_1 can be significantly reduced from 2.67 °C in solution A to 0.011 °C in solution B. This results in a much more stable operation in column C_1 which reduces the purity fluctuation

from 0.52% to 0.3%, while the operation in column C_2 is still very stable. In addition, the temperature driving force in the reboiler of column C_1 increases by 3.5 °C in solution B compared with solution A. This can reduce the transfer area required in the reboiler and makes the process operation much safer. This suggests that solution B is more desirable than solution A. The conclusion is the same as that made by a HYSYS simulator after much more detailed simulation (see Appendix D for detailed steps). The computational results are given in Table 5.6.

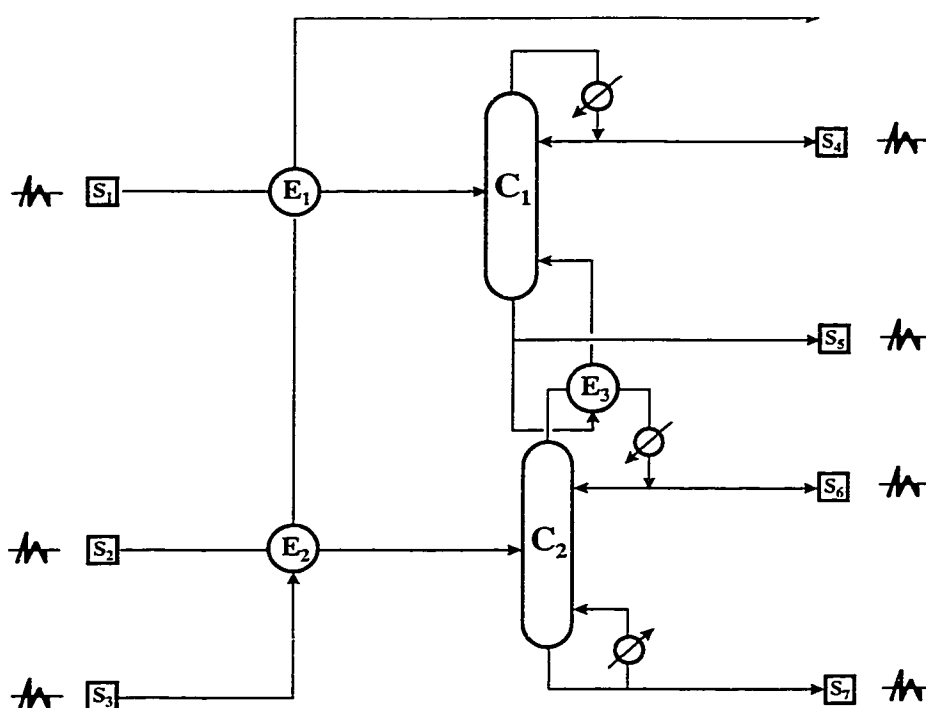


Figure 5.6. A modified distillation process (Solution B).

Table 5.6. Comparison of the Simulations for the Heat Integrated Column Process Alternatives

Output variable	Unit	Solution A			Solution B		
		Model	HYSYS	Prediction Error	Model	HYSYS	Prediction Error
$D_1 + \delta D_1$	kg/h	165.89	165.10	-0.79	165.08	164.3	-0.78
$x_{d_1} + \delta x_{d_1}$	wt. %	98.78	98.56	-0.22	99.0	99.16	0.16
$T_{d_1} + \delta T_{d_1}$	°K	381.28	381.35	0.07	377.48	377.65	0.17
$B_1 + \delta B_1$	kg/h	464.11	464.90	0.79	464.92	465.70	0.78
$x_{b_1} + \delta x_{b_1}$	wt. %	0.30	0.47	0.17	0.38	0.43	0.05
$T_{b_1} + \delta T_{b_1}$	°K	471.91	471.75	-0.16	468.37	468.45	0.08
$D_2 + \delta D_2$	kg/h	234.78	234.40	-0.38	234.77	234.60	-0.17
$x_{d_2} + \delta x_{d_2}$	wt. %	97.13	96.40	-0.73	97.14	96.37	-0.77
$T_{d_2} + \delta T_{d_2}$	°K	482.25	481.95	-0.30	482.22	482.15	-0.07
$B_2 + \delta B_2$	kg/h	320.22	320.60	0.38	320.23	320.40	0.17
$x_{b_2} + \delta x_{b_2}$	wt. %	0.34	0.50	0.16	0.36	0.51	0.15
$T_{b_{21}} + \delta T_{b_2}$	°K	580.55	580.85	0.30	580.54	580.95	0.41

effectively applied to minimize utility consumption in non-isothermal reaction processes (Glavic *et al.*, 1988a,b, 1990). While reaction processes become more and more integrated, various operational and environmental problems can be encountered if the reactor systems are improperly structured. Industrial practices have shown that various disturbances from separation and energy recovery systems surrounding reactor processes may lead to unmanageable reaction operations no matter how control systems are designed. Therefore, it is highly desirable to develop a controllable reaction process capable of rejecting disturbance propagation (DP) through the reaction system, especially for a heat-integrated non-isothermal reaction system.

Heretofore, nearly no publication has been found in the controllability aspect of reactor network synthesis. Shinskey (1995) identified a possible design problem leading to uncontrollable reaction operation. The improvement of structural controllability during reaction process development can greatly benefit process productivity and operability (Orr *et al.*, 1998).

In this chapter, a variety of simplified disturbance models are developed for the quick evaluation of DP through a reaction system and identification of the bottleneck for effective reaction process synthesis. The models are first-principles-based and in the linear form that facilitates to develop a synthesis strategy for integrating highly controllable reaction processes in a system level. The capability of the models is demonstrated by solving two practical example problems.

6.2 Motivation

A reaction is the heart of a chemical process. In most plants, the design of

reactors is the first step toward the overall process development. The success of reactor synthesis can significantly facilitate its relevant process integration to achieve maximum energy recovery, materials reduction and, more importantly, WM. The following example illustrates a typical heat-integrated reaction design problem.

A typical reaction process is depicted in Fig. 6.1. In this process, feed stream *A* is entered to a CSTR (R_1) with cooling jacket where an exothermic, isothermal, irreversible reaction is taken place. Feed stream *C* is in series fed to CSTR's R_2 and R_3 where a reversible and exothermic reaction is carried out adiabatically. In order to achieve higher conversion in reactor R_3 , an intermediate heat exchanger (*E*) is used to cool down the input temperature of the reactant stream in reactor R_3 . Feed stream *B* is used to absorb the heat released by reactor R_1 and then enter heat exchanger *E*. Because the reversible conversion in reactor R_3 is very sensitive to the inlet temperature of the reactant stream, it is highly desirable to maintain optimal inlet temperature to satisfy the productivity requirement. In this process, however, a severe disturbance exists in feed stream *A*, which propagates throughout the system to affect process operations, especially for the reaction conversion in reactor R_3 . The problem is in fact caused by process structural deficiency. Figure 6.2 shows a modified process flowsheet. With the splitting of feed stream *B*, the disturbance from feed stream *A* can be terminated through the reactor (R_3). In this modification, the process operation can be easily maintained regardless of the disturbance.

The example provides an analysis of an existing process structural problem. To identify a superior reaction structure, the quantification of DP is the first step toward disturbance rejection. This requires the development of DP models.

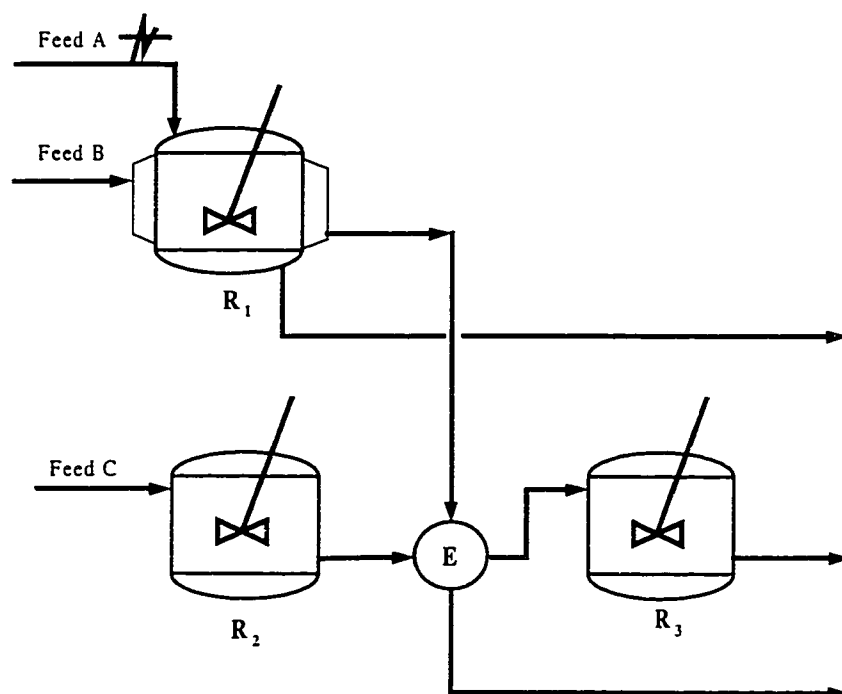


Figure 6.1. Flowsheet of a reactor network.

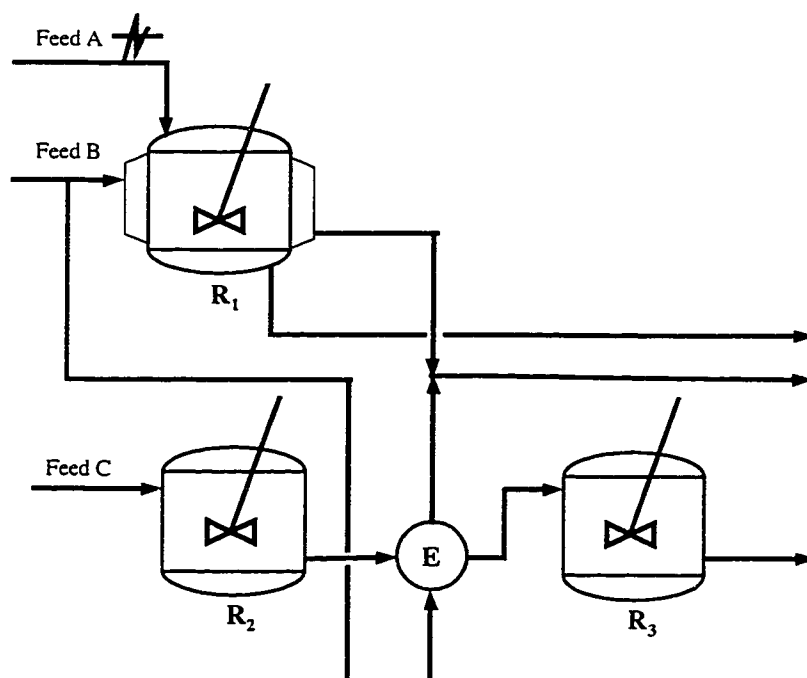


Figure 6.2. Modified process flowsheet.

Fundamental design basis. A general reaction process is depicted in Fig. 6.3. Feed streams containing n different reactants are entered to the reactor process at mole flow rate F_{jo} ($j \in n$); the rate of generation of species j in the reactor with a volume of V is determined by the reactor volume and the rate of formation of species j (r_j); The reaction converts reactants to the product at mole flow rate F_j ($j \in n$). In this process, mass and energy balances are respectively given as follows (Fogler, 1992).

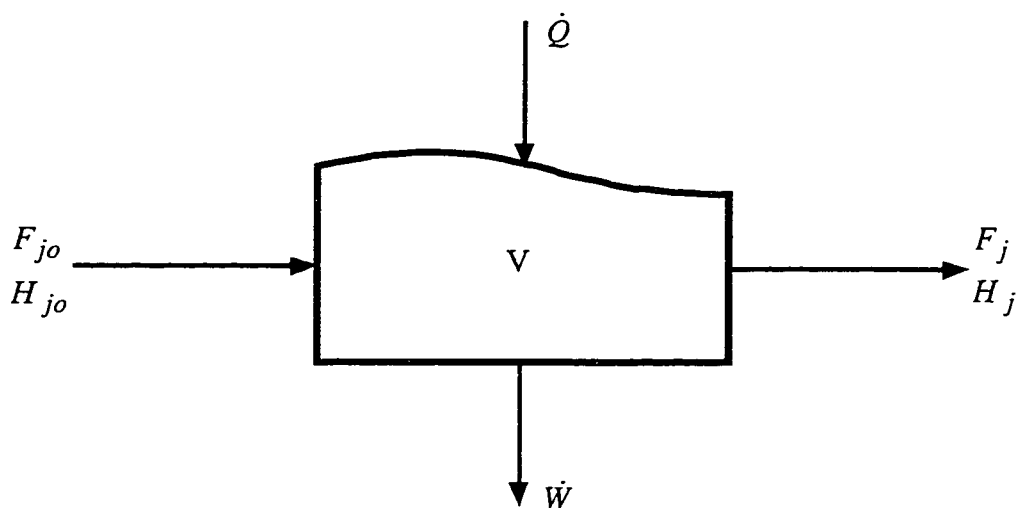


Figure 6.3. A continuous flow reaction process.

$$F_{jo} - F_j + \int_V r_j dV = \frac{dN_j}{dt} \quad (6.1)$$

$$\dot{Q} - \dot{W}_s + \sum_{j=1}^n F_{jo} H_{jo} - \sum_{j=1}^n F_j H_j = \left(\frac{dE}{dt} \right)_{sys} \quad (6.2)$$

where N_j is the number of moles of species j at time t in the system; \dot{Q} and \dot{W}_s are the

heat energy and shaft work flow to the reactor, respectively; H is the mole enthalpy; E is the energy in the system at time t .

In a chemical reaction, the conversion of reactants is largely determined by the kinetic mechanism, which is expressed by the following general rate law.

$$-r_A = k(T)f(C_A, C_B, \dots) \quad (6.3)$$

where k is the rate constant given by Arrhenius equation.

$$k(T) = A \exp\left(-\frac{E}{RT}\right) \quad (6.4)$$

The above fundamental equations can be more specific when typical reaction processes are taken into account. In the following, some homogeneous reaction cases are investigated, and their DP models are developed systematically.

Case 1. Liquid phase CSTR. Consider a simple case of an isothermal, irreversible, and first order reaction ($A \rightarrow B$). A feed stream containing chemical species A with concentration C_{Ao} enters to the reactor at mole flow rate F_{Ao} . After a reaction taken place, a product stream consisting of species A and B is generated at mole flow rate F_A/F_B with concentration C_A/C_B . The steady state mole balance and kinetic equation can be readily derived below based on the following two assumptions (i) constant density or constant volumetric flow rate v_T , and (ii) constant reaction rate r_A over whole reactor volume V .

$$-r_A = \frac{v_T}{V}(C_{Ao} - C_A) \quad (6.5)$$

$$-r_A = k_c C_A \quad (6.6)$$

Solving Eqs. (6.5) and (6.6) yields

$$C_A = \frac{C_{Ao}}{1 + \theta k_c} \quad (6.7)$$

where $\theta \left(= \frac{V}{v_T} \right)$ represents the resident time in a given reactor.

In this reaction process, disturbances include the concentration of species A and volumetric flow rate of the feed stream. These disturbances can propagate through the reactor to affect the reaction conversion and output concentrations of species A and P. To derive the disturbance equation, we start with the differentiation of Eq. (6.7), which gives rise to

$$\delta C_A = \frac{1}{1 + \theta k_c} \delta C_{Ao} + \frac{k_c C_{Ao} \theta}{v_T (1 + \theta k_c)^2} \delta v_T \quad (6.8)$$

$$\delta C_B = \delta C_{Ao} - \delta C_A = \left(1 - \frac{1}{1 + \theta k_c} \right) \delta C_{Ao} - \frac{k_c C_{Ao} \theta}{v_T (1 + \theta k_c)^2} \delta v_T \quad (6.9)$$

or, in the matrix form,

$$\delta \mathbf{C}^t = \mathbf{A} \delta C_{Ao} + \mathbf{B} \delta v_T \quad (6.10)$$

where

$$\delta \mathbf{C}^t = (\delta C_A \quad \delta C_B)^T \quad (6.11)$$

$$\mathbf{A} = (a_I \quad 1 - a_I)^T \quad (6.12)$$

$$\mathbf{B} = (b_I \quad -b_I)^T \quad (6.13)$$

$$a_I = \frac{1}{1 + \theta k_c} \quad (6.14)$$

$$b_I = \frac{k_c C_{Ao} \theta}{v_T (1 + \theta k_c)^2} \quad (6.15)$$

The same modeling approach can be applied to a second order reaction ($A + B \rightarrow$

C). With specification of limiting reactant A, the equations of reaction rate and mole balance for reactant B are given as follows.

$$-r_A = k_c C_A C_B \quad (6.16)$$

$$C_B = (C_{Bo} - C_{Ao}) + C_A \quad (6.17)$$

Solving Eqs. (6.5), (6.16), and (6.17) yields

$$\theta k_c C_A^2 + [1 + \theta k_c (C_{Bo} - C_{Ao})] C_A - C_{Ao} = 0 \quad (6.18)$$

Differentiating Eqs. (6.17) and (6.18), we can obtain the following DP equations.

$$\delta C_A = -a_1 \delta C_{Ao} + a_2 \delta C_{Bo} - b_1 \delta v_T \quad (6.19)$$

$$\delta C_B = -(1 + a_1) \delta C_{Ao} + (1 + a_2) \delta C_{Bo} - b_1 \delta v_T \quad (6.20)$$

$$\delta C_C = (1 + a_1) \delta C_{Ao} - a_2 \delta C_{Bo} + b_1 \delta v_T \quad (6.21)$$

or, in the matrix form,

$$\delta C^t = A \delta C^s + B \delta v_T \quad (6.22)$$

where

$$\delta C^t = (\delta C_A \quad \delta C_B \quad \delta C_C)^T \quad (6.23)$$

$$\delta C^s = (\delta C_{Ao} \quad \delta C_{Bo})^T \quad (6.24)$$

$$A = \begin{pmatrix} -a_1 & a_2 \\ -(1 + a_1) & 1 + a_2 \\ 1 + a_1 & -a_2 \end{pmatrix} \quad (6.25)$$

$$B = (-b_1 \quad -b_1 \quad b_1)^T \quad (6.26)$$

$$a_1 = \frac{1 + \theta k_c C_A}{1 + 2\theta k_c C_A + \theta k_c (C_{Bo} - C_{Ao})} \quad (6.27)$$

$$a_2 = \frac{\theta k_c C_A}{1 + 2\theta k_c C_A + \theta k_c (C_{Bo} - C_{Ao})} \quad (6.28)$$

$$b_I = \frac{\theta k_c C_A (I + C_{Bo} - C_{Ao}) / v_T}{I + 2\theta k_c C_A + \theta k_c (C_{Bo} - C_{Ao})} \quad (6.29)$$

Case 2. Non-isothermal CSTR. For a first order, liquid phase, and irreversible reaction ($A \rightarrow B$) taken place adiabatically in a CSTR, the design equation and rate law in the preceding case can be rewritten below, respectively.

$$V = \frac{F_{Ao} X}{-r_A} \quad (6.30)$$

$$-r_A = kC_A = kC_{Ao}(I - X) \quad (6.31)$$

In Eq. (6.31), reaction constant k is a function of temperature T that is given by the Arrhenius equation below.

$$k = A \exp\left(\frac{-E}{RT}\right) \quad (6.32)$$

Solving X from Eqs. (6.30) and (6.31) and replacing k by Eq. (6.32) yield

$$X = \frac{kV}{v_T + kV} = \frac{VA \exp\left(\frac{-E}{RT}\right)}{v_T + VA \exp\left(\frac{-E}{RT}\right)} \quad (6.33)$$

For an adiabatic CSTR, the energy balance is given by the following equation.

$$-X \left[\Delta H_R^o + \Delta \hat{C}_P (T - T_R) \right] = \tilde{C}_P (T - T_o) \quad (6.34)$$

where T_R is the reference temperature usually using 25 °C; ΔH_R^o is the heat of reaction at the reference temperature; $\Delta \hat{C}_P$ is the heat capacity difference between product and reactant species in the temperature range of interest; \tilde{C}_P is the mean heat capacity of reactant streams. By differentiating Eqs. (6.33) and (6.34), the following disturbance equations can be derived.

$$\delta X = \frac{Vkv_T(E/RT^2)}{(v_T + Vk)^2} \delta T - \frac{Vk}{(v_T + Vk)^2} \delta v_T \quad (6.35)$$

$$\delta X (\Delta H_R^o + \Delta \hat{C}_P(T - T_R)) + (X\Delta \hat{C}_P + \tilde{C}_P) \delta T = \tilde{C}_P \delta T_o \quad (6.36)$$

Solving Eqs. (6.35) and (6.36) gives

$$\delta X = \frac{\tilde{C}_P Vkv_T(E/RT^2)}{\gamma} \delta T_o - \frac{Vk(X\Delta \hat{C}_P + \tilde{C}_P)}{\gamma} \delta v_T \quad (6.37)$$

$$\delta T = \frac{\alpha \tilde{C}_P}{\gamma} \delta T_o + \frac{\beta Vk}{\gamma} \delta v_T \quad (6.38)$$

where

$$\alpha = (v_T + Vk)^2 \quad (6.39)$$

$$\beta = \Delta H_R^o + \Delta \hat{C}_P(T - T_R) \quad (6.40)$$

$$\gamma = \beta Vkv_T(E/RT^2) + \alpha(X\Delta \hat{C}_P + \tilde{C}_P) \quad (6.41)$$

Since we have

$$C_A = C_{Ao}(1 - X) \quad (6.42)$$

$$C_B = C_{Ao}X \quad (6.43)$$

Differentiating Eqs. (6.42) and (6.43) and eliminating δX , we can obtain

$$\delta C_A = (1 - X) \delta C_{Ao} - \frac{\tilde{C}_P Vkv_T(E/RT^2) C_{Ao}}{\gamma} \delta T_o + \frac{Vk(X\Delta \hat{C}_P + \tilde{C}_P) C_{Ao}}{\gamma} \delta v_T \quad (6.44)$$

$$\delta C_B = X \delta C_{Ao} + \frac{\tilde{C}_P Vkv_T(E/RT^2) C_{Ao}}{\gamma} \delta T_o - \frac{Vk(X\Delta \hat{C}_P + \tilde{C}_P) C_{Ao}}{\gamma} \delta v_T \quad (6.45)$$

Equations (6.38), (6.44), and (6.45) can be written in a matrix form relating target fluctuations (δC_A , δC_B , and δT) in terms of source disturbances (δC_{Ao} , δT_o , and δv_T).

Case 3. Reversible and non-isothermal CSTR. For a liquid phase reversible reaction (constant volumetric flow rate),



The net rate of reactant A and the design equation of a CSTR are given in the following equations, respectively.

$$-r_A = k_I \left(C_A - \frac{C_B}{K_e} \right) \quad (6.47)$$

$$V = \frac{F_{Ao} X}{-r_A} \quad (6.48)$$

where

$$C_A = C_{Ao} (1 - X) \quad (6.49)$$

$$C_B = C_{Ao} X \quad (6.50)$$

In Eq. (6.47), K_e is the equilibrium constant that can be determined by the van't Hoff's equation (Folger 1992). Assuming that standard heats of formation ΔH_R is independent of temperature T . The equation of K_e can be derived below.

$$K_e = \frac{k_I}{k_{-I}} = K_o \exp \left(\frac{-\Delta H_R}{RT} \right) \quad (6.51)$$

where K_o is a constant. Combining Eqs. (6.47) through (6.51) yields.

$$X = \frac{VA \exp(-E/RT)}{VA \exp(-E/RT) [1 + (I/K_o) \exp(\Delta H_R/RT)] + v_T} \quad (6.52)$$

According to a reaction carried out adiabatically, the energy balance can be simplified in

the following form.

$$X = \frac{\tilde{C}_P(T - T_o)}{-\Delta H_R} \quad (6.53)$$

Differentiating Eqs. (6.52) and (6.53) and solving δX and δT , we have

$$\delta X = \frac{\phi(\tilde{C}_P / RT^2)}{\phi\tilde{C}_P + \phi(\Delta H_R / RT^2)} \delta T_o - \frac{\tilde{C}_P}{\phi\tilde{C}_P + \phi(\Delta H_R / RT^2)} \delta v_T \quad (6.54)$$

$$\delta T = \frac{\phi\tilde{C}_P}{\phi\tilde{C}_P + \phi(\Delta H_R / RT^2)} \delta T_o + \frac{\Delta H_R}{\phi\tilde{C}_P + \phi(\Delta H_R / RT^2)} \delta v_T \quad (6.55)$$

where

$$\phi = Vk(1 + 1/K_e + v_T/Vk)^2 \quad (6.56)$$

$$\phi = (Ev_T + Vk\Delta H_R / K_e) \quad (6.57)$$

Differentiating Eqs. (6.49) and (6.50) and then substituting δX from Eq. (6.54), we can obtain DP equations below.

$$\delta C_A = (1 - X)\delta C_{Ao} - \frac{\phi(\tilde{C}_P / RT^2)C_{Ao}}{\phi\tilde{C}_P + \phi(\Delta H_R / RT^2)} \delta T_o + \frac{\tilde{C}_P C_{Ao}}{\phi\tilde{C}_P + \phi(\Delta H_R / RT^2)} \delta v_T \quad (6.58)$$

$$\delta C_B = X\delta C_{Ao} + \frac{\phi(\tilde{C}_P / RT^2)C_{Ao}}{\phi\tilde{C}_P + \phi(\Delta H_R / RT^2)} \delta T_o - \frac{\tilde{C}_P C_{Ao}}{\phi\tilde{C}_P + \phi(\Delta H_R / RT^2)} \delta v_T \quad (6.59)$$

Equations (6.55), (6.58), and (6.59) can be rewritten in the matrix form that gives the same model structure as the one in the first case.

Case 4. Gas phase reaction in a PFR. Consider an isothermal, irreversible reaction ($A \rightarrow B + C$). By neglecting pressure drop in the reactor, the design equation

can be developed readily.

$$-r_A = F_{Ao} \frac{dX}{V} = kC_A \quad (6.60)$$

Because of the change of volumetric flow rate, the concentration of reactant A in the product stream need be derived based on stoichiometry, this gives

$$C_A = \frac{F_A}{v_T} = \frac{F_{Ao}(1-X)}{v_o(I+X)} = C_{Ao} \left(\frac{1-X}{I+X} \right) \quad (6.61)$$

Substituting Eqs. (6.61) into (6.60) yields

$$V = F_{Ao} \int_0^X \frac{(I+X)}{kC_{Ao}(I-X)} dX = \frac{F_{Ao}}{kC_{Ao}} \left[2 \ln \left(\frac{I}{I-X} \right) - X \right] \quad (6.62)$$

Since we have

$$X = \frac{C_{Ao} - C_A}{C_{Ao} + C_A}, \quad (6.63)$$

Eq. (6.62) can be rewritten as

$$\frac{Vk}{v_T} = 2 \ln \left(\frac{C_{Ao} + C_A}{2C_A} \right) - \frac{C_{Ao} - C_A}{C_{Ao} + C_A} \quad (6.64)$$

Differentiating Eq. (6.64) yields disturbance equations below.

$$\delta C_A = \frac{C_A}{C_{Ao}} \delta C_{Ao} + \frac{Vk(C_{Ao} + C_A)^2}{2C_{Ao}(C_{Ao} + C_A - I)v_T^2} \delta v_T \quad (6.65)$$

$$\delta C_B = \delta C_C = \delta C_{Ao} - \delta C_A$$

$$= \frac{C_{Ao} - C_A}{C_{Ao}} \delta C_{Ao} - \frac{Vk(C_{Ao} + C_A)^2}{2C_{Ao}(C_{Ao} + C_A - I)v_T^2} \delta v_T \quad (6.66)$$

Equations (6.65) and (6.66) can be written in the matrix form with the same model structure as the one in case 1.

Case 5. Series multiple reaction in a PFR. For an isothermal and liquid phase series reaction,



we can derive the design equation and rate law with neglecting pressure drop through the reactor, which are yielded below.

$$v_T \frac{dC_A}{dV} = r_A = -k_1 C_A \quad (6.68)$$

$$v_T \frac{dC_B}{dV} = r_B = k_1 C_A - k_2 C_B \quad (6.69)$$

$$v_T \frac{dC_C}{dV} = -r_B = k_2 C_B \quad (6.70)$$

Solving Eqs. (6.68) through (6.70) yields

$$C_A = C_{Ao} \exp\left(\frac{-k_1 V}{v_T}\right) \quad (6.71)$$

$$C_B = k_1 C_{Ao} \left[\frac{\exp\left(\frac{-k_1 V}{v_T}\right) - \exp\left(\frac{-k_2 V}{v_T}\right)}{k_2 - k_1} \right] \quad (6.72)$$

$$C_C = \frac{C_{Ao}}{k_2 - k_1} \left[k_1 \exp\left(\frac{-k_2 V}{v_T}\right) - k_2 \exp\left(\frac{-k_1 V}{v_T}\right) - k_1 + k_2 \right] \quad (6.73)$$

Differentiating Eqs. (6.71) through (6.73) with simplification, we can obtain the following disturbance equations, respectively.

$$\delta C_A = \frac{C_A}{C_{Ao}} \delta C_{Ao} + \frac{C_A k_1 V}{v_T^2} \delta v_T \quad (6.74)$$

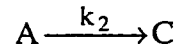
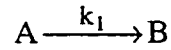
$$\delta C_B = \frac{C_B}{C_{Ao}} \delta C_{Ao} + \frac{k_1 C_{Ao}}{k_2 - k_1} \left[\frac{k_1 V}{v_T^2} \exp\left(\frac{-k_1 V}{v_T}\right) - \frac{k_2 V}{v_T^2} \exp\left(\frac{-k_2 V}{v_T}\right) \right] \delta v_T$$

(6.75)

$$\delta C_C = \frac{C_c}{C_{Ao}} \delta C_{Ao} + \frac{C_B k_2 V}{v_T^2} \delta v_T \quad (6.76)$$

Equations (6.74) through (6.76) can be easily written in a linear matrix form that relates target fluctuations and source disturbances in the reactor operation.

Case 6. Parallel multiple reaction in a PFR. Considering an isothermal, liquid phase parallel reaction,



the design equation and rate law with negligible pressure drop through the reactor can be derived, which gives

$$v_T \frac{dC_B}{dV} = r_B = -r_{A_1} = k_1 C_A \quad (6.77)$$

$$v_T \frac{dC_c}{dV} = r_C = -r_{A_2} = k_2 C_A \quad (6.78)$$

Dividing Eq. (6.77) by Eq. (6.78) yields

$$\frac{dC_B}{dC_C} = \frac{k_1}{k_2} \quad (6.79)$$

Solving the differential equation (6.79), one can obtain

$$C_B = \frac{k_1}{k_2} C_C \quad (6.80)$$

Since we have

$$C_{Ao} = C_A + C_B + C_C, \quad (6.81)$$

solved for C_B and C_C leads to

produced. The reaction can be considered as a first-order irreversible reaction ($A + B \rightarrow$ C). The nominal operating condition of the reactor is listed in Table 6.2.

Table 6.2. Design Data of a Non-Isothermal CSTR

Process variable	Symbol	Unit	Value
Input temperature of the reactant stream	T_o	$^{\circ}\text{K}$	297
Volumetric flow rate of the reactant stream	v_T	m^3/h	9.24
Input concentration of reactant A	C_{Ao}	mol/h	60
Input concentration of reactant B	C_{Bo}	mol/h	1116
Volume of the CSTR	V	m^3	1.14
Conversion of reactant A	X	$\text{mol } \%$	85.73
Output concentration of reactant A	C_A	mol/h	8.53
Output concentration of reactant B	C_B	mol/h	1064.5
Output concentration of reactant C	C_C	mol/h	51.47
Output temperature of the product stream	T	$^{\circ}\text{K}$	340.7
Frequency factor	A	h^{-1}	1.7×10^{13}
Activation energy	E	cal/mol	32400
Enthalpy of formation at a temp. of 293 $^{\circ}\text{K}$	ΔH_R^o	cal/mol	20222
Heat capacity difference between species of products and reactants	\hat{C}_P	$\text{cal}/\text{mol}/^{\circ}\text{K}$	-7
Heat capacity of the reactant stream	\bar{C}_P	$\text{cal}/\text{mol}/^{\circ}\text{K}$	403

The problem is identical to Case 2 discussed in the preceding section. The disturbances in the feed stream are given as follows.

$$\delta X = (\delta C_{Ao} \quad \delta T_o \quad \delta v_T)^T = (-2.27 \quad 1.7 \quad 0)^T \quad (6.88)$$

Rewriting Eqs. (6.38), (6.44), and (6.45), we have

$$\delta Y = A \delta X \quad (6.89)$$

where

$$\delta Y = (\delta C_A \quad \delta C_C \quad \delta T)^T \quad (6.90)$$

The DP matrix A can be obtained based on the given steady-state data, i.e.,

$$A = \begin{pmatrix} 0.1427 & -0.0008 & 0.0001 \\ 0.8573 & 0.0008 & -0.0001 \\ 0 & 1.5517 & -0.0386 \end{pmatrix} \quad (6.91)$$

Each element in matrix A represents the severity of DP from a disturbance source to a process output. To investigate the model prediction precision, Table 6.3 summarizes the results from the simplified model and that from the rigorous model. As a comparison, The prediction errors between their evaluation results are listed in the last column of Table 6.3. Clearly, the model prediction level is well acceptable for process analysis.

Table 6.3. Prediction Precision of the Simplified Model

Process variable	Unit	Rigorous model	Simplified model	Prediction error
$C_A + \delta C_A$	mol/h	6.71	7.17	-0.46
$C_B + \delta C_B$	mol/h	1065	1065.6	-0.6
$C_C + \delta C_C$	mol/h	51.0	50.4	0.6
$T + \delta T$	°K	343.77	343.3	0.43

In this case study, the results have shown that with a mild disturbance of the temperature in the feed stream, the output temperature and productivity can be affected significantly. Therefore, it is very important, in most reaction processes, to carefully examine reaction temperature potentially affecting stable reactor operations, especially when heat integration is taken into account for energy recovery.

Modification of a heat-integrated non-isothermal reaction process. A heat integrated reaction process is depicted in Fig. 6.4. In this system, feed stream S_2 is preheated from 313 °K to 423 °K in heat exchanger E_2 and then fed to reactor R_1 where an adiabatic, exothermic, reversible reaction ($A \longleftrightarrow B$) is taken place. In order to

where

$$\delta T_e^t = \begin{pmatrix} \delta T_h^t & \delta T_c^t \end{pmatrix}^T \quad (6.93)$$

$$\delta T_e^s = \begin{pmatrix} \delta T_h^s & \delta T_c^s & \delta M_{C_{P_h}} & \delta M_{C_{P_c}} \end{pmatrix}^T \quad (6.94)$$

Applying Eq. (6.92) for each heat transfer unit and disturbance equations (6.58) and (6.59) developed in case 3 for each reactor, we can obtain the following system model for the whole process.

$$\delta Y = A_{sys} \delta X \quad (6.95)$$

where

$$\delta Y = \begin{pmatrix} \delta C_{A_3} & \delta T_{R_3}^t & \delta T_{S_1}^t \end{pmatrix}^T \quad (6.96)$$

$$\delta X = \begin{pmatrix} \delta C_{S_1} & \delta C_{S_2} & \delta T_{S_1}^s & \delta T_{S_2}^s & \delta v_T \end{pmatrix}^T \quad (6.97)$$

With given disturbances $\delta X = (-1 \ 0 \ 10 \ 0 \ 0)^T$, the system model in Eq. (6.95) is used to evaluate the stability of the overall process. The result shows that in this design, the disturbances may lead to undesirable reaction conversion and productivity. Through process analysis, it is found that the operational problem in this system is mainly caused by the improper heat integration. To improve process operability, a modified solution is developed as shown in Fig. 6.5. With this modification, the reactor process is much more robust, which naturally enhance process controllability and maintain the chemical conversion. As a comparison, the evaluation results of the original and modified processes are listed in Table 6.5. Clearly, The modified process is superior in terms of disturbance rejection.

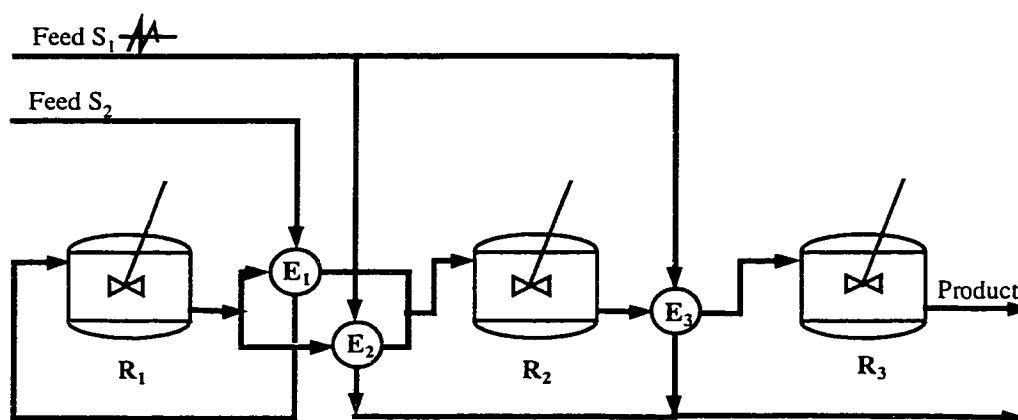


Figure 6.5. Modified process flowsheet of the heat integrated reaction system.

Table 6.5. Comparison of the Results

Process variable	Symbol	Unit	Original	Modified
Conc. of species <i>A</i> in the product	$C_{A_3} + \delta C_{A_3}$	mol/m ³	2.05	1.99
Conc. of species <i>B</i> in the product	$C_{B_3} + \delta C_{B_3}$	mol/m ³	17.95	18.01
Temperature in the product stream	$T'_{R_3} + \delta T'_{R_3}$	°K	614.3	615.2

concentrations in effluent streams. It can be used to identify the bottleneck of a design problem and predict the minimum amount of water required prior to flowsheet development. The design of a system, however, is basically experience based. Moreover, it is difficult to use when multiple pollutants are encountered in design.

Another difficulty involved in the design of cleaning and rinsing processes is the extreme of a variety of uncertain and imprecise process information, such as the chemicals and dirt removal in the process, the driving force of mass transfer between water and process streams, and the description of process behaviors. Thus, it is very difficult to develop disturbance propagation (DP) models to characterize cleaning and rinsing quality during process design stage. It seems that the research focus at this stage should be on the development of an effective design methodology for an optimal plant-wide wastewater reuse network (PWWRN).

In this chapter, an optimization-based approach is developed for designing a PWWRN. The basic element of the approach is the modeling of an elementary wastewater reuse system (EWWRS). This permits the modeling of a PWWRN in which a number of EWWRS's are connected in either series or parallel. The system model formulates a superstructure of a WWRN. An optimization problem is then defined and solved by a nonlinear programming method. Resultant PWWRN features the minimum amount of freshwater consumption while cleaning and rinsing requirement is satisfactory.

7.2 Elementary Wastewater Reuse

A typical wastewater reuse system for a cleaning and rinsing process is depicted in Fig. 7.1. In the process, water is consumed to remove M types of pollutants. In the

$$W^f + W^{ir} + W^{er} = W^{in} \quad (7.2)$$

$$W^{ir} C_i^{out} + W^{er} C_i^{er} = W^{in} C_i^{in} \quad i = 1, 2, \dots, M \quad (7.3)$$

(ii) mass balance for the process

$$q_i = W^{in} (C_i^{out} - C_i^{in}) \quad i = 1, 2, \dots, M \quad (7.4)$$

(iii) mass balance for stream splitting after leaving the process

$$W^{out} = W^{ir} + W^w \quad (7.5)$$

(iv) process constraints

$$C_i^{in} \leq C_{i,max}^{in} \quad i = 1, 2, \dots, M \quad (7.6)$$

$$C_i^{out} \leq C_{i,max}^{out} \quad i = 1, 2, \dots, M \quad (7.7)$$

where $C_{i,max}^{in}$ and $C_{i,max}^{out}$ are, respectively, the maximum permissible concentration of pollutant i in the inlet and outlet of a process. These concentrations are usually determined based on the minimum driving force of mass transfer between a process stream and a water stream. Moreover, it is reasonable to assume that cleaning or rinsing water flow rate is maintained through the process, since the amount of pollutants is negligible, as compared to water flow (i.e., $W^{in} = W^{out}$).

7.3 Modeling for a Plant-Wide Wastewater Reuse Network

Usually, a process plant contains a number of production lines, each of which has a number of cleaning and rinsing steps. A wastewater reuse system in Fig. 7.1 is one of many. A plant-wide wastewater reuse system is essentially a network where water and

in wastewater. These principles can be converted to such design strategies that used water be reused to the maximum extent, and the pollutant concentrations $C_{i,j}^{out}$ of water reach the upper limits. This gives rise to an optimization model shown below.

$$\min \sum_{i=1}^N W_i^f \quad (7.8)$$

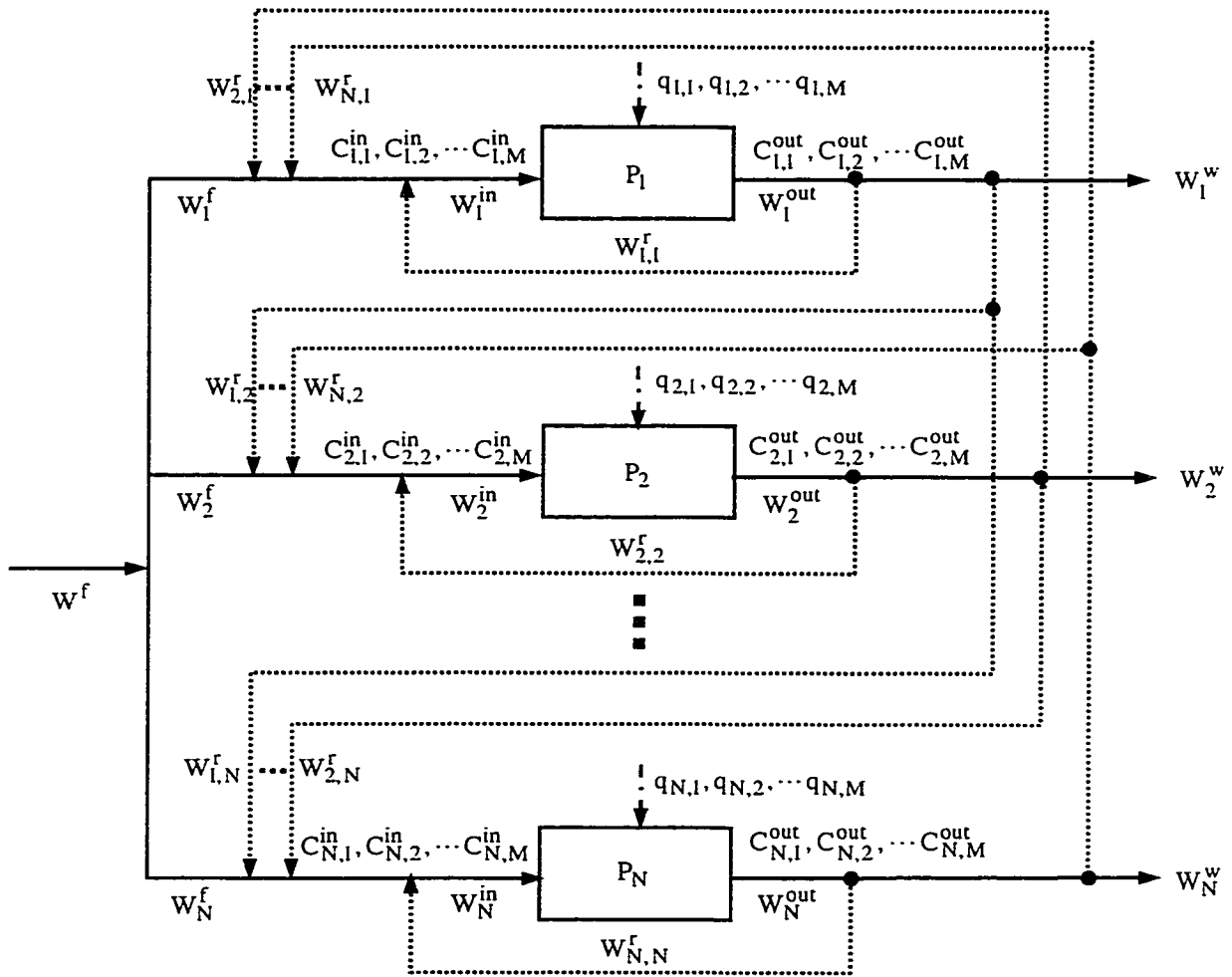
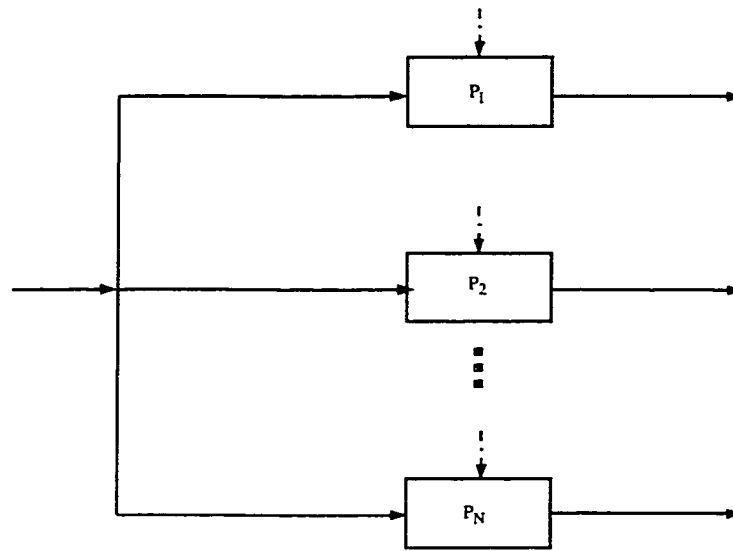
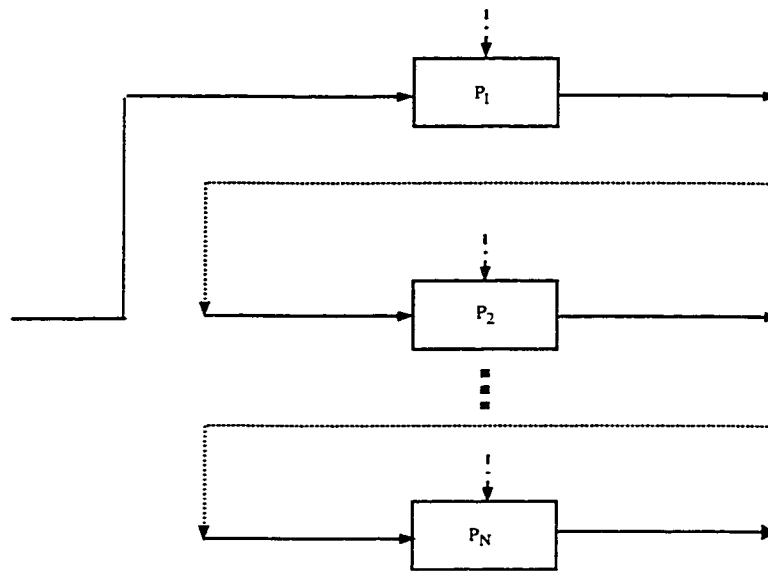


Figure 7.2. Superstructure representation of a water reuse system.



(a)



(b)

Figure 7.3. Potential schemes from the superstructure:
 (a) parallel series;
 (b) complete series.

recycled streams. Such water reuse options should be discarded in practice. Hence, the following constraints should also be included.

$$W_{i,j}^r = 0, \text{ if } W_{i,j}^r < aW_i^{out} \text{ or } W_{i,j}^r < bW_j^{in} \quad (7.17)$$

where a and b are percentages assigned by a designer. The optimization problem can be solved by a non-linear programming method.

7.4 Case Studies

The system model in Eqs. (7.8) through (7.17) has been successfully used to design various PWWRN's. To illustrate the effectiveness of the design strategy, two practical example problems are tackled in this section.

Design of a PWWRN for single pollutant removal in a papermaking process. A pulp and paper plant is one of the major water consumers and wastewater generators in industries. A paper making process consumes a huge amount of water to remove pollutants from paper sheets. In this study, four major sub-processes of a paper making process are considered in which total suspended solids (TSS) is a key pollutant affecting paper quality. Table 7.1 lists the limiting inlet and outlet concentrations and the quantity of TSS to be removed in different shower processes. The optimization model in Eqs. (7.8) through (7.17) is used to determine the most desirable water reuse options. The optimal solution of the WWRN is obtained as shown in Fig. 7.4, where the used water from the head box (P_1) and trim squirt (P_4) need be completely reused, while the major portion of used water from the breast roll process (P_2) is also reused. These three water streams are mixed with fresh water and enter the knockoff process (P_3). This network

Table 7.2. Comparison of Fresh Water Consumption in the Papermaking Process with and without Water Reuse

Process	Fresh water flow rate (t/h)		
	Symbol	Without water reuse	Optimal
Head Box (P_1)	W_1^f	35.0	36.5
Breast Roll (P_2)	W_2^f	44.8	44.8
Knockoff (P_3)	W_3^f	96.2	54.9
Trim Squirt (P_4)	W_4^f	10.0	10.0
Total fresh water	$\sum_{i=1}^4 W_i^f$	186.0	146.2
Water reduction	--	--	21.4%

Design of a PWWRN for multiple pollutant removal in a papermaking process.

In this case, seven sub-processes are considered in a papermaking system. In addition to TSS, the removal of dissolved chemicals (DC) is also considered to ensure the paper quality. The maximum allowable water concentrations in the inlet and outlet of each sub-process and the quantity of pollutants to be removed are listed in Table 7.3.

By solving the optimization model, an optimal solution is obtained. As shown in Fig. 7.5, the used water in processes P_1 , P_4 through P_7 is all reused. The fresh water consumption in this network is 192.7 t/h, which counts 33.4% of fresh water reduction, as compared to the original one without water reuse in these processes (Table 7.4).

Table 7.3. Maximum Water Concentrations and the Quantity of Multiple Pollutants Removed from Seven Major Papermaking Processes

Process	TSS			DC		
	C_{max}^{in} (ppm)	C_{max}^{out} (ppm)	Quantity q (kg/h)	C_{max}^{in} (ppm)	C_{max}^{out} (ppm)	Quantity q (kg/h)
Head Box (P_1)	0	200	7,000	0	200	7,000
Breast Roll (P_2)	100	500	22,400	100	600	28,000
Knockoff (P_3)	200	650	62,550	220	500	38,920
Trim Squirt (P_4)	0	200	2,000	50	300	2,500
Wire Pit (P_5)	50	300	8,750	50	350	10,500
Cooling Water (P_6)	50	200	1,050	50	250	1,400
Vacuum Pumps (P_7)	50	300	13,200	50	200	13,200

Table 7.4. Comparison of Fresh Water Consumption in the Papermaking Process with and without Water Reuse

Process	Fresh water flow rate (t/h)		
	Symbol	Without water reuse	Optimal
Head Box (P_1)	W_1^f	35.0	40.3
Breast Roll (P_2)	W_2^f	46.7	32.7
Knockoff (P_3)	W_3^f	96.2	3.5
Trim Squirt (P_4)	W_4^f	10.0	10.0
Wire Pit (P_5)	W_5^f	30.0	26.8
Cooling Water (P_6)	W_6^f	5.6	13.4
Vacuum Pumps (P_7)	W_7^f	66.0	66.0
Total fresh water	$\sum_{i=1}^7 W_i^f$	289.5	192.7
Water reduction	--	--	33.4%

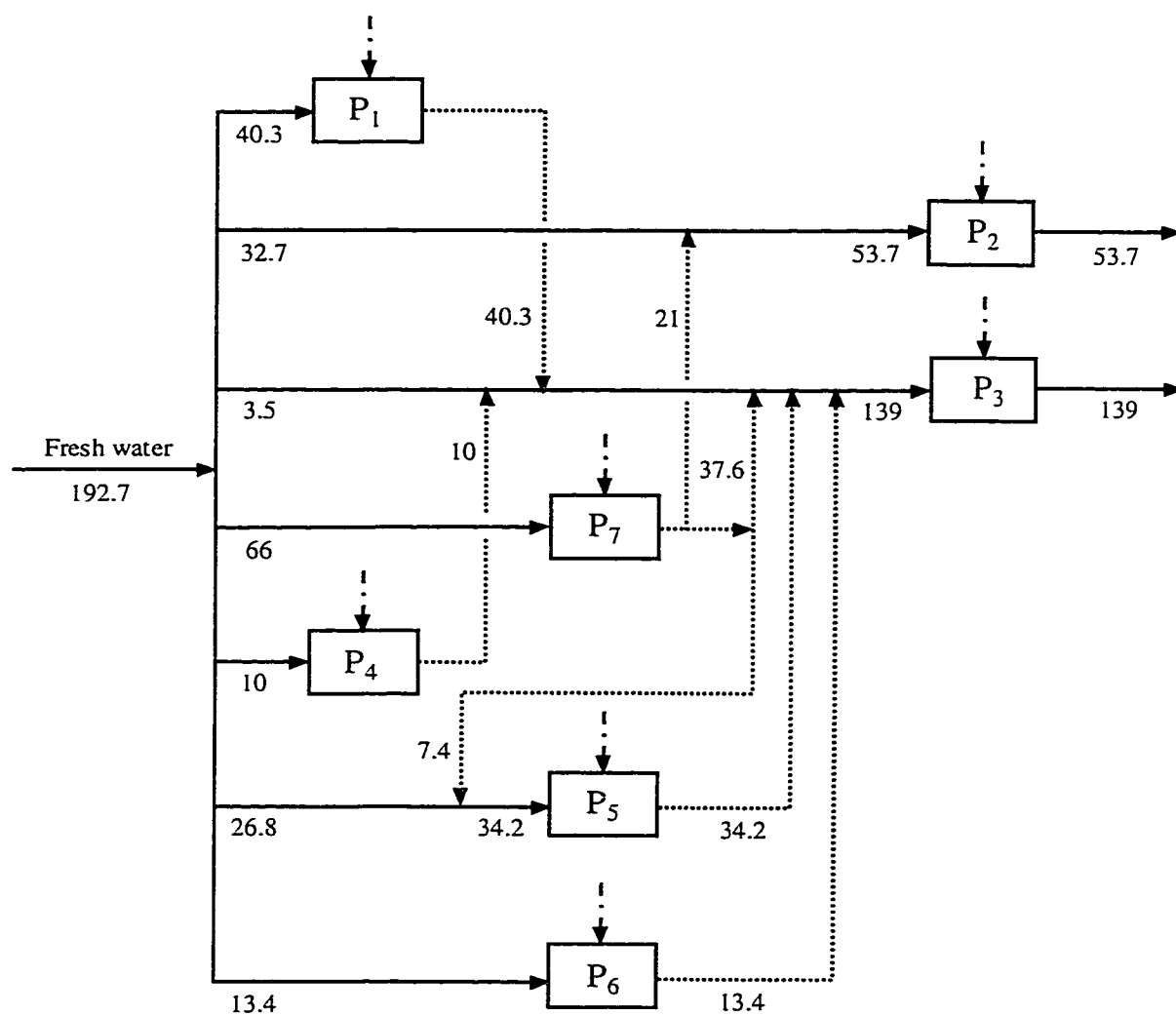


Figure 7.5. Optimal design of a water reuse system with seven sub-water processes.

CHAPTER 8

EXTENDED OPTIMIZATION MODELING FOR DESIGNING A WATER REUSE SYSTEM IN AN ELECTROPLATING PLANT

8.1 Introduction

The electroplating industry is one of the major fresh water consumers and wastewater generators in the manufacturing industries. In an electroplating plant, a huge amount of water is used daily to remove dirt and chemicals on metal parts in various cleaning and rinsing operations. The wastewater generated contains a variety of hazardous or toxic chemicals, metal, and non-metal pollutants that are regulated by EPA (Cherry, 1982). Facing more and more stringently environmental regulations, this industry has been under a constant pressure to significantly reduce fresh water consumption, and certainly wastewater generation.

Over the past decades, tremendous efforts have been made in the industry to design more efficient rinsing systems and in-plant wastewater treatment facilities (Palmer *et al.* 1988; Cushnie, 1994). This has led to tremendous reduction of wastewater. It has been found recently that wastewater can be further reduced if the operations of cleaning, rinsing, and plating processes are optimized. This is a proactive pollution prevention approach that aims at wastewater reduction truly from the first place. In recent year, Huang and Luo (1996), Gong *et al.* (1997), and Luo and Huang (1997) have developed a series of first-principles-based mathematical models for characterizing various cleaning and rinsing operations. With these models, parts cleaning and rinsing standards can be scientifically set; chemical solutions through drag-in and drag-out can be quantified;

water contamination dynamics in any rinsing tanks can be described. More recently, a set of sludge models is also developed to characterize sludge generation through cleaning and rinsing steps (Luo *et al.* 1998). These dynamic and steady-state models can provide deep understanding of cleaning and rinsing operations, which greatly facilitate the development of strategies for optimal water use and reuse in electroplating plants.

In this chapter, the mathematical approach introduced in Chapter 7 is extended to the design of an optimal water reuse system in an electroplating plant for wastewater reduction. This approach focuses on the modification of existing rinsing systems through re-designing water flow patterns and optimizing their flow rates under the constraints of parts rinsing quality and productivity. The approach is applicable to a cleaning-rinsing system containing multiple chemical pollutants.

8.2 Basic Strategies for Wastewater Minimization

A general plating process is depicted in Fig. 8.1. Parts in barrels pass through a series of cleaning-rinsing processes to remove dirt from their surface in order to achieve high plating quality. In the plating process, fresh water enters different rinsing processes to remove drag-out chemical solutions carried by parts from cleaning or plating tanks. The effluent water from rinsing tanks is mixed with different kinds of chemical contaminants. This alerts water use and reuse when quality plating is concerned. To evaluate the feasibility of reusing water, a basic mass balance relationship for all rinsing water streams must be established.

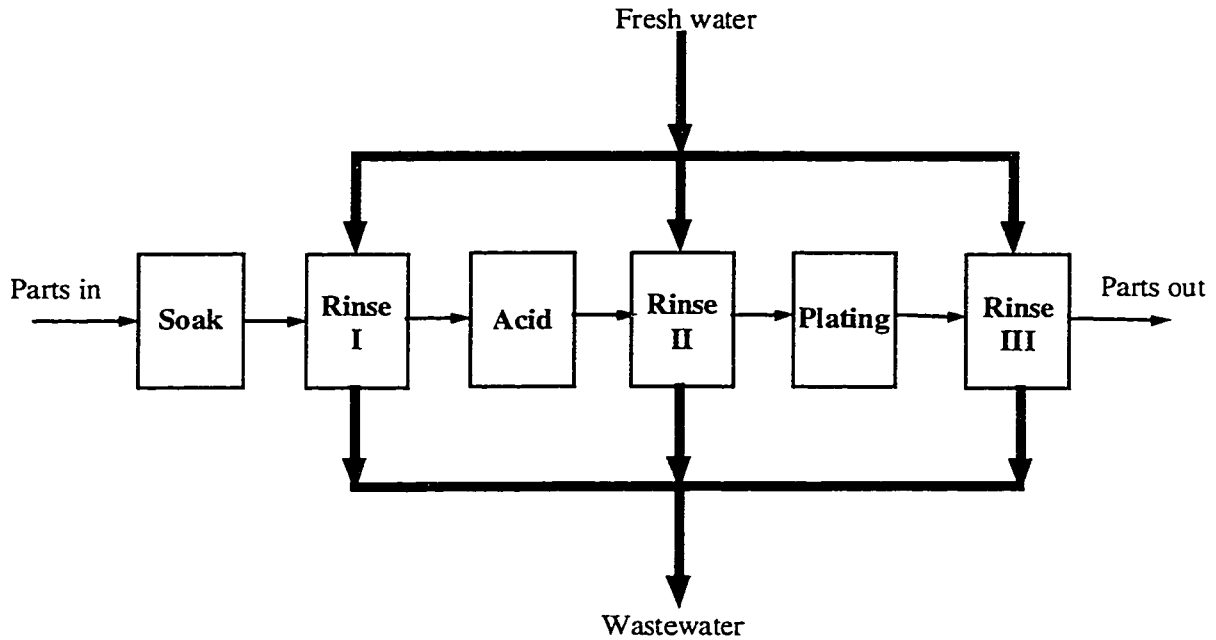


Figure 8.1. Sketch of a conventional electroplating process.

Maximum outlet water concentration. Figure 8.2(a) illustrates a mass transfer process between a pair of contaminated (rich) stream and rinsing water (lean) stream. The concentration in the rich stream, after a certain amount of contaminant is removed, is decreased from C_r^{in} at the inlet to C_r^{out} at the outlet of a rinsing tank. Meanwhile, the concentration in the lean stream is increased from C_l^{in} to C_l^{out} since the stream washes off chemical residue from the surface of parts. Note that the slope of lean-stream line L_R determines the water flow rate; the larger the slope, the smaller the required water flow. If the concentrations at the inlets of both rich and lean streams and at the outlet of the rich stream are specified, the amount of water required will depend on the outlet concentration of the lean stream. When the maximum outlet concentration of the contaminant is reached through mass transfer, water consumption is minimized.

fresh water usage is to maximize the contaminant concentration of rinsing water at the outlet. Figure 8.2(c) shows a rinsing process with two tanks in series. A countercurrent process between parts and water flow is taken place in such a way that water flows through rinsing tanks R_1 and R_2 , and parts are carried over through rinsing tanks R_2 and R_1 . A mass transfer diagram of the process is depicted in Fig. 8.2(d). The slope of line L_{R_1} determines the water flow rate required for a two-tank rinsing process. Obviously, due to the increment of contaminant concentration at the water outlet of the rinsing process, water consumption in this case can be reduced as compared with the one in a single tank that is represented in line L_R . Theoretically, based on a given rinsing requirement, the increment of the number of rinsing tanks in a rinsing process can significantly reduce water consumption. However, this may affect overall process operations, capital cost, and productivity. Industrial experience suggests that two or three rinsing tanks in series for each rinsing step are practical for most cases.

For a plating system containing various rinsing steps, the development of a general mathematical model characterizing a water reuse rinsing system is the first step towards the minimization of water usage.

8.3 Extended System Model

A general rinsing system in a plating process is sketched in Fig. 8.3. This system consists of N sub-rinsing systems, each of which is designed for rinsing out chemical solutions on parts carried by barrels from a preceding cleaning or plating operations. Each sub-rinsing system R_i may contain more than one rinsing tanks. As depicted, fresh

water is sent to each sub-rinsing system. In the figure, dotted lines show all possible water reuse options in the system. The mathematical model to formulate this problem can be developed based on the following assumptions: (i) no chemical reaction in water and (ii) uniform chemical concentration in a rinsing process. This means complete mixing taken place between water flow and chemical residues on the parts. The target is to minimize water usage while a set of process operational requirements is satisfied.

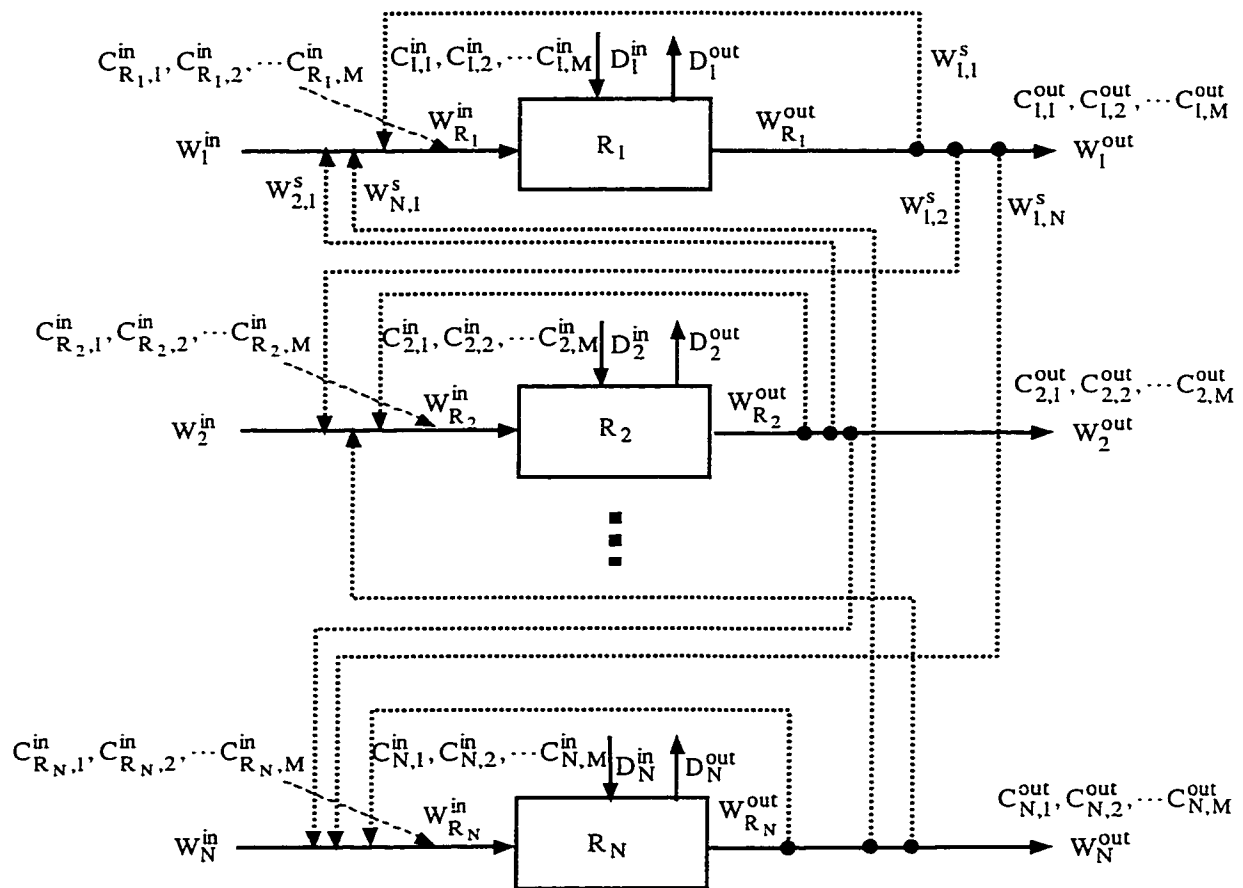


Figure 8.3. System representation of a water-reused rinsing process.

Problems specification. Given drag-in rate D_i^{in} and drag-out rate D_i^{out} in each rinsing process R_i with different contamination levels of chemicals $C_{i,j}^{in}$ and $C_{i,j}^{out}$ ($i \in N; j \in M$), respectively, determine the minimum consumption of fresh water, W_i^{in} ($i \in N$). This eventually can be accomplished by maximizing water reuse and possible outlet wastewater concentration $C_{i,j}^{out}$. Assuming that water can be reused from any effluent water stream to any source water stream with flow rate $W_{i,j}^s$ and concentration $C_{i,j}^{out}$. For the i -th rinsing sub-system, it may receive N recycle streams from N subsystems; these streams are mixed and then enter the subsystem at flow rate $W_{R_i}^{in}$ and concentration $C_{R_i,j}^{in}$. After rinsing, the effluent stream has the increment of chemical concentration to $C_{i,j}^{out}$. Since each sub-system may contain a number of rinsing tanks with drag-in and drag-out, the optimization model derived in Chapter 7 should be extended.

Optimization model. With the characterization of stream concentrations and flow rates for each stream in Fig. 8.3, an optimization model is developed below.

The objective function is defined to minimize the total amount of fresh water used in the system, thus we have

$$\min \sum_{i=1}^N W_i^{in} \quad (8.1)$$

This optimization is subject to four types of constraints:

- (i) Mass balances for mixers:

$$W_{R_i}^{in} = W_i^{in} + \sum_{j=1}^N W_{j,i}^s \quad i = 1, \dots, N \quad (8.2)$$

$$W_{R_i}^{out} = W_{R_i}^{in} + D_i^{in} - D_i^{out} \quad i = 1, \dots, N \quad (8.3)$$

(ii) Mass balances for splitter:

$$W_{R_i}^{out} = W_i^{out} + \sum_{j=1}^N W_{i,j}^s \quad i = 1, \dots, N \quad (8.4)$$

(iii) Mass balances for each component in each rinsing process:

$$C_{R_i,k}^{in} W_{R_i}^{in} = \sum_{j=1}^N C_{j,k}^{out} W_{j,i}^s \quad i = 1, \dots, N; \quad k = 1, \dots, M \quad (8.5)$$

$$C_{R_i,k}^{out} W_{R_i}^{out} = C_{R_i,k}^{in} W_{R_i}^{in} + C_{i,k}^{in} D_i^{in} - C_{i,k}^{out} D_i^{out} \quad i = 1, \dots, N; \quad k = 1, \dots, M \quad (8.6)$$

(iv) Process constraints:

$$C_{i,k}^{lim} \geq C_{i,k}^{out} \geq 0 \quad i = 1, \dots, N; \quad k = 1, \dots, M \quad (8.7)$$

$$C_{R_i,k}^{in} \geq 0 \quad i = 1, \dots, N; \quad k = 1, \dots, M \quad (8.8)$$

$$W_i^{in}, W_{R_i}^{in}, W_{R_i}^{out} \geq 0 \quad i = 1, \dots, N \quad (8.9)$$

$$W_{i,j}^s \geq 0 \quad i = 1, \dots, N; \quad j = 1, \dots, N \quad (8.10)$$

where $C_{i,k}^{lim}$ is the maximum permissible concentration of i -th chemical in the effluent stream of the k -th rinsing process. The optimization is to determine the optimal structure of the water use pattern and the optimal water flow rate in each recycle stream. This can be solved by a non-linear programming approach. It must be pointed out that engineering judgement or common sense knowledge can be used as constraints in the formulation.

This may accelerate the problem solving process.

8.4 Case Study

A rinsing system in an electroplating plant is depicted in Fig. 8.4. The three step rinsing can remove four types of chemical contaminants. In the system, parts are withdrawn from a soak tank to rinsing tanks R_1 and R_2 in series where the concentration of chemical N on parts is reduced from 2,000 ppm to 20 ppm. The parts, after acid cleaning, pass through rinsing tank R_4 where the concentration of chemical H is reduced from 500 ppm to 25 ppm. The effluent water stream from rinsing tank R_4 is then reused to wash out chemical Z on parts in rinsing tank R_3 . After plating, the parts have the final rinsing in tanks R_5 and R_6 in series to remove chemical P on parts through which the concentration is reduced from 10,000 ppm to 20 ppm. The process data and constraints are listed in Table 8.1. Note that drag-out rates D_S , D_A , D_Z , and D_C are from cleaning and plating processes; D_2^{in} and D_6^{in} indicate drag-out rates from tanks R_1 and R_5 , respectively. The chemical concentration on the parts after rinsing in tanks R_2 , R_4 , and R_6 must be strictly controlled within 30 ppm for each chemical contaminant.

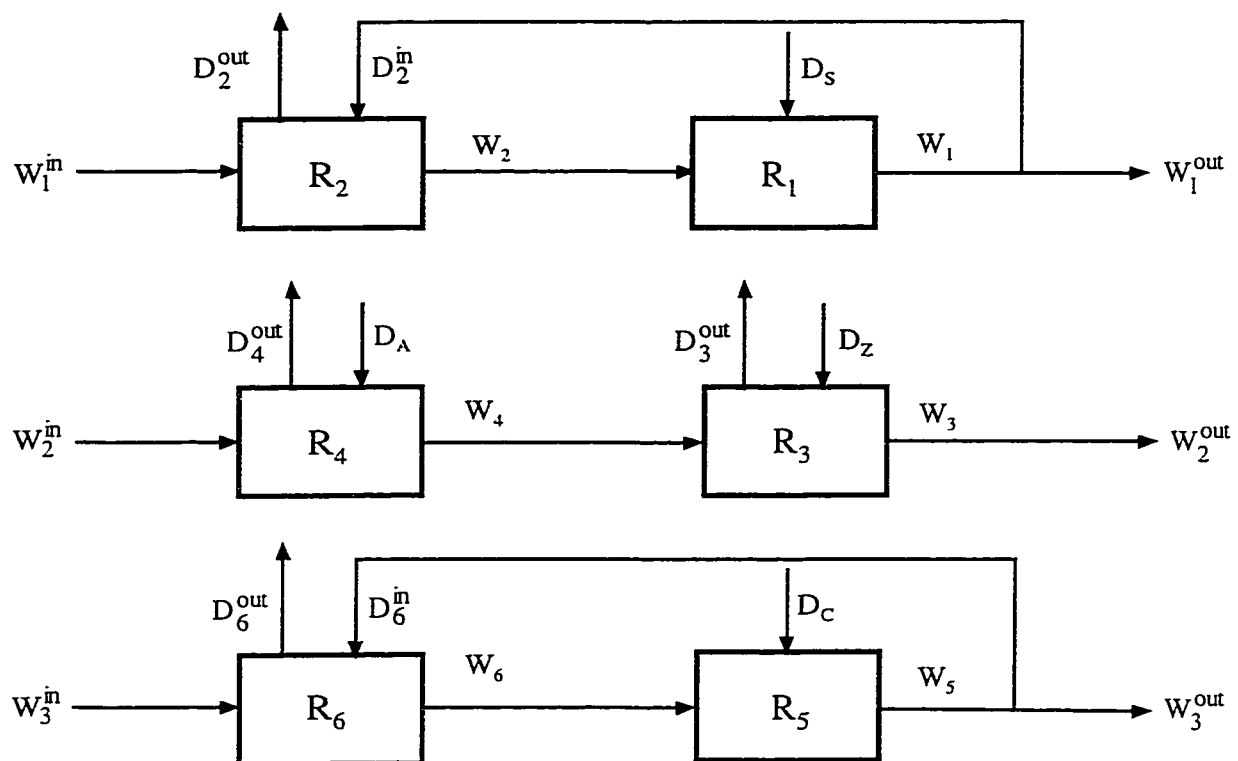


Figure 8.4. Original rinsing system in an electroplating plant.

Table 8.1. Process Data and Constraints in a Rinsing System

Symbol	Flow rate (GPM)	Concentration (ppm)			
		N	H	Z	P
D_A	0.16	0	500.0	0	0
D_C	0.45	0	0	0	10,000.0
D_S	0.52	2,000.0	0	0	0
D_Z	0.24	0	0	13,000.0	0
D_2^{in}	0.75	180.0	0	0	0
D_6^{in}	0.11	0	0	0	1,120.0
D_2^{out}	0.75	--	--	--	--
D_3^{out}	0.24	--	--	--	--
D_4^{out}	0.16	--	--	--	--
D_6^{out}	0.11	--	--	--	--
W_1^{in}	6.0	0	0	0	0
W_2^{in}	3.0	0	0	0	0
W_3^{in}	4.0	0	0	0	0
W_2	6.0	≤ 30.0	≤ 30.0	≤ 30.0	≤ 30.0
W_4	3.0	≤ 30.0	≤ 30.0	≤ 30.0	≤ 30.0
W_6	4.0	≤ 30.0	≤ 30.0	≤ 30.0	≤ 30.0

Operational practice indicates that the effluent stream from R_1 is too dirty so that it is undesirable to be reused for rinsing tanks R_3 through R_6 . Figure 8.5 illustrates a superstructure of the water reuse system for optimization. The models in Eqs. (8.1) through (8.10) are applied to formulate the rinsing process, which leads to the following optimization problem.

$$\min \sum_{i=1}^3 W_i^{in} \quad (8.11)$$

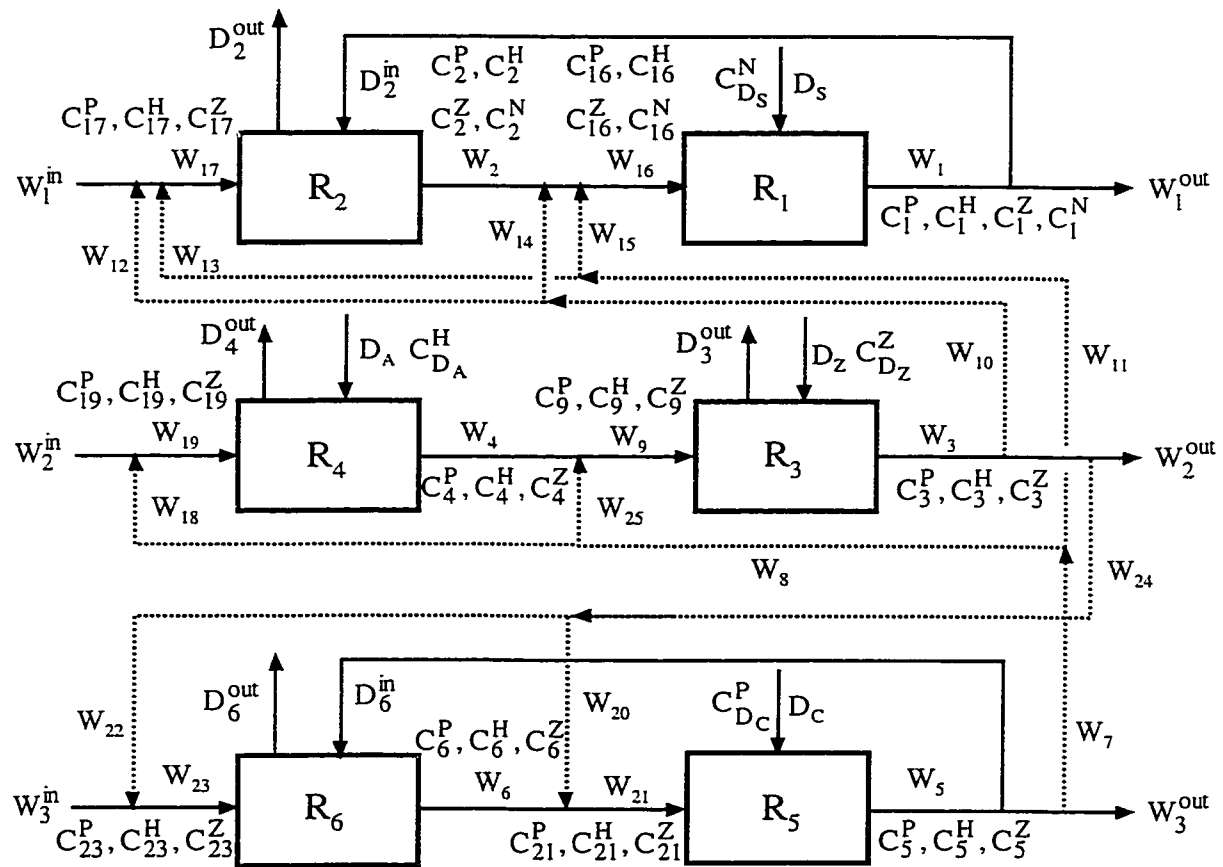


Figure 8.5. Superstructure of the water reuse system for optimization.

$$W_{22} + W_{20} = W_{24} \quad (8.28)$$

$$W_1^{out} + D_2^{in} = W_1 \quad (8.29)$$

$$W_2^{out} + W_{10} + W_{24} = W_3 \quad (8.30)$$

$$W_3^{out} + D_6^{in} + W_7 = W_5 \quad (8.31)$$

(iii) Mass balances for each component in each rinsing process:

$$D_6^{in} C_5^i + W_{23} C_{23}^i = D_6^{out} C_6^i + W_6 C_6^i \quad i = P, H, Z \quad (8.32)$$

$$W_{22} C_3^i = W_{23} C_{23}^i \quad i = P, H, Z \quad (8.33)$$

$$W_6 C_6^i + W_{20} C_3^i = W_{21} C_{21}^i \quad i = P, H, Z \quad (8.34)$$

$$W_{21} C_{21}^i + D_C C_{D_C}^i = W_5 C_5^i \quad i = P, H, Z \quad (8.35)$$

$$W_{19} C_{19}^i = W_{18} C_5^i \quad i = P, H, Z \quad (8.36)$$

$$W_{19} C_{19}^i + D_A C_{D_A}^i = W_4 C_4^i + D_4^{out} C_4^i \quad i = P, H, Z \quad (8.37)$$

$$W_4 C_4^i + W_{25} C_5^i = W_9 C_9^i \quad i = P, H, Z \quad (8.38)$$

$$W_9 C_9^i + D_Z C_{D_Z}^i = W_3 C_3^i + D_3^{out} C_3^i \quad i = P, H, Z \quad (8.39)$$

$$W_{12} C_3^i + W_{13} C_5^i = W_{17} C_{17}^i \quad i = P, H, Z \quad (8.40)$$

$$W_{17} C_{17}^i + D_2^{in} C_1^i = D_2^{out} C_2^i + W_2 C_2^i \quad i = P, H, Z, N \quad (8.41)$$

$$W_2 C_2^i + W_{14} C_3^i + W_{15} C_5^i = W_{16} C_{16}^i \quad i = P, H, Z, N \quad (8.42)$$

$$W_{16} C_{16}^i + D_S C_{D_S}^i = D_2^{in} C_1^i + W_1 C_1^i \quad i = P, H, Z, N \quad (8.43)$$

(iv) Concentration requirements:

Table 8.2. Optimal Water Flow Rates in the Water Reuse System

Symbol	Flow rate (GPM)	Concentration (ppm)			
		<i>N</i>	<i>H</i>	<i>Z</i>	<i>P</i>
W_1^{in}	4.010	0	0	0	0
W_2^{in}	2.445	0	0	0	0
W_3^{in}	2.924	0	0	0	0
W_{12}	0.015	0	27.41	1,136.37	27.41
W_{13}	0.0	0	11.41	461.80	828.27
W_{14}	0.289	0	27.41	1,136.37	27.41
W_{15}	1.242	0	11.41	461.80	828.27
W_{18}	0.098	0	11.41	461.80	828.27
W_{20}	2.203	0	27.41	1,136.37	27.41
W_{22}	0.036	0	27.41	1,136.37	27.41
W_{25}	0.0	0	11.41	461.80	828.27
W_1^{out}	4.576	191.03	4.06	168.26	190.48
W_2^{out}	0.0	0	27.41	1,136.37	27.41
W_3^{out}	4.163	0	11.41	461.80	828.27

Table 8.3. Comparison of Fresh Water Consumption
between the Original and Modified Processes

Water stream	Flow rate (GPM)		
	Symbol	Original	Modified
Fresh water 1	W_1^{in}	6.0	4.13
Fresh water 2	W_2^{in}	3.0	2.51
Fresh water 3	W_3^{in}	4.0	2.81
Wastewater 1	W_1^{out}	6.52	4.46
Wastewater 2	W_2^{out}	3.0	0.0
Wastewater 3	W_3^{out}	4.45	4.35
Reused water 1	W_{15}	--	1.31
Reused water 2	W_{20}	--	2.51
Total fresh water	$\sum_{i=1}^3 W_i^{in}$	13.0	9.45
Water reduction	--	--	27.3 %

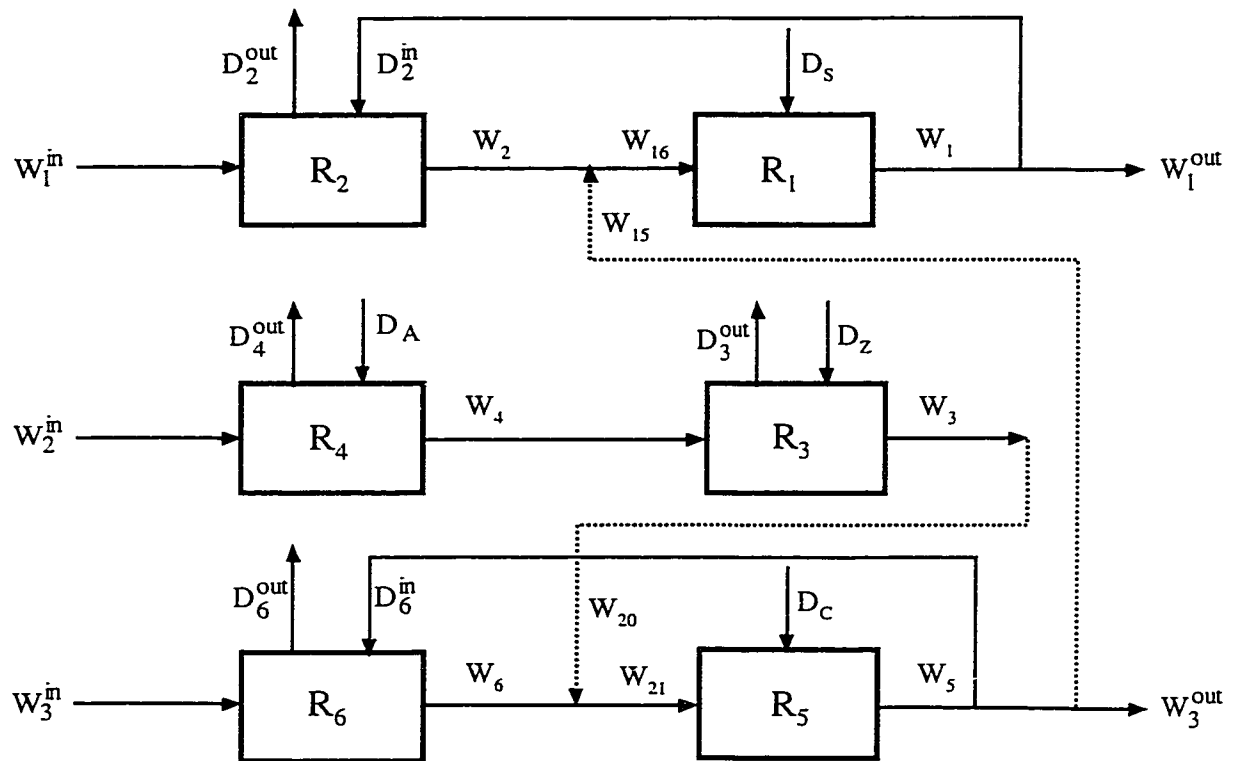


Figure 8.6. Modified rinsing system.

CHAPTER 9

CONCLUSIONS AND RECOMMENDATIONS

9.1 Conclusions

Process integration, in particular, heat and mass integration, in specific, is one of the most important concept and industrial practice in the process systems engineering during the past two decades. Successful process integration, process design and control (PD&C) must be effectively integrated. Naturally, the integration of PD&C become a hot topic in process integration. This research is focused on the development of a model-based synthesis methodology. It has the following unique features:

(i) The earliest integration of PD&C. The integration at the process synthesis phase is the most difficult integration, but the most effective way for preventing or eliminating process operational problems, and eventually simplifying control system design.

(ii) Simple, yet effective integration of PD&C. Various disturbance propagation (DP) models have been developed for characterizing DP through all types of major chemical processes and identifying the most effective way for maximum disturbance rejection. The models are first-principles-based and in a linear form, which permit quick and accurate process evaluation, and facilitate the incorporation of the models into process synthesis. These models have a general and unified structure so that the model structure is applicable to any type of processes, such as heat exchanger networks (HEN's), mass exchanger network (MEN's), reactor networks (RN's), distillation column networks (DCN's), and any of their combinations.

9.2 Recommendations

The model-based methodology for the earliest integration of process design and control developed in this dissertation has demonstrated the great potentials for advancing existing process integration technologies. It is conceivable that if it is further extended in depth and breath, the methodology will have much broader application opportunities in industries.

As shown in Chapter 6, the DP models for heat-integrated distillation column are applicable to the standard units for which feed streams have no more than three components. Industrial practice shows, however, that columns may have multiple feed streams, side streams, and intermediate heat exchangers. The components in feed streams may be more than three. These systems are much more complicated in terms of heat and mass transfer. The basic principles of the DP models developed so far are entirely applicable to these more complicated systems. In this direction, a specific attention should be paid to column decomposition. A more precise model, instead of the Fenske equation, is needed to improve the DP prediction.

For reactor systems, especially non-isothermal reactor systems, some operating ranges demonstrate highly nonlinear behaviors. Thus, it is desirable to carefully examine how DP affects overall process operability under those operation conditions. Nonlinear DP models are permitted to assess DP more accurately. Note that a RN system is structurally less complicated than a HEN or MEN, and a RN is always to be synthesized first. Thus, a nonlinear model for enhancing the structural controllability for it will be computationally acceptable.

A future trend in this study of the integration of PD&C is to incorporate process

dynamics into the overall integration activity. Hitherto, the progress is only restricted to the design of a simple system with one or two units. Certainly, if the system is network-structured, it will be extremely difficult to consider the dynamics of the network during the process synthesis stage. Our suggestion is the incorporation of dynamics for key unit(s).

As shown in Chapters 7 and 8, the superstructure developed for a WWRN is to include all possible wastewater reuse options. This work can be extended by including all possible fresh water distribution options in the superstructure. This may further reduce fresh water consumption, and thereby wastewater generation. The DP modeling of a cleaning and rinsing process should be also conducted to ensure process cleaning and rinsing quality. It can be achieved by extending the DP models developed for a mass-separating-agent-based mass exchanger in Chapter 4. Since the driving force in the cleaning and rinsing process is varies with time, the incorporation of dynamic models for characterizing the chemicals and dirt removal in the cleaning and rinsing process into WWRN design should have lots of opportunities to improve cleaning quality and to reduce wastewater generation.

APPENDIX A

DERIVATION OF UNIT-BASED DISTURBANCE PROPAGATION MODEL FOR A HEAT EXCHANGER

The derivation of the unit-based disturbance propagation model in Eq. (2.11) can be initiated by rewriting Eqs. (2.7) and (2.10). This gives rise to:

$$Q + \delta Q = Mc_{P_h} \Delta T_h + Mc_{P_h} (\delta T_h^s - \delta T_h^t) + \delta Mc_{P_h} \Delta T_h + \delta Mc_{P_h} (\delta T_h^s - \delta T_h^t) \quad (A-1)$$

$$= Mc_{P_c} \Delta T_c + Mc_{P_c} (\delta T_c^t - \delta T_c^s) + \delta Mc_{P_c} \Delta T_c + \delta Mc_{P_c} (\delta T_c^t - \delta T_c^s) \quad (A-2)$$

$$= UA \frac{\Delta T_{hc}^{st} + \Delta T_{hc}^{ts}}{2} + UA \frac{(\delta T_h^s - \delta T_c^t) + (\delta T_h^t - \delta T_c^s)}{2} \quad (A-3)$$

By applying Eq. (2.9) and neglecting the second order term, the following relationship holds,

$$\frac{UA}{2} [(\delta T_h^s - \delta T_c^t) + (\delta T_h^t - \delta T_c^s)] = \delta Mc_{P_h} \Delta T_h + Mc_{P_h} (\delta T_h^s - \delta T_h^t) \quad (A-4)$$

$$\frac{UA}{2} [(\delta T_h^s - \delta T_c^t) + (\delta T_h^t - \delta T_c^s)] = \delta Mc_{P_c} \Delta T_c + Mc_{P_c} (\delta T_c^t - \delta T_c^s) \quad (A-5)$$

Substitutes Eq's. (2.1), (2.2), and (A-5) into Eq. (A-4) gives:

$$\frac{\Delta T_h}{\Delta T_{hc}^{st} + \Delta T_{hc}^{ts}} (\delta T_h^s - \delta T_c^t + \delta T_h^t - \delta T_c^s) = \frac{\Delta T_h}{Mc_{P_h}} \delta Mc_{P_h} + (\delta T_h^s - \delta T_h^t) \quad (A-6)$$

Similarly, the following relationship can be obtained:

$$\frac{\Delta T_c}{\Delta T_{hc}^{st} + \Delta T_{hc}^{ts}} (\delta T_h^s - \delta T_c^t + \delta T_h^t - \delta T_c^s) = \frac{\Delta T_c}{Mc_{P_c}} \delta Mc_{P_c} + (\delta T_c^t - \delta T_c^s) \quad (A-7)$$

Dividing Eq. (A-7) by Eq. (A-6) gives:

$$\frac{\Delta T_h}{\Delta T_c} = \frac{\frac{\Delta T_h}{Mc P_h} \delta Mc P + (\delta T_h^s - \delta T_h^t)}{\frac{\Delta T_c}{Mc P_c} \delta Mc P_c + (\delta T_c^t - \delta T_c^s)} \quad (\text{A-8})$$

or

$$\delta T_h^t = \delta T_h^s + \frac{\Delta T_h}{\Delta T_c} \delta T_c^s - \frac{\Delta T_h}{\Delta T_c} \delta T_c^t + \frac{\Delta T_h}{Mc P_h} \delta Mc P_h - \frac{\Delta T_h}{Mc P_c} \delta Mc P_c \quad (\text{A-9})$$

Substituting Eq. (A-9) into Eq. (A-6) and neglecting the second order term gives:

$$\delta T_c^t = \frac{\Delta T_c}{\Delta T_{hc}^{ss}} \delta T_h^s + \frac{\Delta T_{hc}^{st}}{\Delta T_{hc}^{ss}} \delta T_c^s + \frac{\Delta T_h \Delta T_c}{2 \Delta T_{hc}^{ss} Mc P_h} \delta Mc P_h - \frac{\Delta T_c (\Delta T_{hc}^{ss} + \Delta T_{hc}^{st})}{2 \Delta T_{hc}^{ss} Mc P_c} \delta Mc P_c \quad (\text{A-10})$$

Similarly, substituting Eq. (A-10) into Eq. (A-7), gives:

$$\delta T_h^t = \frac{\Delta T_{hc}^{ts}}{\Delta T_{hc}^{ss}} \delta T_h^s + \frac{\Delta T_h}{\Delta T_{hc}^{ss}} \delta T_c^s + \frac{\Delta T_h (\Delta T_{hc}^{ss} + \Delta T_{hc}^{ts})}{2 \Delta T_{hc}^{ss} Mc P_h} \delta Mc P_h - \frac{\Delta T_c \Delta T_h}{2 \Delta T_{hc}^{ss} Mc P_c} \delta Mc P_c \quad (\text{A-11})$$

These two equations can be expressed into the following matrix form.

$$\begin{pmatrix} \delta T_h^t \\ \delta T_c^t \end{pmatrix} = \mathbf{A} \begin{pmatrix} \delta T_h^s \\ \delta T_c^s \end{pmatrix} + \mathbf{B} \begin{pmatrix} \delta Mc P_h \\ \delta Mc P_c \end{pmatrix} \quad (\text{A-12})$$

where

$$\mathbf{A} = \begin{pmatrix} \frac{\Delta T_{hc}^{ts}}{\Delta T_{hc}^{ss}} & \frac{\Delta T_h}{\Delta T_{hc}^{ss}} \\ \frac{\Delta T_c}{\Delta T_{hc}^{ss}} & \frac{\Delta T_{hc}^{st}}{\Delta T_{hc}^{ss}} \end{pmatrix} = \begin{pmatrix} I - \frac{\Delta T_h}{\Delta T_{hc}^{ss}} & \frac{\Delta T_h}{\Delta T_{hc}^{ss}} \\ \frac{\Delta T_c}{\Delta T_{hc}^{ss}} & I - \frac{\Delta T_c}{\Delta T_{hc}^{ss}} \end{pmatrix} \quad (\text{A-13})$$

$$\begin{aligned}
\mathbf{B} &= \begin{pmatrix} \frac{\Delta T_h (\Delta T_{hc}^{ss} + \Delta T_{hc}^{ts})}{2\Delta T_{hc}^{ss} Mc P_h} & -\frac{\Delta T_h \Delta T_c}{2\Delta T_{hc}^{ss} Mc P_c} \\ \frac{\Delta T_h \Delta T_c}{2\Delta T_{hc}^{ss} Mc P_h} & -\frac{\Delta T_c (\Delta T_{hc}^{ss} + \Delta T_{hc}^{st})}{2\Delta T_{hc}^{ss} Mc P_c} \end{pmatrix} \\
&= \begin{pmatrix} \frac{\Delta T_h}{2Mc P_h} (2 - \frac{\Delta T_h}{\Delta T_{hc}^{ss}}) & -\frac{\Delta T_c \Delta T_h}{2Mc P_c \Delta T_{hc}^{ss}} \\ \frac{\Delta T_h \Delta T_c}{2Mc P_h \Delta T_{hc}^{ss}} & -\frac{\Delta T_c}{2Mc P_c} (2 - \frac{\Delta T_c}{\Delta T_{hc}^{ss}}) \end{pmatrix}
\end{aligned} \tag{A-14}$$

$$\begin{aligned}
& \frac{(\Delta C_{lel}^{st} + \Delta C_{lel}^{ts})}{2\Delta C_r} \left[\frac{\delta M_r}{M_r} \Delta C_r + (\delta C_r^s - \delta C_r^t) \right] \\
& = n \left(\frac{\delta M_r}{M_r} + \frac{\delta M_l}{M_l} \right) \frac{(\Delta C_{lel}^{st} + \Delta C_{lel}^{ts})}{2} + \frac{\left(\frac{\delta C_r^s}{m} - \delta C_l^t \right) + \left(\frac{\delta C_r^t}{m} - \delta C_l^s \right)}{2}
\end{aligned} \quad (B-3)$$

From Eqs. (B-2) and (B-3), we have

$$\delta C_l^t = \delta C_l^s + \frac{\Delta C_l}{\Delta C_r} \delta C_r^s - \frac{\Delta C_l}{\Delta C_r} \delta C_r^t + \frac{\Delta C_l}{M_r} \delta M_r - \frac{\Delta C_l}{M_l} \delta M_l \quad (B-4)$$

Substituting Eq. (B-4) into Eq. (B-3) and neglecting the second order terms yield

$$\begin{aligned}
\delta C_r^t = & \frac{\Delta C_{lel}^{ts}}{\Delta C_{lel}^{ss}} \delta C_r^s + \frac{\Delta C_r}{\Delta C_{lel}^{ss}} \delta C_l^s + \frac{\Delta C_r \left[(\Delta C_{lel}^{ss} + \Delta C_{lel}^{ts}) - n(\Delta C_{lel}^{st} + \Delta C_{lel}^{ts}) \right]}{2 M_r \Delta C_{lel}^{ss}} \delta M_r \\
& - \frac{\Delta C_r \left[\Delta C_l + n(\Delta C_{lel}^{st} + \Delta C_{lel}^{ts}) \right]}{2 M_l \Delta C_{lel}^{ss}} \delta M_l
\end{aligned} \quad (B-5)$$

Substituting Eq. (B-5) into Eq. (B-4) leads to

$$\begin{aligned}
\delta C_l^t = & \frac{\Delta C_l}{m} \delta C_r^s + \frac{\Delta C_{lel}^{st}}{\Delta C_{lel}^{ss}} \delta C_l^s + \frac{\Delta C_l \left[\Delta C_{lel} + n(\Delta C_{lel}^{st} + \Delta C_{lel}^{ts}) \right]}{2 M_r \Delta C_{lel}^{ss}} \delta M_r \\
& - \frac{\Delta C_l \left[(\Delta C_{lel}^{ss} + \Delta C_{lel}^{st}) - n(\Delta C_{lel}^{st} + \Delta C_{lel}^{ts}) \right]}{2 M_l \Delta C_{lel}^{ss}} \delta M_l
\end{aligned} \quad (B-6)$$

The above equations can be written in the following matrix form.

$$\begin{pmatrix} \delta C_r^t \\ \delta C_l^t \end{pmatrix} = A_e \begin{pmatrix} \delta C_r^s \\ \delta C_l^s \end{pmatrix} + B_e \begin{pmatrix} \delta M_r \\ \delta M_l \end{pmatrix} \quad (B-7)$$

where

APPENDIX C

DERIVATION OF CONVERSION FACTORS IN EQ. (4.78)

The conversion factors in Eq. (4.78) can be determined based on the following three types of mass flow rate disturbances in a process system.

Mass flow rate disturbance at the Inlet of a mass exchanger. The mass flow rate disturbance at the inlet of a mass exchanger (δM_e^{in}) comes from three difference sources.

Case a. As shown in Fig. C-1(a), δM_e^{in} is equal to δM_r^s if the source is directly from a rich stream, or equal to δM_l^s if the source is directly from a lean stream. In either case, conversion factor f is 1. For instance, for the former case,

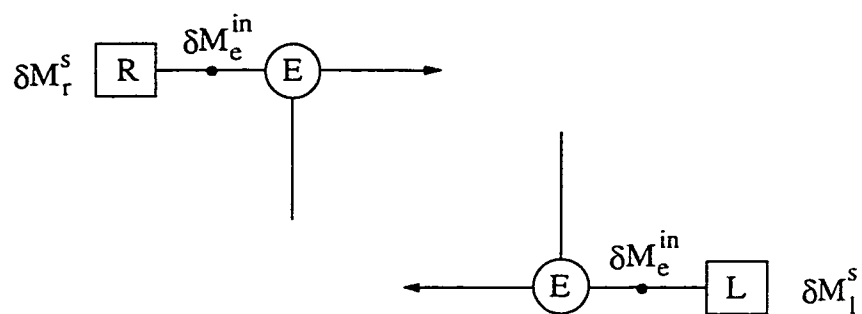
$$f = \frac{\delta M_e^{in}}{\delta M_r^s} = 1 \quad (C-1)$$

Case b. The inlet of an exchanger is the outlet of a branch of a splitter (Fig. C-1(b)). In this case, the conversion factor relating δM_e^{in} and δM_s^{in} can be determined as follows.

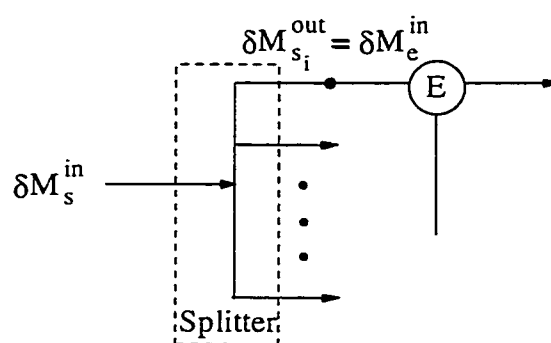
$$f = \frac{\delta M_e^{in}}{\delta M_s^{in}} = \frac{\delta M_{s_i}^{out}}{\delta M_s^{in}} = \frac{M_{s_i}^{out}}{M_s^{in}} \quad (C-2)$$

Case c. The outlet of a mixer can be the inlet of a exchanger (Fig. C-1(c)). Thus, the conversion factor relating δM_e^{in} and $\delta M_{m_i}^{in}$ is

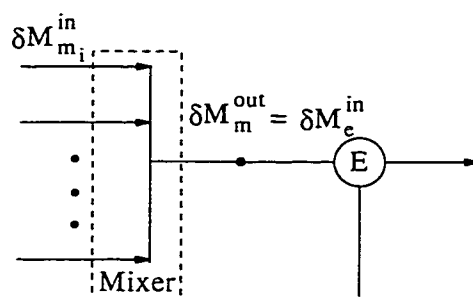
$$f = \frac{\delta M_e^{in}}{\delta M_{m_i}^{in}} = \frac{\delta M_m^{out}}{\delta M_{m_i}^{in}} = \frac{M_m^{out}}{M_{m_i}^{in}} \quad (C-3)$$



(a)



(b)



(c)

Figure C-1. Mass flow rate disturbance at the inlet of a mass exchanger.

$$f = \frac{\delta M_s^{in}}{\delta M_{m_i}^{in}} = \frac{\delta M_m^{out}}{\delta M_{m_i}^{in}} = \frac{M_m^{out}}{M_{m_i}^{in}} \quad (\text{C-6})$$

Case c. Connection to the outlet of an exchanger (Fig. C-3(c)). The conversion involved in this case is straightforward, i.e.,

$$f = \frac{\delta M_s^{in}}{\delta M_e^{in}} = \frac{\delta M_e^{in}}{\delta M_e^{in}} = 1 \quad (\text{C-7})$$

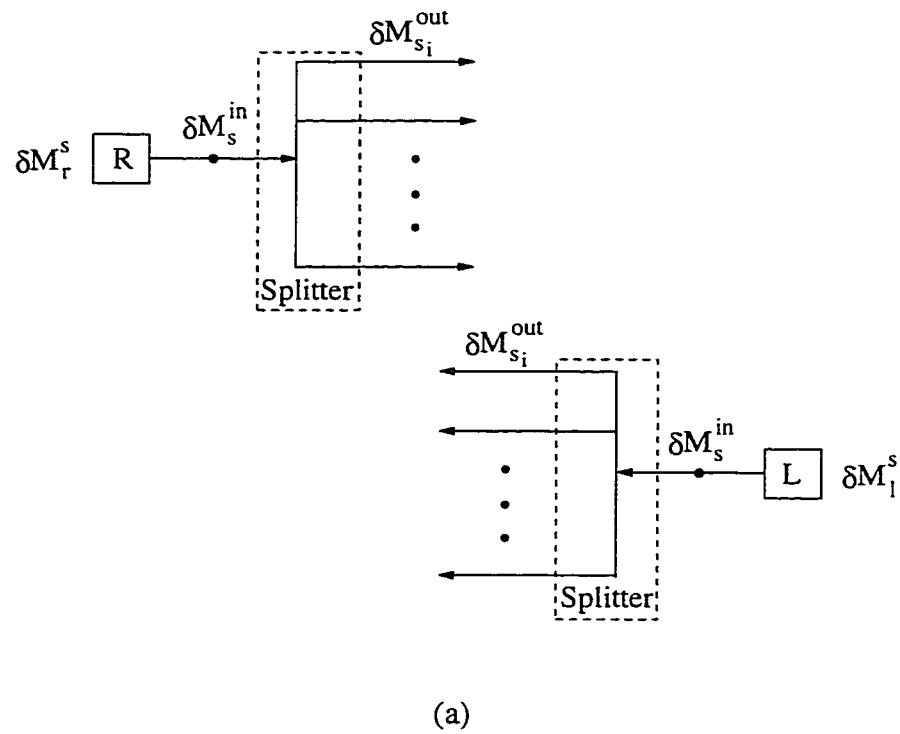
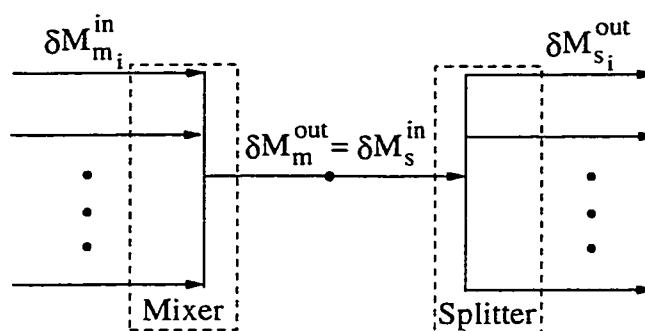
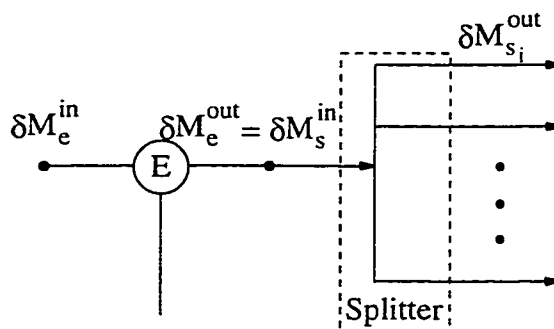


Figure C-3. Mass flow rate disturbance at the inlet of a splitter.



(b)



(c)

Figure C-3. Mass flow rate disturbance at the inlet of a splitter (cont'd).

Overall conversion factor. For any of the three types of mass flow rate disturbances, we can always trace a DP path and convert an intermediate disturbance to a source disturbance of mass flow rate. The relevant conversion factors obtained should be multiplied to obtain an overall conversion factor which usually has the following form.

$$f = \prod_{i=1}^N f_i \quad (\text{C-8})$$

where N is the total number of conversions involved.

Illustrative example. Figure C-4 shows a partial network system containing six mass exchangers, two splitters, and one mixer. We intend to show how to use the

formulas in Eqs. (C-1) through (C-8) to derive an overall conversion factor which relates $\delta M_{e_5}^{in}$ at point g and δM_r^s at point a in the figure. In derivation, we need to have seven conversion factors between every pair of adjacent points (f_1 through f_7). Their values are listed in Table C-1. The overall conversion factor f for converting $\delta M_{e_5}^{in}$ to δM_r^s can be obtained by multiplying the conversion factors f_1 through f_7 , which results in

$$f = \prod_{i=1}^7 f_i = \frac{M_{e_5}^{in}}{M_r^s} \quad (C-9)$$

Note that this f represents only one diagonal element of matrix F in Eq. (4.78). Other elements can be derived by the same approach.

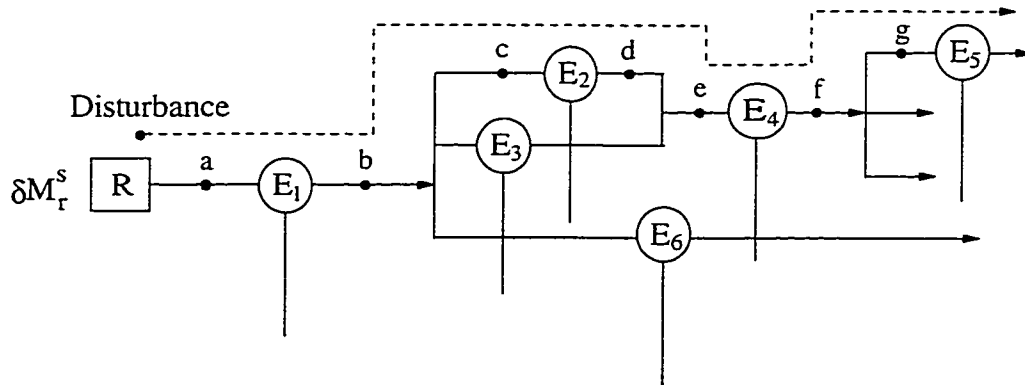


Figure C-4. Partial network system for evaluating a conversion factor.

APPENDIX D

HYSYS SIMULATION

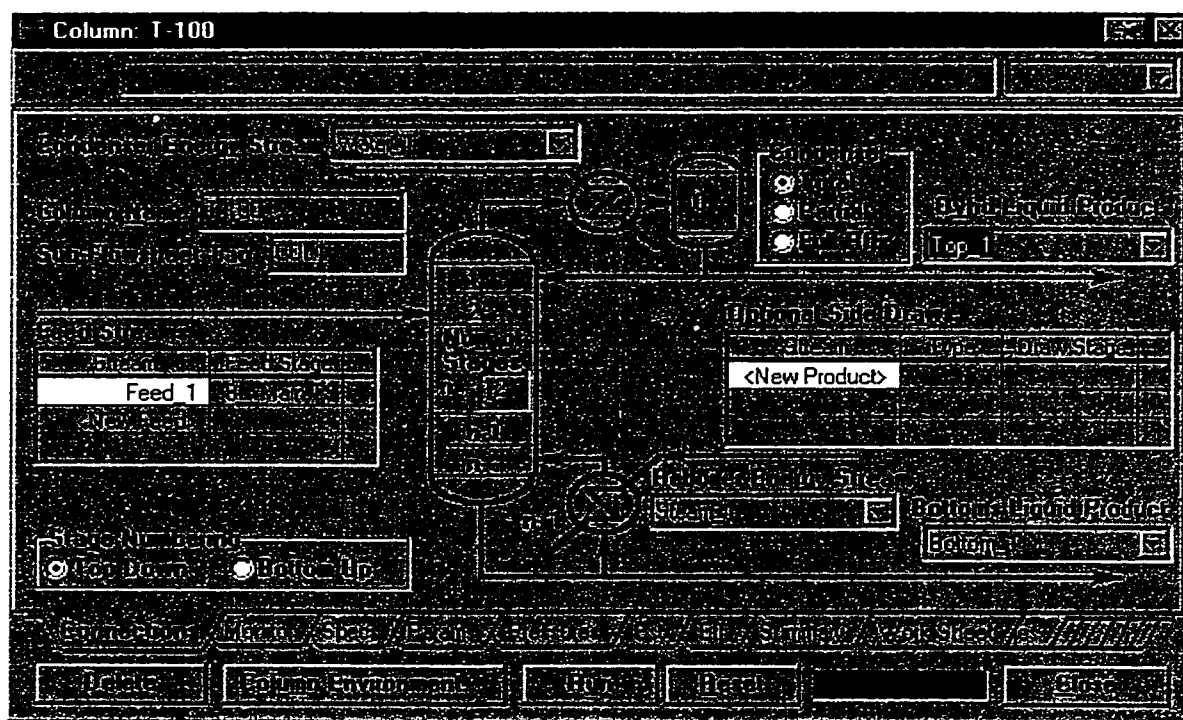
Heat-integrated distillation column processes in Figs. 5.5 and 5.6 are simulated by the HYSYS simulator. The overall simulation procedure is given by the following steps:

Step 1. Build a fluid package including the components, property method, etc. As shown in Fig. D-1, three components, Benzene, Cumene, and n-Nonane, are selected into the fluid package. The thermodynamic physical properties are to be estimated using the SRK method.

Step 2. Input feed stream data including temperatures, pressures, mass flow rates, and compositions for each component (Fig. D-2).

Step 3. Install unit operations and specify their stream connections. Figure D-3(a) shows stream connections and specifications in distillation column T-100. Figures D-3(b) and (c) respectively illustrate the specified value of reflux ratio and the summary of simulation results, such as the profiles of temperature, pressure, liquid flow rate, and vapor flow rate, as well as heat duties for the condenser and the reboiler in the column. Figure D-4(a) depicts stream connections of a heat exchanger; its specified values and simulation results are illustrated in Figs. D-4(b) and (c), respectively. In the HYSYS simulator, stream splitting and mixing is treated as a type of unit operation; the specified stream connections and simulation results are given in Figs. D-5(a) and (b) for the splitter and D-6(a) and (b) for the mixer.

Step 4. Simulate the overall process system. The results of stream outputs in all unit operations are shown in the main workbook (Fig. D-7); a process flowsheet diagram (PFD) is depicted in Figs. D-8(a) and (b).



(a) stream connections

	Specified Value	Control Variable	Unit	Active	Estimate
Feed Rate	1.550	1.55	kmol/h	<input checked="" type="checkbox"/>	<input checked="" type="checkbox"/>
Distillate Rate	empty	2.11	kmol/h	<input checked="" type="checkbox"/>	<input checked="" type="checkbox"/>
Bottoms Rate	empty	3.25	kmol/h	<input checked="" type="checkbox"/>	<input checked="" type="checkbox"/>
Reflux Ratio	empty	3.38	kmol/h	<input checked="" type="checkbox"/>	<input checked="" type="checkbox"/>

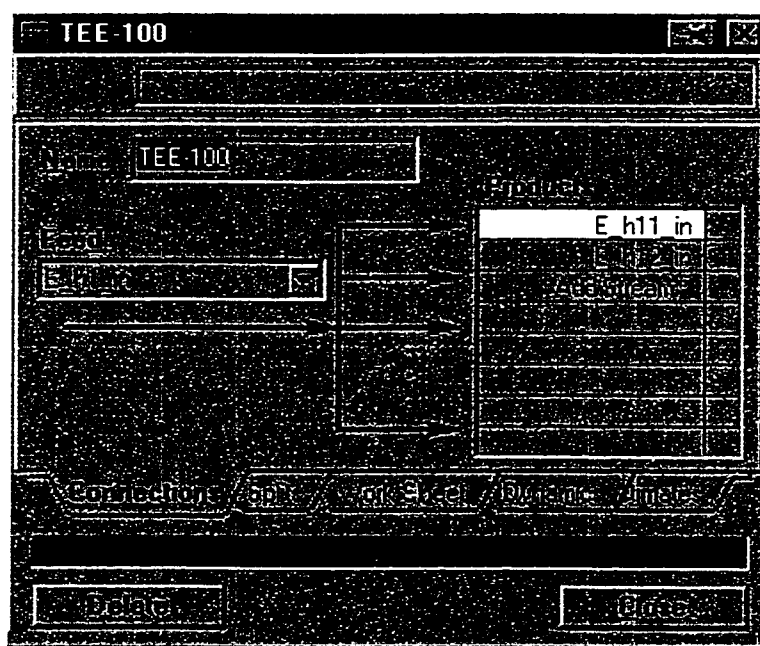
(b) specified value for simulation

Figure D-3. Column specifications and simulation results.

Column: T-100									
<input type="radio"/> Off <input type="radio"/> On <input checked="" type="radio"/> Simulation									
Refin Ratio: 5500									
	Flow (lb)	Pressure (PSI)	Temp (°F)	Temp (°F)	Temp (°F)		Temp (°F)	Temp (°F)	
1. Inlet	105.21	220.10	325.68				210.8	L	2160.85
2. Inlet	105.10	220.10	318.90	535.27					
3. Inlet	107.48	225.82	275.58	209.05					
4. Inlet	105.22	233.5	275.21	183.61					
5. Inlet	105.27	240.45	238.98	158.73					
6. Inlet	105.34	248.25	238.20	129.04					
7. Inlet	102.42	257.15	210.35	102.71					
8. Inlet	105.26	260.81	210.85	100.88					
9. Inlet	105.58	257.73	228.10	151.19	5.38	L			
10. Inlet	105.22	274.55	227.48	138.64					
11. Inlet	107.03	281.36	269.05	105.72					
12. Inlet	105.89	288.10	239.77	104.9					
13. Inlet	105.65	295.10	210.00	145.41					
14. Inlet	105.55	295.10		222.6			138.73	L	1516.05

(c) simulation result

Figure D-3. Column specifications and simulation results (cont'd).

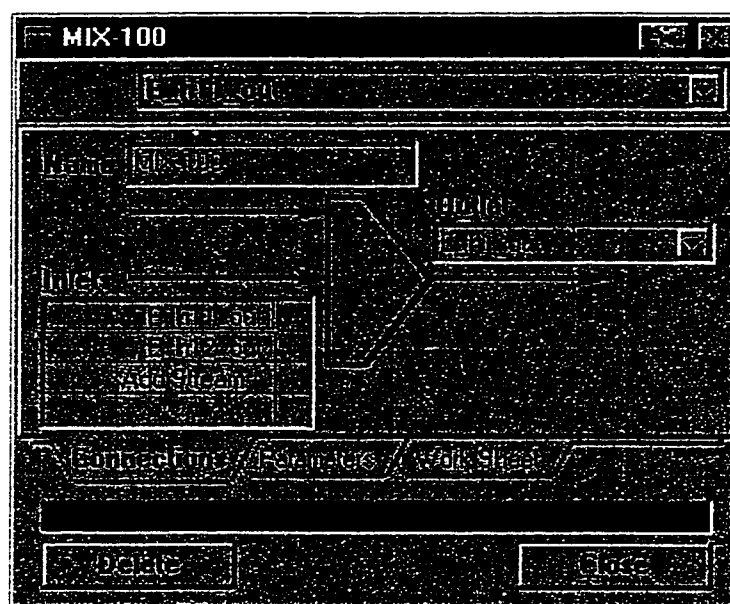


(a) stream connections

Name	Value	Units
Feed	1000000	kg/h
Temperature (C)	263.0000	
Pressure (kPa)	2000.0000	
Molar Flow (kmol/h)	85.4000	
Mass Flow (kg/h)	9000.0000	
Crude Oil Flow (kg/h)	1000.0000	
Crude Oil Flow (kg/h)	1000.0000	
Crude Oil Flow (kg/h)	1000.0000	

(b) simulation result

Figure D-5. Stream specifications and simulation results for a splitter.

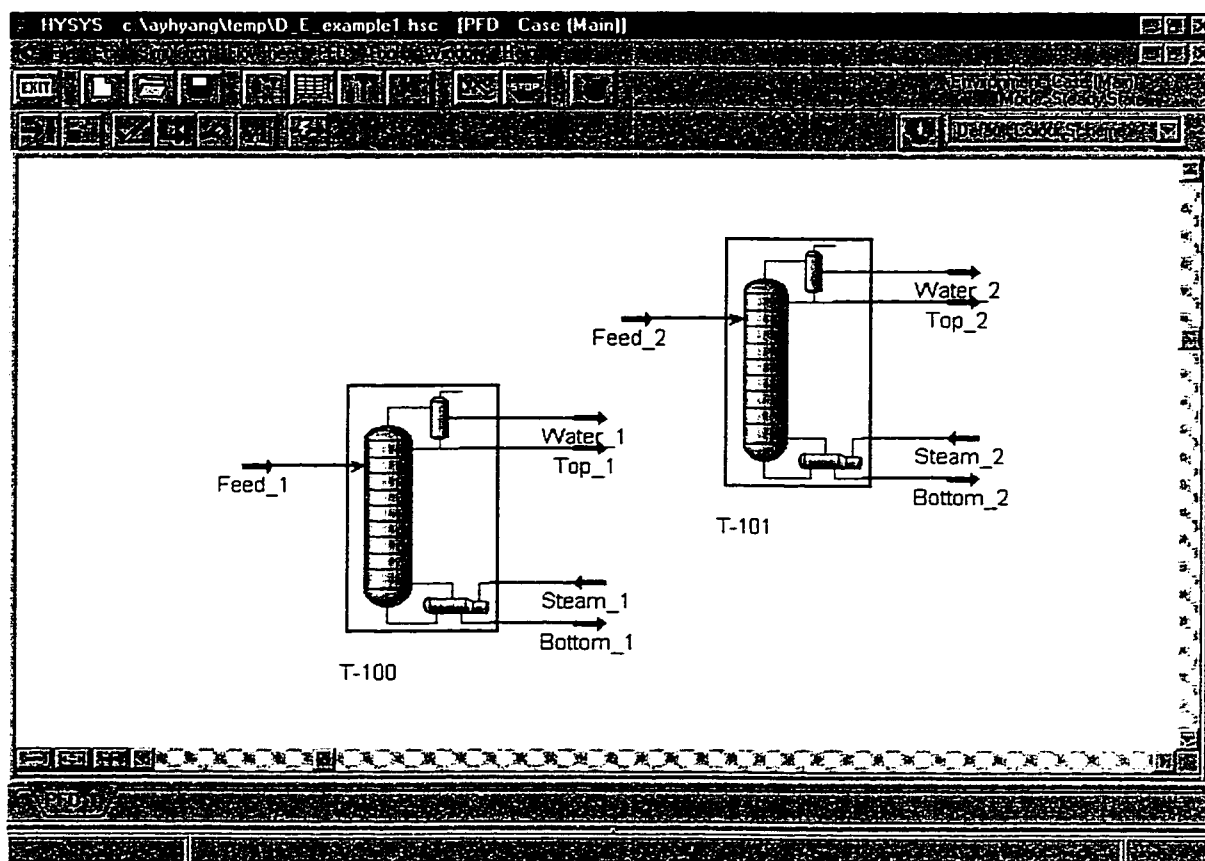


(a) stream connections

Name	F100-001	F100-002	F100-003
Various	0.0000	0.0000	0.0000
Temperature (K)	180.59 (1)	175.15 (1)	177.34 (1)
Pressure (kPa)	2000.0000	2000.0000	2000.0000
Molar Flow (kmol/h)	3.466	5.725	8.5408
Mass Flow (kg/h)	360.0000	5.0000	900.0000
Enthalpy (kJ/h)	0.4892	0.6509	0.0982
Heat Flow (kW)	34.586 (1)	1.474 (1)	24.988 (1)

(b) simulation result

Figure D-6. Stream specifications and simulation results for a mixer.



(a) the PFD for distillation columns

Figure D-8. The PFD of the heat-integrated distillation column process.

REFERENCES

- Alsop, A. W. *Nonlinear Chemical Process Control by Means of Linearizing State and Input Variable Transformations*. Ph.D. Dissertation, University of Texas at Austin, TX, 1987.
- Bagajewicz, M. J. and V. Manousiouthakis, "Mass/Heat-Exchange Network Representation of Distillation Networks," *AIChE J.*, **38**, 1769-1800, 1992.
- Balakrishna, S. and L. T. Biegler, "A Unified Approach for the Simultaneous Synthesis of Reaction, Energy, and Separation Systems," *Ind. Eng. Chem. Res.*, **32**, 1372, 1993.
- Barton, G. W., M. A. Padley, and J. D. Perkins, "Incorporating Operability Measures into the Process Synthesis Stage of Design," in *Proceedings of the IFAC Workshop on Integration of Process Design and Control*, London, U. K., 1992.
- Calandranis, J. and G. Stephanopoulos, "Structural Operability Analysis of Heat Exchanger Networks," *Chem. Eng. Res. Des.*, **64**, 347-364, 1986.
- Calandranis, J. and G. Stephanopoulos, "A Structural Approach to the Design of Control Systems in Heat Exchanger Networks," *Comp. Chem. Eng.*, **12**, 651-669, 1988.
- Cherry, K. F., "Plating Waste Treatment," *Ann Arbor Science*, Ann Arbor, MI, 1982.
- Chitra, S. P. and R. Govind, "Synthesis of Optimal Series Reactor Structures for Homogeneous Reactions. II. Nonisothermal Reactors," *AIChE J.*, **31**, 185-194, 1985.
- Commault, C., J. M. Dion, and S. Perez, "Transfer Matrix Approach to the Disturbance Decoupling Problem," IFAC World Congress, Budapest, Hungary, 1984.
- Commault, C., J. M. Dion, and S. Perez, "Disturbance Rejection for Structural Systems," *IEEE Trans. Automatic Control*, **36**, 884, 1991.
- Cushnie, G. C. Jr., "Pollution Prevention and Control Technology for Plating Operations," *National Center for Manufacturing Sciences*, Ann Arbor, MI, 1994.
- Dion, J. M., C. Commault, and J. Montoya, "Simultaneous Decoupling and Disturbance Rejection - A Structural Approach," *Int. J. Control*, **59**, 1325, 1994.
- Douglas, J. M., "A Hierarchical Decision Procedure for Process Synthesis," *AIChE J.*, **31**, 353, 1985.
- Downs, J. J. and J. Siirola, "Challenges of Integrated Process and Control Systems Design for Operability," *AIChE Annual Meeting*, Los Angeles, CA, November 16-21, 1997.

- El-Halwagi, M. M. and V. Manousiouthakis, "Automatic Synthesis of Mass Exchange Networks," *AIChE Annual Meeting*, Washington, D. C., November 1988.
- El-Halwagi, M. M. and V. Manousiouthakis, "Synthesis of Mass Exchange Networks," *AIChE J.*, **35**, 1233-1244, 1989.
- El-Halwagi, M. M. and V. Manousiouthakis, "Automatic Synthesis of Mass Exchange Networks with Single-Component Targets," *Chem. Eng. Sci.*, **45**, 2813-2831, 1990a.
- El-Halwagi, M. M. and V. Manousiouthakis, "Simultaneous Synthesis of Mass-Exchange and Regeneration Networks," *AIChE J.*, **36**, 1209-1219, 1990b.
- El-Halwagi, M. M. and B. K. Srinivas, "Synthesis of Reactive Mass-Exchange Networks," *Chem. Eng. Sci.*, **47**, 2113-2119, 1992.
- El-Halwagi, M. M., A. A., Hamad, and G. W., Garrison, "Synthesis of Waste Interception and Allocation Networks," *AIChE J.*, **42**, 3087-3101, 1996.
- Elliott, T. R. and W. L. Luyben, "Capacity-Based Approach for the Qualitative Assessment of Process Controllability during the Conceptual Design State," *Ind. Eng. Chem. Res.*, **34**, 3907-3915, 1995.
- Fisher, W. R., M. F. Doherty, and J. M. Douglas, "The Interface between Design and Control. 1. Process Controllability," *Ind. Eng. Chem. Res.*, **27**, 597-605, 1988a.
- Fisher, W. R., M. F. Doherty, and J. M. Douglas, "The Interface between Design and Control. 2. Process Operability," *Ind. Eng. Chem. Res.*, **27**, 606-611, 1988b.
- Fisher, W. R., M. F. Doherty, and J. M. Douglas, "The Interface between Design and Control. 3. Selecting a Set of Controlled Variables," *Ind. Eng. Chem. Res.*, **27**, 611-615, 1988c.
- Floudas, C. A. and Grossmann, I. E., "Synthesis of Flexible Heat Exchanger Networks for Multiperiod Operation," *Comput. Chem. Eng.*, **10**, 153-168, 1986.
- Fogler, H. S., *Elements of Chemical Reaction Engineering*. Prentice Hall: New Jersey, NJ, 1992.
- Georgiou, A. and C. A. Floudas, "Simultaneous Process Synthesis and Control: Minimization of Disturbance Propagation in Heat Recovery Systems," in *Proceedings of the Third International Conference on Foundations of Computer-Aided Process Design*, J. J. Siirola, I. E. Grossmann, and G. Stephanopoulos (eds.), Elsevier, New York, NY, pp. 435-450, 1990.
- Galli, M. R. and J. Cerda, "Synthesis of Flexible Heat Exchanger Networks – III: Temperature and Flowrate Variations," *Comput. Chem. Eng.*, **15**, 7-24, 1991.

- Integration of Process Design and Control," *Ind. Eng. Chem. Res.*, **33**, 1174-1187, 1994.
- Huang, Y. L. and T. F. Edgar, "Knowledge-Based Design Approach for the Simultaneous Minimization of Waste Generation and Energy Consumption in Petroleum Refineries," in *Waste Minimization through Process Design*, A. P. Rossiter (ed.), McGraw-Hill: New York, NY, pp. 181-196, 1995.
- Huang, Y. L. and L. T. Fan, "Analysis of Work Exchanger Networks," *Ind. Eng. Chem. Res.* **35**, 3528-3538, 1996.
- Huang, Y. L. and K. Q. Luo, "Intelligent Decision Support System for Source Waste Reduction in Metal Finishing Plants," in *Intelligent Systems in Process Engineering*, J. F. Davis, G. Stephanopoulos, and V. Venkatasubramanian (eds.), AIChE Symposium Series, Vol. 92, 405-409, 1996.
- Jacobs, R., Wouter N. H. Jansweijer, and P. Iedema, "A Knowledge Based System for Reactor Selection," *Comp. Chem. Eng.*, **20**, S165-S170, 1996.
- Johnson, G. and O. P. Palsson, "Use of Empirical Relations in the Parameters of Heat-Exchanger Models," *Ind. Eng. Chem. Res.*, **30**, 1193, 1991.
- King, C. J., *Separation Processes*. 2nd ed., McGraw-Hill: New York, NY, 1980.
- Kern, D. Q., *Process Heat Transfer*. McGraw-Hill: New York, NY, 1950.
- Koggersbol, A., B. R. Andersen, J. S. Nielsen, and S. B. Jorgensen, "Control Configurations for an Energy Integrated Distillation," *Comp. Chem. Eng.*, **20**, S853-S858, 1996.
- Kokossis, A. C. and C. A. Floudas, "Optimization of Complex Reactor Networks. I. Isothermal Operation." *Chem. Eng. Sci.*, **45**, 595, 1990.
- Kotjabasakis, E. and B. Linnhoff, "Sensitivity Tables for the Design of Flexible Process (I) - How Much Contingency in Heat Exchanger Networks Is Cost-Effective?" *Chem. Eng. Res. Des.*, **64**, 197-211, 1986.
- Lakshmanan, Ajay and L. T. Biegler, "Synthesis of Optimal Chemical Reactor Networks with simultaneous Mass Integration," *Ind. Eng. Chem. Res.*, **35**, 4523-4536, 1996.
- Li, G. Q., B. Hua, B. L. Liu, and G. R. Wu, "The Study for Flexibility Analysis Method in Heat Exchanger Network," in *Proceedings of PSE '94*, 407-413, 1994.
- Linnhoff, B., D. W. Townsend, D. Boland, G. F. Hewitt, B. E. A. Thomas, A. R. Guy, and R. H. Marsland, *User Guide on Process Integration for the Efficient Use of Energy*. The Institute of Chemical Engineers, London, U. K. 1982.

- Linnhoff, B. and E. Kotjabasakis, "Downstream paths for Operable Process Design," *Chem. Eng. Prog.*, **82**(5), 23-28, 1986.
- Luo, K. Q. and Y. L. Huang, "Intelligent Decision Support for Waste Minimization in Electroplating Plants," *Int. J. Engng. Applic. Artif. Intell.*, **10**(4), 321-334, 1997.
- Luo, K. Q., J. P. Gong, and Y. L. Huang, "Modeling for Sludge Estimation and Reduction," in press, *Plat. & Surf. Fin.*, **84**(10) 1998.
- Luyben, M. L., *Analyzing the Interaction between Process Design and Process Control*. Ph.D. Dissertation, Princeton University, NJ, 1993.
- Luyben, M. L. and C. A. Floudas, "Analyzing the Integration of Design and Control — 1. A Multiobjective Framework and Application to Binary Distillation Synthesis," *Comp. Chem. Eng.*, **18**, 933-969, 1994a.
- Luyben, M. L. and C. A. Floudas, "Analyzing the Integration of Design and Control — 2. Reactor-Separator-Recycle System," *Comp. Chem. Eng.*, **18**, 970-994, 1994b.
- McLane, P. J. and E. J. Davison, "Disturbance Localization and Decoupling in Stationary Linear Multivariable Systems," *IEEE Trans. Automatic Control*, **15**, 133, 1970.
- McAvoy, T. J., "Integration of Process Design and Process Control," in *Recent Development in Chemical Process and Plant Design*, Y. A. Liu, H. A. McGee, Jr., and W. R. Epperly (eds.), John Wiley & Sons: New York, NY, pp. 289-325, 1987.
- McCabe, W. L., J. C. Smith, and P. Harriott, *Unit Operations of Chemical Engineering*. 5th ed., McGraw-Hill: New York, NY, 1993.
- Morari, M., "Flexibility and Resiliency of Process Systems," in *Proceedings of the International Symposium on Process Systems Engineering*, pp. 223-237, Kyoto, Japan, August 23-27, 1982.
- Morari, M., "Effect of Design on the Controllability of Chemical Plants," in *Preprints of the IFAC Workshop on Interactions between Process Design and Process Control*, pp. 3-16, London, UK, September 7-8, 1992.
- Nelson, K. E., "Process Modifications That Save Energy, Improve Yields and Reduce Waste," in *Waste Minimization through Process Design*, A. P. Rossiter (ed.), McGraw-Hill: New York, NY, pp. 119-132, 1995.
- Nelson, W. L., *Petroleum Refinery Engineering*. 4th ed., McGraw-Hill: New York, NY, 360-362, 1969.
- Nishida N., G. Stephanopoulos, and A. W. Westerberg, "A Review of Process Synthesis," *AIChE J.*, **27**, 321-351, 1981.

- Noyes, R., *Handbook of Pollution Control Processes*, Noyes Publications: New Jersey, NJ, 1991.
- Orr, C. P., Y. H. Yang, and Y. L. Huang, "Waste Minimization in CSTR Systems by Disturbance Simulation for Improved Design," *AIChE Spring Meeting*, New Orleans, LA, March 1998.
- Palmer, S. A. K., M. A. Breton, T. J. Nunno, D. M. Sullivan, and N. F. Surprenant, "Metal/Cyanide Containing Wastes, Treatment Technology," Noyes Data Corp., Park Ridge, NJ, 1988.
- Papalexandri K. P. and E. N. Pistikopoulos, "A Multiperiod MINLP Model for the Synthesis of Flexible Heat and Mass Exchange Networks," *Comp. Chem. Eng.*, **18**, 1125-1139, 1994a
- Papalexandri K. P. and E. N. Pistikopoulos, "Synthesis and Retrofit Design of Operable Heat Exchanger Network: 1. Flexibility and Structural Controllability Aspects," *Ind. Eng. Chem. Res.*, **33**, 1718-1737, 1994b.
- Perry, R. H., D. W. Green, and J. O. Maloney, *Perry's Chemical Engineers' Handbook*. 6th ed., Section 18, McGraw-Hill: New York, NY, 1984.
- Ratnam, R. and V. S. Patwardhan, "Sensitivity Analysis for Heat Exchanger Networks," *Chem. Eng. Sci.*, **46**, 451-458, 1991.
- Rossiter, A. P., H. D. Spriggs, and H. Klee, "Apply Process Integration to Waste Minimization," *Chem. Eng. Prog.*, **89**(1), 30-36, 1993.
- Rossiter, A. P. and J. D. Kumana, "Pollution Prevention and Process Integration – Two Complementary Philosophies," in *Waste Minimization through Process Design*, A. P. Rossiter (ed.), McGraw-Hill: New York, NY, pp. 43-52, 1995.
- Sabharwal, A, T. F. Edgar, and Y. L. Huang, "A Knowledge Engineering Approach to Waste Minimization," *AIChE Spring Meeting*, Houston, TX, March 1995.
- Saboo, A. K., M. Morari, and D. C. Woodcock, "Design of Resilient Processing Plants – VIII. A Resilience Index for Heat Exchanger Networks," *Chem. Eng. Sci.*, **40**, 1553-1565, 1985.
- Seader, J. D. and E. J. Henley, *Separation Process Principles*. John Wiley & Sons: New York, NY, 1998.
- Sheffield, R. E., "Integrate Process and Control System Design," *Chem. Eng. Prog.*, **88**, 30-35, 1992.
- Shinskey, F. G., *Process Control Systems*, 4th ed., McGraw-Hill: New York, NY, 1995.

- Smith, J. M. and H. C. Van Ness, *Introduction to Chemical Engineering Thermodynamics*, 4th ed.; McGraw-Hill: New York, NY, 1987.
- Smith, R., *Chemical Process Design*, McGraw-Hill, New York, NY, 1995.
- Terrill, D. L. and J. M. Douglas, "Heat-Exchanger Network Analysis – 2: Steady-State Operability Evaluation," *Ind. Eng. Chem. Res.*, **26**, 691-696, 1987.
- Wang, Y. P. and R. Smith, "Wastewater Minimization," *Chem. Eng. Sci.*, **49**(7), 981-1006, 1994.
- Wang, Y. P. and R. Smith, "Wastewater Minimization with Flowrate Constraints," *Chem. Eng. Res. Des.*, Part A **73**, 889-904, 1995.
- Yang, Y. H. and Y. L. Huang, "Extended Distributed Strategy for Process Modification," *AIChE Spring Meeting*, New Orleans, LA, February 1996.
- Yang, Y. H., J. P. Gong, and Y. L. Huang, "A Simplified System model for Rapid Evaluation of Disturbance Propagation through a Heat Exchanger Network," *Ind. Eng. Chem. Res.*, **35**, 4550-4558, 1996.
- Yang, Y. H. and Y. L. Huang, "Modeling for Evaluation of Disturbance Propagation through a Heat Integrated Distillation Process," accepted, *Chem. Eng. Res. Des.*, 1998.
- Yang, Y. H. and Y. L. Huang, "A Unified Model for the Prediction of Structural Disturbance Propagation in Mass Exchanger Networks," submitted, *Chem. Eng. Res. Des.*, 1998.
- Zhu, M. J. and M. M. El-Halwagi, "Synthesis of Flexible Mass-Exchange Network," *Chem. Eng. Comm.*, **138**, 193-211, 1995.
- Zhu, Z. X., J. Lee, and T. F. Edgar, "Steady State Structural Analysis and Interaction Characterization for Multivariable Control Systems," *Ind. Eng. Chem. Res.*, **36**, 3718-3726, 1997.

ABSTRACT

MODEL-BASED INTEGRATION OF PROCESS DESIGN AND CONTROL VIA PROCESS SYNTHESIS: *DEVELOPMENT OF HIGHLY CONTROLLABLE AND ENVIRONMENTALLY BENIGN PROCESSES*

by

YIHUA YANG

May 1999

Advisor: Prof. Yinlun Huang
Major: Chemical Engineering
Degree: Doctor of Philosophy

Process integration techniques have been increasingly employed in the process and allied industries to reduce energy and material costs and, more recently, to minimize waste. Industrial practice has shown, however, that improper integration can cause various operational problems, and may make economic and environmental goals unachievable. Consequently, to ensure successful process integration, an integrated process must be structurally highly controllable. Naturally, the integration of process design and control is becoming one of the most promising, but most difficult area in the process systems engineering.

This dissertation is a fundamental study of the earliest integration of process design and control in the overall process engineering activities. The main focus is on the development of a novel and systematic model-based integration methodology for synthesizing cost-effective, highly structurally controllable, and environmentally benign process plants. The research interest is in the synthesis of complex network-structured

AUTOBIOGRAPHICAL STATEMENT

EDUCATION

May 1996 **M.S., Chemical Engineering**, Wayne State University, Detroit, MI
July 1983 **B.S., Chemical Engineering**, South China University of Technology,
GuangZhou, China

PROFESSIONAL EXPERIENCE

1994-present **Graduate Research Assistant**, Wayne State University, Detroit, MI
1983-1993 **Process Engineer**, China Petrochemical Corporation (SINOPEC),
Beijing, China

AWARDS AND MEMBERSHIPS

- **Advanced Science and Technology Awards**, SINOPEC, Beijing, China
 - * Synthesis and Design of cost-effective Industrial-Scale Heat Exchanger Networks 1992
 - * Novel Simulating Approach for Heat Exchanger Networks 1988
- **Excellent Software Development Award**, SINOPEC, Beijing, China
 - * Simulator for Evaluating Performance of Heat Exchanger Networks 1988
- **American Institute of Chemical Engineers (AIChE)**
- **American Chemical Society (ACS)**

PUBLICATIONS (SELECTED)

1. Huang, Y. L. and Yang, Y. H., "Knowledge- and Model-based Process Modification Approach for In-Plant Waste Minimization," invited chapter, in *Knowledge-Based Systems Techniques and Applications*, C. T. Leondes (ed.), Academic Press, 1999.
2. Yang, Y. H., Lou, H. R., and Huang, Y. L., "Optimal Design of a Water Reuse System in an Electroplating Plant," to appear, *Plat. & Surf. Fin.*, 1998.
3. Yang, Y. H., Lou, H. R., and Huang, Y. L., "Synthesis of an Optimal Wastewater Reuse Network," submitted, *Waste Management*, 1998.
4. Luo, K. Q., Yang, Y. H., Gong, J. P., and Huang, Y. L., "Modeling for Sludge Estimation & Reduction," *Plat. & Surf. Fin.*, **85**, 59-63, October, 1998.
5. Yang, Y. H. and Huang, Y. L., "A Unified Model for the Prediction of Structural Disturbance Propagation in Mass Exchanger Networks," accepted, *Chem. Eng. Res. & Des.*, 1998.
6. Yang, Y. H. and Huang, Y. L., "A Shortcut Model for Disturbance Prediction in a Non-Sharp Ternary Separation System," submitted, *Can. J. Chem. Eng.*, 1998.
7. Yang, Y. H. and Huang, Y. L., "Modeling for Evaluation of Disturbance Propagation through a Heat Integrated Distillation Process," submitted, *Chem. Eng. Res. & Des.*, 1998.
8. Yang, Y. H., Gong, J. P., and Huang, Y. L., "A Simplified System Model for Rapid Evaluation of Disturbance Propagation through a Heat Exchanger Network," *Ind. & Eng. Chem. Res.*, **35**, 4550-4558, 1996.